Histochemical Features and Oil Production in Relation to the Reproductive Modes of Physic Nut (*Jatropha curcas* L.) during in vivo Seed Development and Cell Suspension Culture

Nilubol Nuanjunkong

A Thesis Submitted in Fulfillment of the Requirements for the Degree of Doctor of Philosophy in Biology

Prince of Songkla University

2018

Histochemical Features and Oil Production in Relation to the Reproductive Modes of Physic Nut (*Jatropha curcas* L.) during in vivo Seed Development and Cell Suspension Culture

Nilubol Nuanjunkong

A Thesis Submitted in Fulfillment of the Requirements for the Degree of
Doctor of Philosophy in Biology
Prince of Songkla University
2018

Thesis Title Histochemical features and oil production in relation to the reproductive modes of physic nut (*Jatropha curcas* L.) during in vivo seed development and cell suspension culture

Author Miss Nilubol Nuanjunkong

Major Program Biology

Major Advisor

……
(Assoc. Prof. Dr. Upatham Meesawat)

Co-advisor

……
(Assoc. Prof. Dr. Chakrit Tongurai)

Examining Committee:

..…….Chairperson
(Prof. Dr. Sompong Te-chato)

..……..Committee
(Assoc. Prof. Dr. Upatham Meesawat)

..……..Committee
(Assoc. Prof. Dr. Chakrit Tongurai)

..……..Committee
(Asst. Prof. Dr. Natthaya van Beem)

The Graduate School, Prince of Songkla University, has approved this thesis as fulfillment of the requirements of the Doctor of Philosophy Degree in Biology.

…….
(Prof. Dr. Damrongsak Faroongsarng)
Dean of Graduate School

This is to certify that the work here submitted is the results of candidate's own investigations. Due acknowledgement has been made of any assistance received.

…….Signature
(Assoc. Prof. Dr. Upatham Meesawat)
Major Advisor

……...Signature
(Nilubol Nuanjunkong)
Candidate

I hereby certify that this work has not already been accepted in substance for any degree, and is not being concurrently submitted in candidature for any degree.

…….Signature

(Nilubol Nuanjunkong)

Candidate

ชื่อวิทยานิพนธ์ ลักษณะทางฮีสโตเคมีและการสร้างน้ำมันที่เกี่ยวข้องกับระบบสืบพันธุ์ของสบู่ดำในระหว่างการเจริญของเมล็ดและการเพาะเลี้ยงเซลล์แขวนลอย

ผู้เขียน นางสาวนิลุบล นวลจันทร์คง

สาขาวิชา ชีววิทยา

ปีการศึกษา 2560

บทคัดย่อ

สบู่ดำสามารถใช้ผลิตไบโอดีเซลที่มีคุณสมบัติตรงตามมาตรฐาน เนื่องจากพืชชนิดนี้สร้างน้ำมันที่บริโภคไม่ได้ และมีกรดไขมันชนิดโอเลอิกสูง อย่างไรก็ตาม ความเป็นไปได้ในทางการค้ายังไม่ประสบความสำเร็จ เนื่องด้วยการให้น้ำมัน การติดผล และเมล็ด ยังค่อนข้างต่ำ เป็นผลสืบเนื่องมาจากขาดการปรับปรุงพันธุ์และองค์ความรู้ที่ไม่สมบูรณ์ ดังนั้นงานวิจัยฉบับนี้ จึงมีวัตถุประสงค์เพื่อเพิ่มเติมองค์ความรู้ในด้าน 1) การเจริญและความมีชีวิตของแกมีโทไฟต์เพศผู้และเพศเมีย 2) ความสัมพันธ์ระหว่างรูปแบบการผสมเกสรและคุณลักษณะของน้ำมันในเมล็ด และ 3) น้ำมันในเซลล์แขวนลอย จากการศึกษาพบว่า ขนาดเส้นผ่านศูนย์กลางตาดอกสามารถใช้เป็นเกณฑ์ในการระบุระยะการเจริญของเรณูและถุงเอ็มบริโอได้ ความมีชีวิตของเรณูและการพร้อมรับของยอดเกสรเพศเมียสูงในระยะดอกบาน ปริมาณน้ำมันในเมล็ดที่ได้จากการผสมเกสรแบบธรรมชาติ ผสมข้าม ผสมตัวเอง และไม่ผสมเกสร (แอโพมิกซิส) ไม่มีความแตกต่างทางสถิติ อย่างไรก็ตาม การผสมธรรมชาติมีการติดผล จำนวนเมล็ด และกรดโอเลอิกสูงที่สุด นอกจากนี้ยังพบว่า เอนโด-สเปิร์ม สะสมน้ำมันและกรดโอเลอิกสูงกว่าเอ็มบริโอ ออยบอดีที่สกัดจากเมล็ดสะสมไขมันในรูปไตรเอซิลกลีเซอรอล (TAG) เป็นส่วนใหญ่ และมีโปรตีนแทรกชื่อ caleosin และ oleosins (ทั้งชนิดน้ำหนักโมเลกุลสูงและน้ำหนักโมเลกุลต่ำ) เป็นองค์ประกอบ เซลล์แขวนลอยถูกเพาะเลี้ยงจากแคลลัสชนิดเกาะกันแน่น (compact callus) ในอาหารสูตร MS เติมด้วย 2, 4-dichlorophenoxyacetic acid (2, 4- D) 1 มิลลิกรัมต่อลิตร และ kinetin (KN) 0.5 มิลลิกรัมต่อลิตร จากการศึกษาพบว่าปริมาณน้ำมันและกรดโอเลอิกในเซลล์แขวนลอยต่ำกว่าในเมล็ด อย่างไรก็ตาม เซลล์แขวนลอยสะสมกรดโอเลอิกในปริมาณสูงกว่ากรดไขมันชนิดอื่นๆ ทั้งหมดที่พบภายในเซลล์ ซึ่งบ่งชี้ถึงศักยภาพของเซลล์แขวนลอย ที่จะสามารถใช้เป็นแหล่งน้ำมัน สำหรับผลิตไบโอดีเซลที่มีคุณภาพตามมาตรฐานได้ ถึงกระนั้นก็ตาม การปรับปรุงเพิ่มเติมยังมีความจำเป็น เพื่อที่จะเพิ่มปริมาณของเซลล์ และปริมาณน้ำมันที่สะสมในเซลล์แขวนลอยดังกล่าว เพื่อตอบสนองความต้องการในเชิงการค้าได้

Thesis Title Histochemical features and oil production in relation to the reproductive modes of physic nut (*Jatropha curcas* L.) during in vivo seed development and cell suspension culture

Author Miss Nilubol Nuanjunkong

Major Program Biology

Academic Year 2017

ABSTRACT

Physic nut (*Jatropha curcas* L.) is promising for biodiesel production due to its inedible oil and high oleic acid content which leads to the standard-satisfied biodiesel. However, commercial feasibility has not been achieved due to its low oil content, fruit and seed set ascribed to the lack of crop improvement and incomplete knowledge. Thus, this study aims to fulfill the gap knowledge on 1) development and fertility of male and female gametophytes, 2) relationship between pollination method and oil features and 3) lipid storage in cell suspension. The results showed that bud diameter could be used as criteria for identifying the stages of pollen and embryo sac. The pollen viability and the stigma receptivity were high at anthesis. There was no significant difference of seed oil content after open-, cross-, self- pollination and non-pollination (apomixis). However, the open-pollination provided maximal fruit, seed set and oleic acid content. Besides, the endosperm reserved greater oil and oleic than the embryo. The seed oil bodies were mainly composed of triacylglycerol (TAG) and integral proteins named caleosin and oleosins (both high and low molecular weight isoforms). Cell suspension was established, from the compact callus, in liquid MS media added with 1 mg L^{-1} 2, 4-dichlorophenoxyacetic acid (2, 4- D) and 0.5 mg L^{-1} kinetin (KN). This study revealed that both oil content and oleic acid were lower in the cell suspension than in the seed. However, the cell suspension accumulated higher oleic acid than all other fatty acid types found within the cell, indicating its potential for using as a source of oil for producing the standard-satisfied biodiesel. Further improvement, nevertheless, is needed in order to increase the biomass and oil content of the cell suspension – for meeting the commercial demand.

ACKNOWLEDGMENTS

I would like to express my special appreciation to my advisor, Assoc. Prof. Dr. Upatham Meesawat, for being an outstanding mentor, providing valuable advices on research, and all her charitable helps in supporting me throughout my study. I am grateful to Assoc. Prof. Dr. Chakrit Tongurai, my co-advisor from Department of Chemical Engineering, Faculty of Engineering, Prince of Songkla University (PSU), for his valuable guidance and generous supports. I would especially like to thank Professor Dr. Jason T. C. Tzen, Graduate Institute of Biotechnology, National Chung Hsing University, Taiwan, for all his kind helps during my five-month stay in Taiwan as a research exchange student. Special thanks to Dr. Pei-Luen Jiang and her staffs, Institute of Marine Biotechnology, National Dong-Hwa University, Pingtung, Taiwan, for a priceless assistance in extraction and analysis of oil body. I would also like to thank Prof. Dr. Sompong Te-chato, Department of Plant Science, Faculty of Natural Resources, PSU, and Asst. Prof. Dr. Natthaya van Beem, Department of Biology, Faculty of Science, Thaksin University, for serving as my committee members and for their brilliant comments and criticism.

I would like to take this opportunity to thank all staffs and laboratory members from Department of Biology, Faculty of Science and Department of Chemical Engineering, Faculty of Engineering, PSU for every laboratory techniques they have taught me and meaningful aids. I wish to acknowledge Science Achievement Scholarship of Thailand (SAST) for Ph.D. financial support and Graduated school, PSU for research funding and scholarship for support exchange students and international credit transferred through ASEAN Community. As well as, I would like to thank Trang Agricultural Occupation Promotion and Development Center, Thailand, for generous permission in employing physic nut plantation.

Finally, I would love to manifest a special gratitude to my family. Words cannot express how grateful I am to my parents, brothers, and my beloved husband for spending difficult time with me and giving worthy encouragement.

Nilubol Nuanjunkong

CONTENTS

CONTENTS (CONTINUED)

CONTENTS (CONTINUED)

CONTENTS (CONTINUED)

LIST OF TABLES

LIST OF FIGURES

LIST OF FIGURES (CONTINUED)

LIST OF ABBREVIATIONS

2, 4-D	=	2, 4-dichlorophenoxyacetic acid
BA	=	6-Benzyladenine
BAP	=	6-Benzylaminopurine
BCIP	=	5-Bromo-4-chloro-3-indolyl phosphate
DAF	=	Days after flowering
DAG	=	Diacylglycerol
DGAT	=	Diacylglycerol acyltransferase
DIC	=	Differential interference contrast
FAA	=	Formalin-aceto-alcohol
FAD2	=	Omega-6 desaturase
FAD3	=	Omega-3 desaturase
FAME	=	Fatty acid methyl ester
FDA	=	Fluorescein diacetate
FID	=	Flame ionization detector
FW	=	Fresh weight
H-form	=	High molecular weight
HAF	=	Hours after flowering
IBA	=	Indole-3-butyric acid
JcOle	=	*J. curcas* oleosin
KN	=	Kinetin
L-form	=	Low molecular weight
LACS	=	Long-chain acyl CoA synthetases
LC-MS/MS	=	Liquid chromatography-tandem mass spectrometry
LPA	=	Lysophosphatidic acid
LPAAT	=	Lysophosphatidic acid acyltransferase
MaCoA	=	Malonyl-coenzyme A
MAT	=	Malonyltransferase

LIST OF ABBREVIATIONS (CONTINUED)

MS	=	Murashige and Skoog
MSO	=	MS-zero
MUFA	=	Monounsaturated fatty acid
NAA	=	1-Naphthaleneacetic acid
NBT	=	Nitro blue tetrazolium chloride
PGRs	=	Plant growth regulators
PUFA	=	Polyunsaturated fatty acid
SDS-PAGE	=	Sodium dodecyl sulfate-polyacrylamide gel electrophoresis
SEM	=	Scanning electron microscope
SFA	=	Saturated fatty acid
SPA	=	Stigmatic peroxidase activity
TAG	=	Triacylglycerol
TBA	=	Tert-butyl alcohol series
TBS	=	Tris-buffered saline
TIBA	=	2, 3, 5-Triiodobenzoic acid
TLC	=	Thin-later chromatography
TTBS	=	Tris-buffered saline plus with tween 20
TTC	=	Triphenyl tetrazolium chloride
tTCL	=	Transverse thin cell layer
UNE-EN 14214	=	Automotive fuels-Fatty acid methyl esters (FAME) for diesel engines-Requirements and test methods

CHAPTER 1
INTRODUCTION

1.1 Introduction

As continuous rising of energy demand and getting extinct of petroleum fuels, biodiesel becomes more attractive. It outweighs the traditional fossil fuel by both sustainability and better gas emission profiles (Demirbas, 2003). Approximately 95% biodiesel are produced from edible oil feedstock such as *Glycine max*, *Brassica napus*, *Elaeis guineensis* and *Helianthus annuus* (Ramos et al., 2009; Mazumdar et al., 2012), which can cause the food supply reduction and raise the cost of biodiesel (Wang et al., 2006). Accordingly, physic nut (*Jatropha curcas* L.) is promising for an alternative source of renewable biodiesel due to its inedible oil and fatty acid composition that is analogous to that of fossil fuel. The oil was composed of high monounsaturated fatty acid (MUFA) especially oleic acid, which made the biodiesel match to an acceptable range specified by European and American standard (Akbar et al., 2009; Mazumdar et al., 2012). Despite those advantages, using physic nut as a biodiesel source can lead to a risky business due to a lack of varieties with high oil content and a low productivity of fruit and seed (Akbar et al., 2009; Wu et al., 2011). Thus, much understanding on fruit and seed production and lipid profiles is necessary – to fulfill the biological gaps and improve oil productivity. This is also useful for estimating the feasibility of this plant for a commercially biodiesel production.

For increasing a genetic variability of desired traits and homozygous genotypes essentially for breeding program, haploid and dihaploid production may require for physic nut (Currais et al., 2012). Appropriate stage of microspore and embryo sac was one of the most critical parameters for the success of the haploid culture and this varied among the species (Lauxen et al., 2003; Malik et al., 2007; Chen et al., 2010). For this reason, sequential events of male and female gametophyte development relating to floral features are prioritized information providing bud selection at accurately developmental stage required for such culture. In order to

heighten the fruit and seed fecundity, both pollen and stigma at high capability period for pollination set have been required (Stone et al., 1995; Hedhly et al., 2003). Therefore, the study on longevity of pollen and stigma fertility, which is now scarce, is also demanded for this species. It has been evidently examined that pollination method could improve oil content and fatty acid composition of *Prunus amygdalus* (Kodad and Socias i Company, 2008) and *Brassica napus* (Hua et al., 2012). However, there is no available report about an effect of pollination methods on oil features of physic nut grew locally in Thailand. Thus, association between pollination route and seed lipid profiles is needed for this plant – for applying the best pollination which gives the best productivity in the plantation. Moreover, lipid accumulation could successfully be induced via plant tissue culture technique in many plant species such as *Lesquerella fendleri* (Kharenko et al., 2011), *Boerhaavia paniculata* (Souza et al., 2014) and *Capparis spinosa* (Yin et al., 2014). Hence, using in vitro culture materials such as callus and cell suspension for a source of biodiesel would be optional for a large-scale production of physic nut. Furthermore, this in vitro system could be benefit for characterizing the mechanisms related to oil accumulation (Kharenko et al., 2011). However, the pervious experiments on physic nut exhibited that the oil obtained from somatic embryos was not suitable for biodiesel production due to high accumulation of saturated fatty acid (Ismidianty and Esyanti, 2010). Plant growth regulators (PGRs) could influence the variation of lipid compositions in plant materials (Sauerwein et al., 1992). 2, 4-dichlorophenoxyacetic acid (2, 4-D) and kinetin (KN), for example, have been mentioned influencing on features of lipid accumulation in *Glycine max* (Liu et al., 1995) and *Carthamus tinctorius* (Ullah and Bano, 2011), respectively.

Consequently, this work aims to determine (i) the development and fertility of male and female gametophytes, (ii) the effects of pollination methods on fruit development and oil accumulation in seed and (iii) the features of oil reserved in cell suspension culture of physic nut.

1.2 Literature review

1.2.1 The background of *J. curcas* L.

A. Botanical characteristics

Physic nut is classified into the Euphorbiaceae family (Divakara et al., 2009; Moore et al., 2017) (Figure 1). Though its native distribution is the tropical America, the species can now be found in the regions of Africa and Asia (Figure 2) (Silitonga et al., 2013). This species is a small perennial tree or large shrub (Figure 3A) and can live for up to 50 years (Achten et al., 2008). It is a monoecious plant and produces both female and male flowers in the same cymose inflorescence (Kumar and Sharma, 2008; Rao et al., 2008) (Figure 3B), exhibiting male to female ratio at 105.73: 14.4 (Pranesh et al., 2010). This ratio was very low and indicated the low fruit production. The anthesis times of male and female flower varied as respectively occurring between 05.30 - 06.30 a. m. for both male and female flower by Raju and Ezradanam (2002) but during 06.00 - 07.00 and 07.00 - 08.00 a. m. by the report of Kaur et al. (2011). The stigma was receptive after the flowers blooming and remained for three days, while the male flower exhibited the relatively high pollen viability at 9 hours after flowering and could maintain about two days (Divakara et al., 2009). The pollen tube entered the ovary within about 8 hours after pollination (Abdelgadir et al., 2012). The pollinated pistils took over a two-month to become mature fruit (Figure 3C). The previous study showed that this species could produce fruit via three reproductive modes; cross-pollination, self-pollination and apomixis which gave 93.2, 72.2 and 36.2% fruit set, respectively (Kaur et al., 2011). *Jatropha* seed was albuminous which endosperm acts as a main source of nutrient storages (Reale et al., 2012). At maturity, the outer layer of seed coat is black and hardened (Figure 3D, arrowhead), while the inner layer appear as a shrunken layer like tissue attached to the thick endosperm (Figure 3D, arrow). The existence of apomixis (asexual reproduction) possibly results in high degrees of homozygosity, thus lead to the lack of high oil yielding varieties for this species (Ambrosi et al., 2010).

Kingdom: Plantae

Division: Magnoliophyta (Flowering plants)

Class: Magnoliopsida (Dicotyledens)

Order: Euphorbiales

Family: Euphorbiaceae

Genus: *Jatropha*

Species: *Jatropha curcas* L.

Figure 1 Classification of physic nut (*J. curcas*)
(Source: Moore et al., 2017)

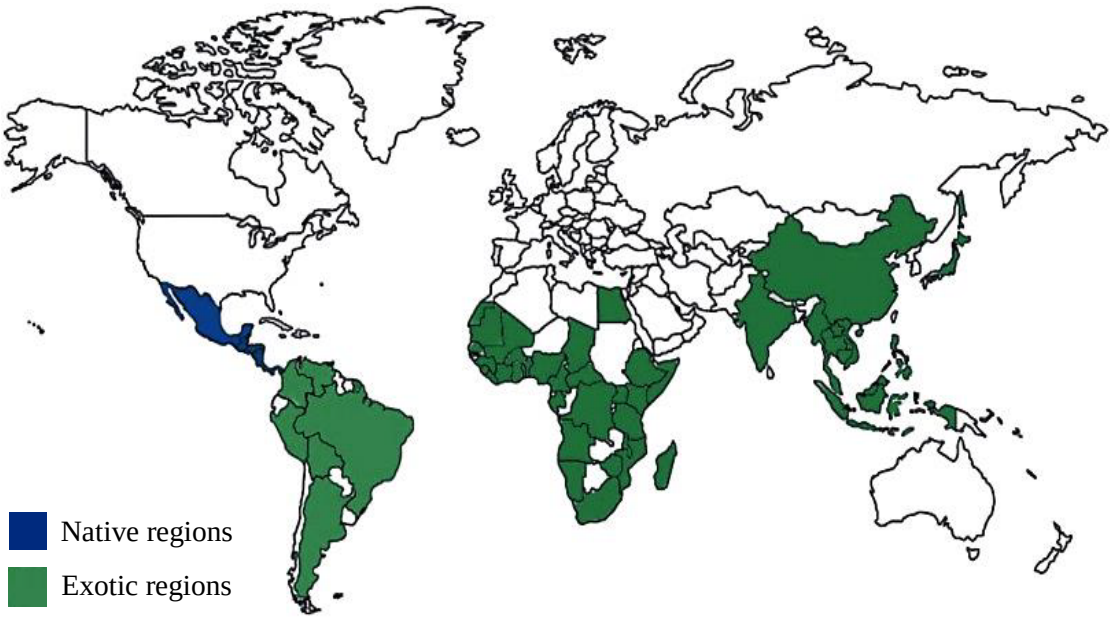

Figure 2 Distribution of physic nut (*J. curcas*)
(Source: Silitonga et al., 2013)

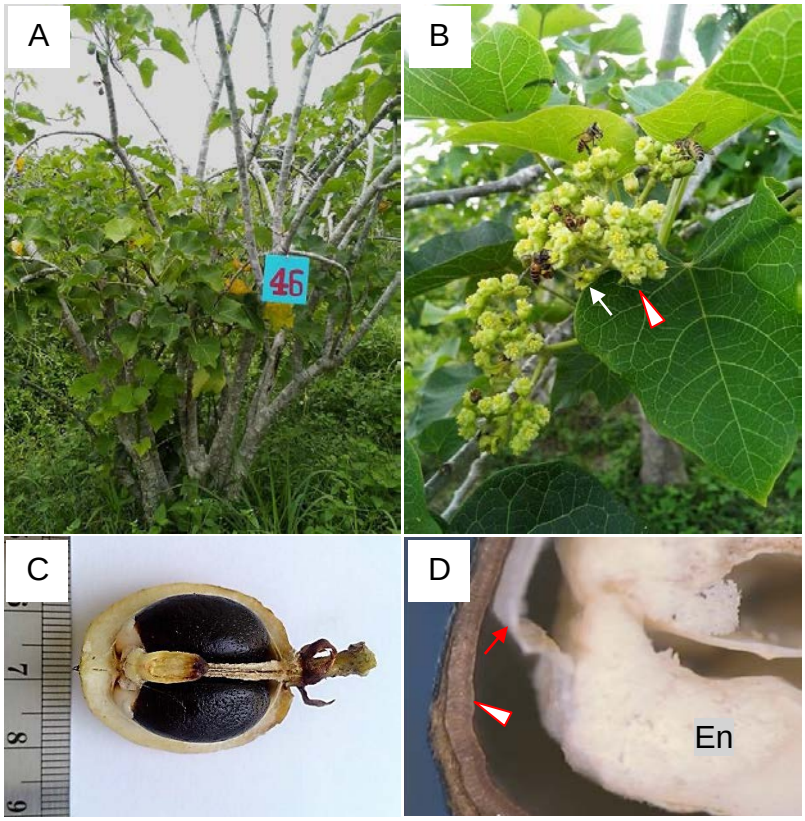

Figure 3 Physic nut characteristics

(**A**) Large shrub physic nut; (**B**) A cymose inflorescence with female (arrow) and male flowers (arrowhead); (**C**) Mature fruit with seeds; (**D**) Dissected seed representing the hardened outer layer (arrowhead) and the shrunken layer like tissue (arrow) attached to the endosperm (En)

(Source for D: Reale et al., 2012)

B. Breeding studies

Carvalho et al. (2008) revealed that chromosomes of physic nut are very small sizes and have a diploid state of 2n = 2x = 22 (a genome size of 416 Mbp and 2C = 0.85 pg). For genetic improvement, gene expressions for fatty acid and lipid biosynthesis genes in developing endosperm of this plant have been studied. From *c*DNA library of developing endosperm, sixty eight genes that encode enzymes, proteins or their subunits involved in fatty acid and lipid biosynthesis were recognized. It was established that the majority of fatty acid and lipid biosynthesis genes expressed in consistent with the development of oil bodies and endosperm (Gu

et al., 2012). After examination at gene, transcript and protein levels, it appeared that oleosins were the major component protein of *J. curcas* oil body. Three putative oleosins, *JcOle1, JcOle2, JcOle3*, have been identified, suggesting that *JcOle3* could potentially be used as a co-dominant marker in phylogenetic and *Jatropha* breeding studies, especially for qualitative/quantitative seed oil improvement (Popluechai et al., 2011). Notably, some experts have tried to make *Jatropha* desired traits by using breeding technique combined with genetic engineering such as intra-specific hybridization, gene transfer through inter-specific hybridization (Divakara et al., 2009). To increase genetic diversity and add new alleles, inter-specific cross pollination between *J. curcas* and other *Jatropha* species was reported (Parthiban et al., 2009). In addition, new hybrids with higher yield potential and resistance to diseases have been generated, showing that the cross between *J. curcas* and *J. integerrima* produced successful hybrids with more seed production, while the other crosses failed to generate seeds due to an appearance of cross-ability obstacles (Parthiban et al., 2009).

C. Advantages

Physic nut is multiple uses and considerable potential. Its reserved TAG exhibited good physicochemical properties; hence, become one promising alternative source for biodiesel production and several industrial applications such as alkyd resin, shoe polish and varnishes (Akbar et al., 2009). Especially, the *Jatropha* oil showed the satisfiable engine performance after tested in Thailand (Takeda, 1982) and was used as an engine fuel during World War II (Kumar and Sharma, 2008). Ong et al. (2013) displayed that properties of biodiesel made from high oleic (44.5%) or MUFA (45.2%) *Jatropha* oil (Table 1) was similar to the petro diesel and matched to the specified range imposed by both American (ASTMD 6751) and European (EN 14214) standard (Table 2). More interesting, oleic acid accumulated in physic nut (44.7%) was higher than those of *Elaeis guineensis* (39.2%), *Helianthus annuus* (21.21%) and *Glycine max* (23.4%) (Akbar et al., 2009). In a view of agricultural practice, this plant could be grown in an area with extreme climates and soil conditions such as drought, soil salinity and water logging (Staubmann et al., 1999). It

can also be used to control erosion and reclaim land. Moreover, since this oil is inedible and without competition with food sector, it became less expensive and could reduce the biodiesel production cost as well as it would arouse rustic economic development (Akbar et al., 2009). Correspondingly, an ambitious plan to enhance *Jatropha* plantation has been made in several Asian countries particularly Indonesia, India and China (Cai et al., 2011).

Table 1 Fatty acid contents of oil obtained from Indonesian variety of physic nut

Fatty acid types	**Composition (%)**
Lauric acid (C12:0)	0.1
Myristic acid (C14:0)	0.1
Palmitic acid (C16:0)	13.0
Palmitoleic acid (C16:1)	0.7
Stearic acid (C18:0)	5.8
Oleic acid (C18:1)	44.5
Linoleic acid (C18:2)	35.4
Linolenic acid (C18:3)	0.3
Arachidic acid (C20:0)	0.2
SFA	19.1
MUFA	45.2
PUFA	35.7

MUFA, monounsaturated fatty acid; PUFA, polyunsaturated fatty acid; SFA, saturated fatty acid

(Source: Ong et al., 2013)

Table 2 Properties of biodiesel made from high oleic acid *Jatropha* oil

Properties	Physic nut biodiesel	Petro diesel	ASTM D6751[a]	EN 14214[b]
Kinematic viscosity at 40 °C (mm^2/s)	3.91	2.91	1.9 - 6.0	3.5 - 5.0
Density at 15 °C (kg/m^3)	838.8	839.0	880	860-900
Flash point (°C)	161.5	71.5	100 - 170	>120
Pour point (°C)	2.0	1.0	-15 to -16	–
Cloud point (°C)	3.0	2.0	-3 to -12	–
Cloud filter plugging point (°C)	0.0	-8	19	+5 (max)
Calorific value (MJ/kg)	40.427	45.825	–	35
Acid value (mg KOH per g)	0.24	0.17	0.5 (max)	0.5 (max)
Iodine value (g I_2/100 g)	105	–	–	120 (max)
Sulfate ash content (% w/w)	0.006	0.02	0.02	0.02
Oxidation stability 110 °C	9.40 h	23.7 h	3 (min)	6 (min)
Cetane number	58.2	49.7	47 (min)	51 (min)

– , not specified (Adapted from: Ong et al., 2013)

[a] American standard

[b] European standard

1.2.2 Gametophyte developments and events after fertilization

Male gametophyte or pollen is important to transfer a male gamete (sperm cells) to a female gametophyte (embryo sac) – to produce the next descendants. Typically, the pollen develops from the pollen mother cell (PMC) located in anther locule which is surrounded by anther walls consisting of epidermis, endothecium, middle layer and tapetum (Ma et al., 2008; Kawashima and Berger, 2014) (Figure 4A). The PMC enters a sporogenesis process in which the meiosis takes place to produce four microspores (tetrad microspores) (Figure 4B). The adherent tetrad is released to free microspores which afterwards undergo gametogenesis and generate the mature pollen (bicellular) with vegetative and generative cells. Around 70% of flowering plants liberated pollen at the bicellular stage, but for some species such as *Liriodendron tulipifera* produced tricellular pollen with vegetative nucleus

and two sperm cells before pollen tube germination (Lora et al., 2009). Pollen at high fertility is demanded for the pollination process to ensure fruit and seed fecundity. Cytochemical staining including fluorochromatic reaction (FCR) and 2, 3, 5-triphenyl tetrazolium chloride (TTC) tests were extensively used to evaluate the pollen viability by checking enzymatic activity and membrane integrity (Lyra et al., 2011; Abdelgadir et al., 2012). Germination assay was also widely employed to define the true ability of pollen to germinate under in vitro conditions (Li et al., 2010).

Pollen development in *J. curcas* has been carried out and found that it was related to anther long (Liu et al., 2007; Currais et al., 2012). However, the correlation between pollen ontogeny and bud diameter, as an alternative choice for more convenience in bud selection, has never been reported. In addition, longevity of the pollen is still limited in this plant.

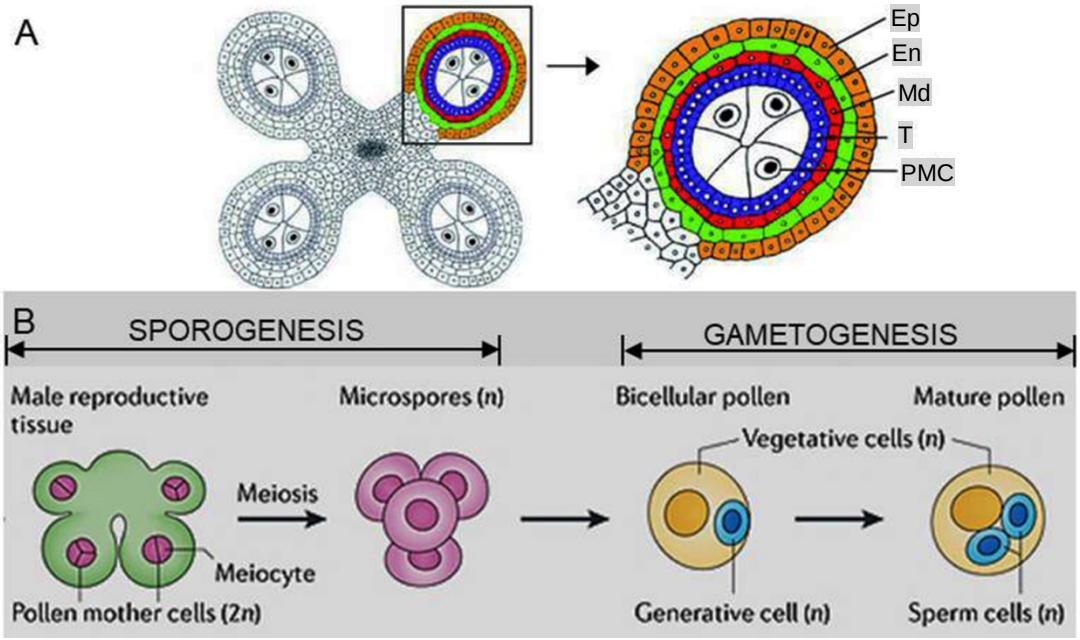

Figure 4 Diagram showing (**A**) anther wall structure and (**B**) pollen development
En, endothecium; Ep, epidermis; Md, middle layer; PMC, pollen mother cell; T, tapetum
(Source: Ma et al., 2008; Kawashima and Berger, 2014)

Meanwhile, the embryo sac originates from a megaspore mother cell (MMC) settled in nucellar region of ovule (Figure 5A). The common type for embryo sac development in several species, for example *Arabidopsis thaliana* (Olsen, 2004) and *Agave tequilana* (González-Gutiérrez et al., 2014) is polygonum (Figure 5B). The MMC gets in the meiosis and produces four megaspores which are arranged in linear pattern. Three of these megaspores at micropylar area are degenerated while the rest one at chalazal region is survived and become a functional megaspore. This megaspore then undergoes three rounds of mitosis and finally creates a mature polygonum embryo sac comprising of one egg cell and two synergids at micropylar, two polar nuclei at the central and three antipodal cells at the chalazal end (Chaudhury et al., 1998). For the success in pollination set and breeding manipulation, receptivity of pistil is also required and this receptive could be qualified by high activity of enzymes such as peroxidase, esterase, alcohol dehydrogenase and acid phosphatase (Gupta et al., 2015). Checking of stigmatic peroxidase activity with hydrogen peroxide was common for pistil receptivity test (Pio et al., 2004; Lankinen et al., 2007). Embryo sac development in physic nut has been previously performed by Soares et al. (2017). Nevertheless, relationship between embryo sac development and bud diameter, as well as the duration of stigma receptivity is still scant for this plant.

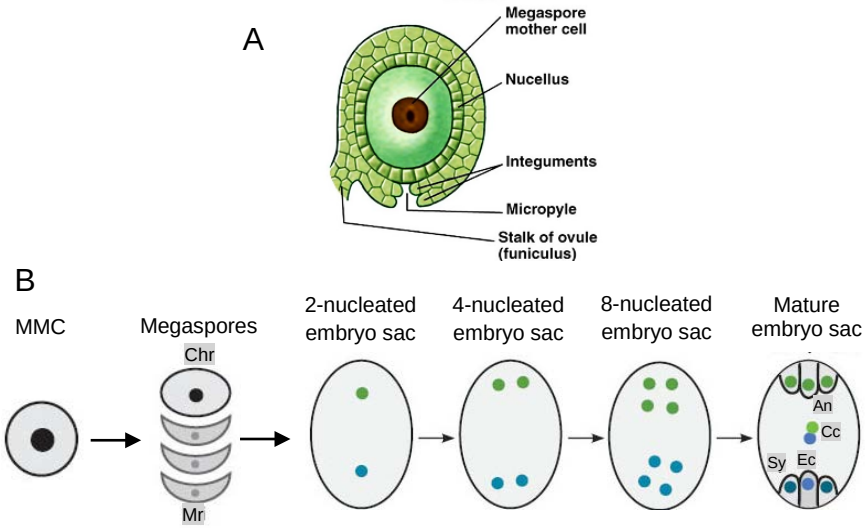

Figure 5 Diagram showing (**A**) ovule and (**B**) polygonum embryo sac development
An, antipodal cells; Cc, central nuclei; Chr, chalazal region; Ec, egg cell; Mr, micropylar region; MMC, megaspore mother cell; Sy, synergid
(Adapted from: Reece et al., 2011; Pires, 2014)

After the deposition of compatible pollen grains on the stigma surface, the germinated pollen tube penetrates towards the micropyle to start double fertilization in which the one sperm cell is fused with egg cell and another with polar nuclei to produce embryo and endosperm, respectively (Chaudhury et al., 1998). In general, the embryo develops through globular, heart, torpedo, cotyledonary and mature embryo (Figure 6A). Three types of endosperm development – the nuclear, cellular and helobial are elucidated for angiosperm (Figure 6B); however, the most common one is the free nuclear type which produces numerous free nuclei at early stage and cellularlized nuclei at later stage (Taiz et al., 2015). The fertilization is essential for the success of seed development and guarantees the survival of embryo and seedling by provided the nutrient-supplied endosperm. However, some flowering plants such as *Citrus* and *Hieracium* species can proceed seed development by avoiding the fertilization of egg cell via the process called apomixis (Koltunow, 1993). The formation of the apomictic embryo in the ovule can be through sporophytic or gametophytic pathway. The former refers to the development of embryo from nucellus or the integument (adventitious embryony), while the latter mentions to the embryo that autonomously originates from cells in the embryo sac which is formed without meiotic division (Koltunow et al., 1995). Most apomictic seeds are pseudogamous, which the pollination and fertilization are demanded for polar nuclei to develop into endosperm, but in some plants (like *Taraxacum*) the endosperm autonomously develops from the central cells by lacking fertilization (Vinkenoog and Scott, 2001).

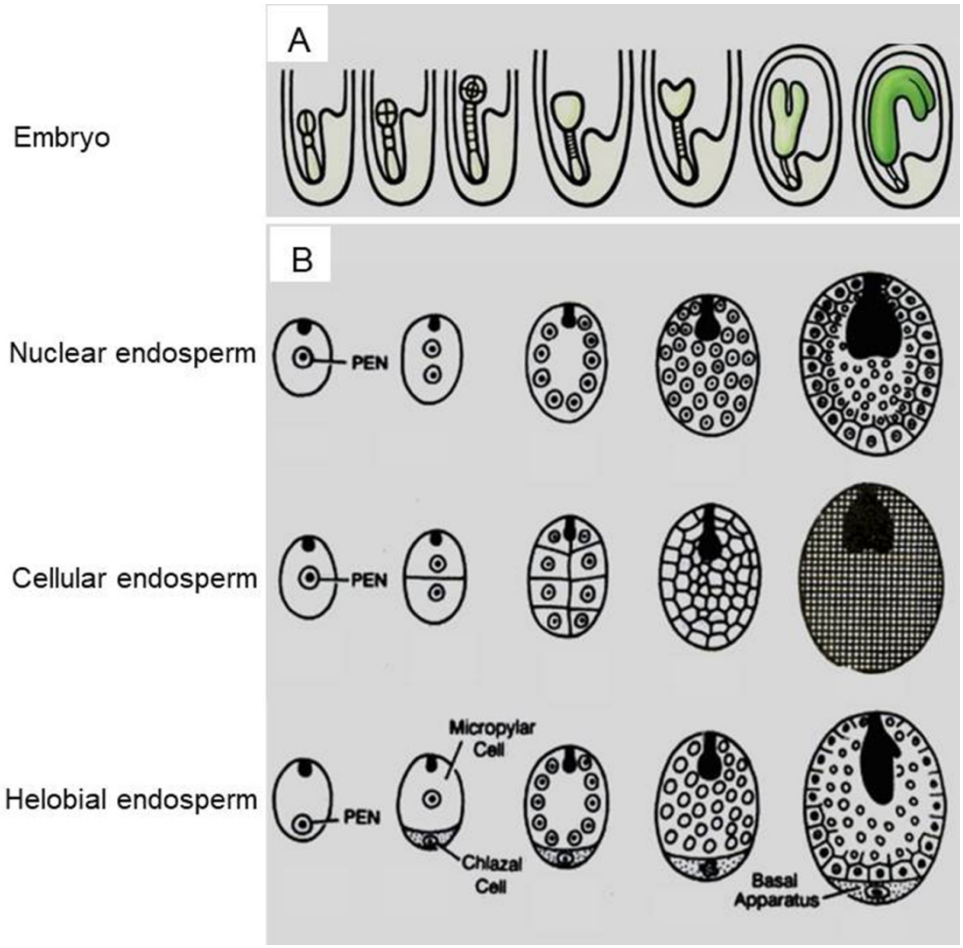

Figure 6 Development of (**A**) embryo and (**B**) endosperm
PEN, primary endosperm nucleus
(Source: Le et al., 2010; Gaur, 2017)

1.2.3 Callus and cell suspension culture

Plant tissue culture is an effective technique for a rapid propagation of the plant materials, production of desirable compounds and biotechnological applications (Thepsamran et al., 2006; Khanpour-Ardestani et al., 2015). Once the plant tissue was cultured on an artificial solid medium under sterile condition, the tissue develops into undifferentiated tissue termed callus. This callus can be divided into various groups based on macroscopic features such as friable and compact callus (no obvious organ regeneration), root, shooty and embryonic callus (organ regeneration capability) (Ikeuchi et al., 2013). Intermediate ratio between auxin and

cytokinin, which stimulates cell cycle reentry, is essential for the callus formation (Skoog and Miller, 1957; Ikeuchi et al., 2013; Schaller et al., 2014). Alternatively, tissue culture can be manipulated using a shaking liquid medium to produce cell suspension comprising of single or aggregated cells (Chawla, 2003). This cell suspension is more benefit than the callus in providing higher propagated competency and homogeneity, thus this culture has widely been applied in secondary metabolite production for fragrances, drugs, flavorings and oil (Figueiredo et al., 1995; Baraki and Kenji, 2001). For example, the highest and more diverse ingredients of volatile oil could be obtained in *Achillea millefolium* cell suspension established in B5+ medium supplemented by a medium-chain triglyceride termed Miglyol 812 (Figueiredo et al., 1995). Cells of *Panax quinquefolium* cultured in a medium combined with 2.5 mg L^{-1} indole-3-butyric acid (IBA) and 0.1 mg L^{-1} KN produced sufficient amount of ginsenoside saponin and higher than that contributed by original explant (Zhong et al., 1996). A production of acteoside, the medicinal compound related to biological activities such as antioxidant and tumor cell battle, was optimized in cell suspension which was cultured in liquid MS medium added with 0.5 mg L^{-1} naphthalene acetic acid (NAA) and 2.0 mg L^{-1} 6-benzyladenine (BA) for *Scrophularia striata* (Khanpour-Ardestani et al., 2015).

For physic nut, callus formation has been achieved for further application on hybrid combinations and mass multiplication (Soomro and Memon, 2007; Mohan et al., 2011). The success in callus induction from such experiments depended on type of explants, hormone and medium compositions. For example, the friable green callus (100% induction) could be obtained from the culture of hypocotyl explants on MS medium containing 0.5 mg L^{-1} 2, 4-D alone as well as in combination with 2% v/v coconut water (Soomro and Memon, 2007). Friable callus (100% induction) could also be induced from hypocotyl segment in semisolid MS medium mixed with 1.5 mg L^{-1} 2, 4-D (Ramos et al., 2013). However, the compact callus (38 - 49% induction) could be observed in MS medium added with 0.5 mg L^{-1} 2, 4-D alone or in combination with 2% v/v coconut water when using leaf as the explants (Soomro and Memon, 2007). Additionally, supplementation of 2, 4-D at high concentration (2.98 mg L^{-1}) along with KN at low concentration (0.95 mg L^{-1}) and vitamin B5 to MS medium allowed hypocotyl explants developing into an embryogenic callus

(Ismidianty and Esyanti, 2010). For Chinese-variety physic nut, supplementation of 1 mg L^{-1} NAA and 0.1 mg L^{-1} KN to the medium placed in dark condition sufficiently induced the callus (90 - 100%) from epicotyl, hypocotyl, petiole and cotyledon. Furthermore, this combination of NAA and KN stimulated the highest growth of callus (Li et al., 2012). Leaf- and petiole-derived calli were successfully induced on the MS medium combined with both 0.5 mg L^{-1} BA and 1.0 mg L^{-1} 2, 4- D in this physic nut (Ramrao et al., 2016). Combinations of BA (1, 2 and 3 mg L^{-1}) and IBA (0.1, 0.25 and 0.5 mg L^{-1}) could also stimulate the compact callus induction (100%) from embryo culture of this species. However, the combination of 3 mg L^{-1} BA and 0.25 mg L^{-1} IBA promoted the highest growth of callus (3.45 mg) (Kaewpoo, 2010). Thus, from all above details, it seems that auxin and cytokinin are essential for callus induction in physic nut. This relates to the role of auxin on allowing the cell to reach G1/S transition and the role of KN on regulation kinase complex at G1/S and G2/M transition; hence, promoting mitosis and cell proliferation (Pasternak et al., 2000; Perrot-Rechenmann, 2010; Schaller et al., 2014). Besides the application on propagation, callus in this species was recently established for an evaluation of its feasibility to accumulate oil storage, which revealed the callus cultured in 0.5 mg L^{-1} 2, 4-D alone could reserve 18% oil content. However, the lipid composition of the oil was different from the seed and carried the highest palmitic acid (55.4%) (Costa et al., 2015). This indicates the improvement of the fatty acid composition is further required for the callus of this species.

The friable green or yellow callus induced from diverse *Jatropha* explants has been employed for cell suspension establishment in liquid media supplemented with several PGRs (Ismidianty and Esyanti, 2010; Siang et al., 2012). The friable callus was inoculated into liquid MS medium comprising of 0.5 mg L^{-1} 2, 4-D in order to induce cell suspension in Pakistan-variety physic nut (Soomro and Memon, 2007). Under that condition, the cell suspension gave high fresh weight (~5 g per 25 ml culture), dry weight (~0.33 g per 25 ml culture) and total chlorophyll content (50.7 to 75.2 µg per gram fresh weight). This cell suspension was classified into green culture type because its chlorophyll content was within 30 to 2, 000 µg per g fresh weight imposed by Widholm (1992) – which might attribute to the role of 2, 4 -D on promoting chlorophyll accumulation as previously suggested in *Chlorella*

vulgaris and *Spirulina platensis* cells (Saygideger and Okkay, 2008). For the future investigation on innovative compounds for medicinal purposes or industrial applications, method for a long-term maintenance of cell suspension was established for Costa Rican *J. curcas* (Ramos et al., 2013). The highest cell growth (fresh weight, 194.9 g L^{-1}; dry weight, 6.52 g L^{-1}) was obtained after culturing 1 g of 35-day-old friable callus in 50 ml liquid MS media added with 1.5 mg L^{-1} 2, 4-D and 30 g L^{-1} sucrose. For the optimized maintenance, the cell suspension was subcultured at 20-day intervals. Added to these, by initiating from hypocotyl-derived callus, embryogenic cell suspension was successfully developed in MS medium added with vitamin B5, 1.49 mg L^{-1} 2, 4-D, 0.95 mg L^{-1} KN and 20 g L^{-1} sucrose for this species (Ismidianty and Esyanti, 2010). Characterizations of lipid storage in *Jatropha* materials cultured in liquid system have been provided by some researchers (Ismidianty and Esyanti; 2010; Correa and Atehortua, 2012). For instance, the *Jatropha* somatic embryo developed in ½ macro element MS media contained approximately 30% total oil content and 82% saturated fatty acids (palmitic and stearic acid) (Ismidianty and Esyanti, 2010). Thus, it seems that a further modification is needed for reducing the saturated fatty acids as enhancing the oleic acid in such cell suspension. Contrarily, it revealed that cell suspensions cultured in Lloyd and McCown modified liquid medium provided high oleic acid for some varieties of *Jatropha* (Correa and Atehortua, 2012). These authors, however, suggested that the main factor affecting high accumulation of oleic acid in such cell suspension might be *Jatropha* variety rather than the medium composition or culture conditions.

1.2.4 Factors affecting lipid profiles in plant species

A. Plant growth regulators (PGRs)

By foliar spraying to the plant cultivated in an orchard or a greenhouse, various PGRs were effective to improve the lipid content and compositions of many crop species. In the research farm, the spraying of indole acetic acid (IAA) on the 60-day-old plants could heighten the oil productivity (both per leaf and per plant) of *Cymbopogon martinii* and *C. winterianus* (Farooqi et al., 2005). More recently, 50

ppm IAA could increase up to 60% oil content in *C. martinii* seedling in comparison to the control plant (Khan et al., 2015). However, 2, 4-D caused a reduction of oil content when applied to flax (*Linum usitatissimum*) (Dunham, 1951). The KN enhanced the seed oil content of *L. usitatissimum* (Faizanullah et al., 2010) and *Carthamus tinctorius* (Ullah and Bano, 2011). The KN could also induce more accumulation of oleic acid but reduce the level of linoleic acid in *C. tinctorius* seed (Ullah and Bano, 2011). Moreover, the KN application could produce more biodiesel yield after transesterification of *L. usitatissimum* (Faizanullah et al., 2010) and *C. tinctorius* seed oil (Ullah and Bano, 2011). In *Brassica napus*, however, the KN did not significantly increase the oil content comparing with the KN-free treatment (Sharma et al., 2017). Gibberellic acid (GA_3) and salicylic acid (SA) could promote more accumulation of oil in *C. tinctorius* (Baydar, 2000) and *B. napus* (Ullah et al., 2012), respectively. In the latter case, oleic acid content was also increased under drought condition.

Several PGRs have also been accounted for the alteration of oil amount and fatty acid contents in in vitro culture plant materials. The supplementation of 4 mg L^{-1} 2, 4-D could increase linolenic acid (C18:3) as decrease oleic acid (C18:1) and linoleic acid (C18:2) content in cotyledons of soybean (*Glycine max*) embryo cultured in MSO (MS-zero) medium (Liu et al., 1995). The combination of 2, 4-D and BA could arise the linoleic acid and linolenic acid while reduce the oleic and palmitic acid in *Simmondsia chinensis* callus (Aly et al., 2008). However, the combination of 2, 4-D and 6-benzylaminopurine (BAP) decreased the oil content in the callus of *S. chinensis*. Fortunately, high accumulation of oil could be observed in callus of the same species cultured on the medium containing NAA combined with BAP (Taha, 2014). Application of KN could induce oil-like drops in cell suspension of *Coffea arabica* (Townsley, 1974).

B. Pollination method

The influence of reproductive mode on the features of storage oil seemed to fluctuate among species considered. The significant increase in oil content could be obtained after open-pollination of *Zea mays* (Letchworth and Lambert, 1998). Similarly, the open-pollinated seeds of *Sesamum indicum* contained superior oil capacity than the seeds derived from other pollination routes (Blal et al., 2013). In addition, this pollination method also produced 9.76-fold higher oil yielding in *Brassica campestris* (Mishra et al., 2011). It was proposed that the pollinator and pollen resources, available during open-pollination, may play role in improving fruit and seed composition (Abdelal et al., 1983; Mishra et al., 2011). In *Prunus amygdalus*, oil content and fatty acid compositions also varied among pollination types (Kodad and Socias i Company, 2008). A cross-pollination gave higher oil content but lower oleic acid percentage than self-treatment. Meanwhile, the open-pollination resulted in the highest linoleic acid content. In *B. napus*, however, mother plant genotype rather than the pollination method fundamentally controlled the lipid features (Hua et al., 2012).

1.2.5 Fatty acid synthesis and the effect of fatty acid on biodiesel properties

A. Fatty acid synthesis

The storage lipid of seed is synthesized by the cooperation of plastid and endoplasmic reticulum (ER). The fatty acids are firstly synthesized in plastid and then transported to ER where the TAG assembly is taken place (Baud and Lepiniec, 2010). Once TAG assembly is completed, the TAG is reserved in the special organelle called oil body which is composed of a single layer of phospholipid embedded by integral proteins such as oleosin, caleosin and steroleosin (Tzen, 2012).

The fatty acid synthesis starts by a conversion of the acetyl-CoA (AcCoA) to malonyl-CoA (MaCoA) by activity of acetyl-CoA carboxylase (ACC) (Figure 7) (Baud and Lepiniec, 2010). The malonyl group is then moved from CoA to

acyl carrier protein (ACP) by the action of MaCoA: acyl carrier protein S-malonyltransferase (MAT) (Figure 7). By using AcCoA as a starting unit and malonyl-ACP as the elongator, 4:0-ACP is stepwise elongated to 18:0-ACP by ketoacetyl-ACP synthases (KAS). After acyl group removing, the free fatty acids are activated to CoA ester by long-chain acyl CoA synthetases (LACS) and exported to ER. Even though 18:0-ACP is dominantly produced from this machinery, the fatty acids exported to ER can be diverse depended on plant species. The plant species that accumulate fatty acid whose carbon chain is shorter than 18 evolved the acyl-ACP thioesterases in order to prematurely hydrolyze the developing acylthioesters and then result in the export of capric acid (C10:0), laurate (C12:0) and palmitic acid (C16:0) to ER. For MUFA like oleic acid (C18:1), its double bond is inserted by the plastidial stearoyl-ACP desaturase at the Δ^9 position before transferred to ER. The formation of polyunsaturated fatty acid (PUFA, such as linoleic acid and linolenic acid), however, is taken place in the ER. The oleoyl-CoA is jointed into membrane phosphatidylcholine (PC) and desaturased to 18:2-PC by the action of omega-6 desaturase (FAD2) to form linoleic acid (C18:2). Afterwards, the produced 18:2-PC can further be desaturated to 18:3-PC by the omega-3 desaturase (FAD3) and results in the linolenic acid (C18:3).

TAG assembly happens in specialized sub-domains of ER by using acyl-CoA for the sequential acylation of G3P (Figure 7) (Shockey et al., 2006; Baud and Lepiniec, 2010). Glycerol-3-phosphate acyltransferase (GPAT) catalyzes the first acylation and produces lysophosphatidic acid (LPA) which is then being a substrate for the second acylation to produce phosphatidic acid by activity of lysophosphatidic acid acyltransferase (LPAAT). This phosphatidic acid is afterwards changed to diacylglycerol (DAG) by phosphatidic acid phosphatase (PAP). The third fatty acid is moved to the DAG by enzyme named diacylglycerol acyltransferase (DGAT) to produced triacylglycerol (TAG) (Cao and Huang, 1986; Baud and Lepiniec, 2010).

The synthesized TAG is stored in the spherical oil body whose diameter ranged from 0.2 to 2.5 μm (Tzen, 2012). The oil body is composed of the TAG matrix encompassed by a layer of phospholipid where buried some unique proteins named oleosin, caleosin and steroleosin (Figure 8A) (Huang, 1992; Tzen, 2012). Oleosin, the relative small protein of 15 - 20 kDa, has been known to stabilize

the seed oil body, thus preventing coalescence of oil bodies during seed desiccation and maintaining their discrete and small spherical shape (Tzen and Huang, 1992). At least two isoforms of oleosin, the high molecular weight (H-form) and the low molecular weight (L-form) can be observed in several species of angiosperm, for example, *Zea may*, *Glycine max* and *Brassica napus* (Tzen et al., 1990). The caleosin (~27 kDa) served as a stabilizer of oil body and also related to the mobilization of the organelle (Wu et al., 1998; Jiang et al., 2009). The steroleosin (around 39 kDa), possessing sterol-regulatory dehydrogenase domain, may play a role in regulating the caleosin and activating of sterol signal transduction involving oil body mobilization in germinating seed (Lin et al., 2002; Tzen, 2012). Remarkably, a model describing targeting of oil body proteins to maturing oil body has been established (Figure 8B). In that model, the oleosin and caleosin seemed to unite directly to maturing oil bodies, while steroleosin might firstly be recognized by signal recognition particle (SRP) and guided to incorporate into the phospholipid bilayer of ER membrane before the development of TAG between ER membranes (Tzen, 2012).

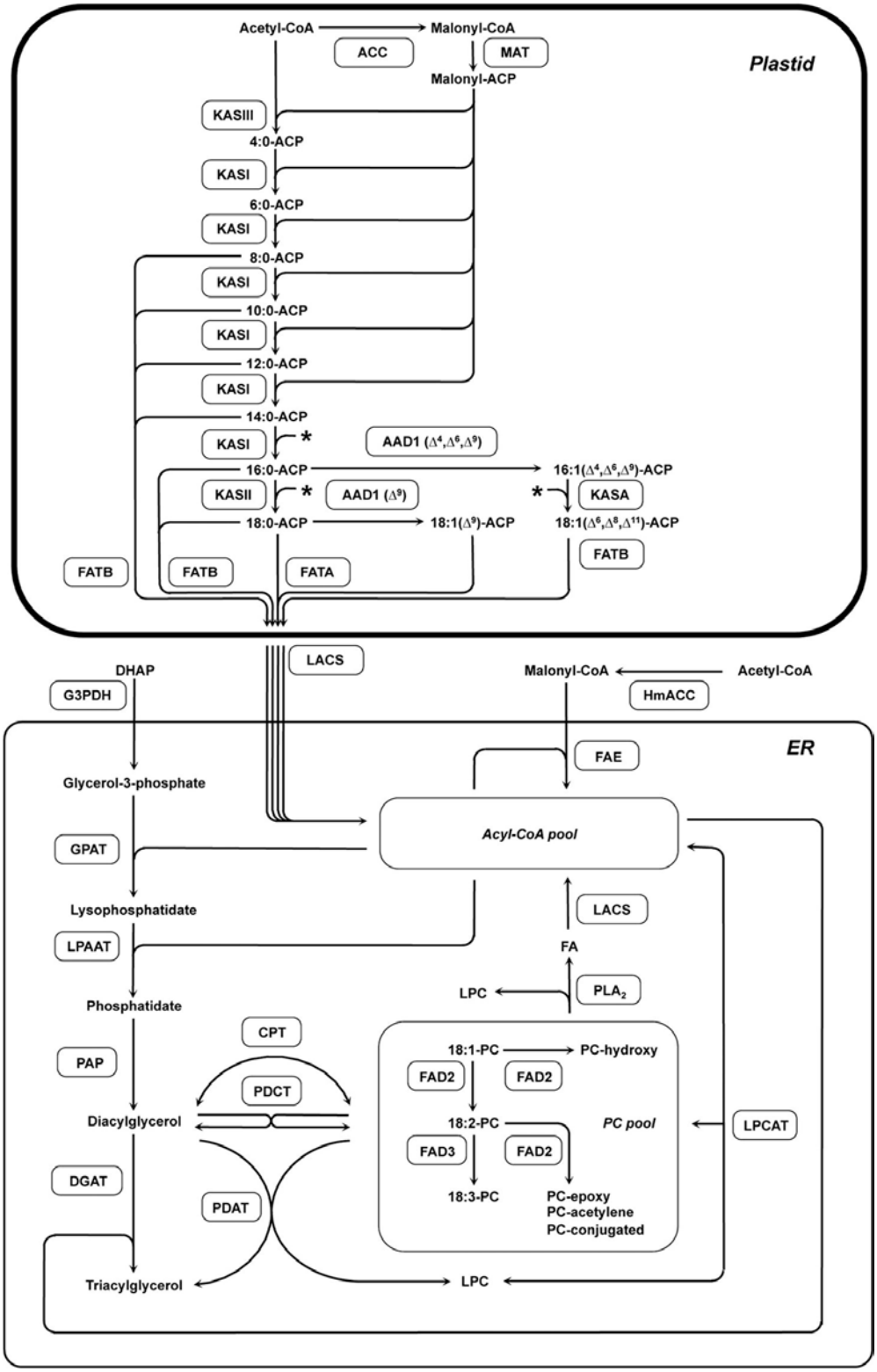

Figure 7 Scheme of pathways involved fatty acid synthesis and TAG assembly in oilseeds

(Source: Baud and Lepiniec, 2010)

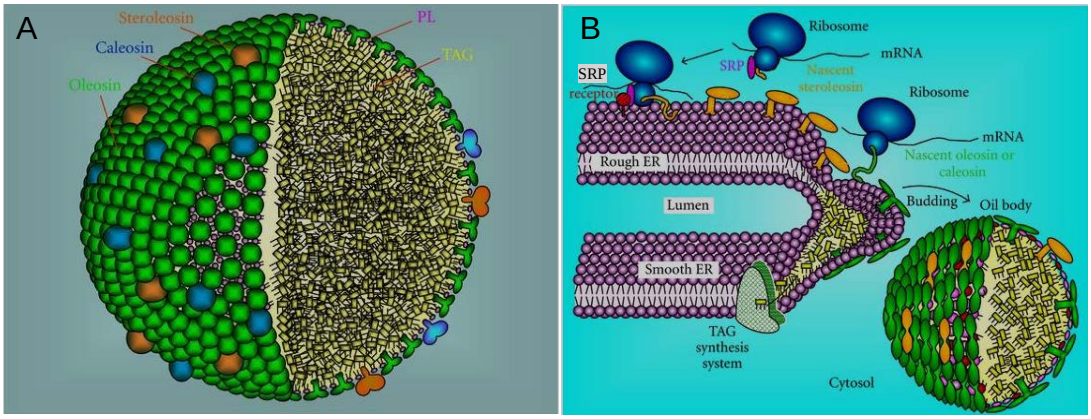

Figure 8 Structure of oil body

(**A**) TAG matrix enclosed by phospholipid monolayer which is rooted by protein oleosin, caleosin and steroleosin; (**B**) Targeting of oil body proteins to maturing oil body. PL, phospholipids; SRP, signal recognition particle; TAG, triacylglycerol

(Source: Tzen, 2012)

B. Effect of fatty acid composition of oil on some crucial parameters of biodiesel

Biodiesel is generally produced from an organic reaction namely transesterification. In this reaction, one mole of triglyceride reacts to three moles of alcohols to form a mole of glycerol and three moles of fatty acid alkyl esters (Schuchardt et al., 1998; Verma et al., 2015). After this transesterification, fatty acid compositions of oil are not modified and they still play a significant role in determining some crucial parameters of biodiesel, especially, cetane number, iodine value, cold filter plugging point and oxidation stability (Ramos et al., 2009).

Generally, the fatty acids can be categorized into three major groups – the saturated fatty acid (SFA, number of carbon chain length: number of unsaturated bonds = Cn: 0), monounsaturated fatty acid (MUFA, Cn: 1) and polyunsaturated fatty acid (PUFA, Cn: 2, 3). The oil containing high SFA (such as stearic and palmitic acid) and long carbon chain fatty acid (like behenic and lignoceric acid) provided high cetane number biodiesel. The adequate cetane number is required for the better

combustion properties of engine and reducing white smoke formation; accordingly, its value should not be lower than 51 by UNE-EN 14214 standard (Meher et al., 2006; Ramos et al., 2009). In addition, biodiesels from high SFA content have low iodine value and then prevents the glyceride polymerization caused by the heating of unsaturated fatty acid (Mittelbach, 1996). Unfortunately, the high SFA, especially the stearic and palmitic acid, could give poor cool filter plugging point when the biodiesel experiences to the cool temperature, resulting in the wax settling and plugging of engine filters (Dunn and Bagby, 1996). High level of unsaturated fatty acid, however, could make the biodiesel worse on iodine value and oxidation stability (Ramos et al., 2009). The iodine value, which is a measure of total unsaturation and is reported in the gram of iodine reacting with a hundred gram of biodiesel sample, is restricted to 120 g I_2 100^{-1} g^{-1} by UNE-EN 14214 due to its effect on lubricating degeneration as mentioned above. While, the oxidation stability, the factor relates to the stability of biodiesel during stretch preservation, is limited at a minimum of six hours by UNE-EN 14214. High proportion of PUFA reduces the biodiesel oxidation stability by the reaction of its double bonds to oxygen, which diminishes the quality of fuel and then the engine efficiency (Pullen and Saeed, 2012). It can be seen that very high saturation and unsaturation level made the biodiesel better on some as worse on other parameters. Accordingly, high monounsaturated oleic acid content, which balanced the degree of saturation and unsaturation in the raw oil provided the global better properties of biodiesel including cetane number, iodine value and filter plugging point (Ramos et al., 2009).

1.3 Objectives

1.3.1 To examine the development and fertility of male and female gametophytes

1.3.2 To determine the effect of pollination methods [open-, cross-, self- and non-pollination (apomixis)] on fruit, embryo and endosperm development and seed oil accumulation

1.3.3 To establish cell suspension and analyze its lipid accumulation

CHAPTER 2
RESEARCH METHODS

This research was composed of three parts (Figure 9); (1) the development and the fertility of male and female gametophytes (Topic 2.1), (2) the effects of pollination methods on fruit development and lipid accumulation in seed (Topic 2.2) and (3) the establishment of cell suspension and its oil accumulation (Topic 2.3). Local *J. curcas* plants grown, on the sandy loam soil, at Trang Agricultural Occupation Promotion and Development Center (TAOPDC), Trang Province were used as materials. All experiments were carried out during 2012 - 2016 at TAOPDC and Prince of Songkla University, Hat Yai, Thailand.

2.1 Development and fertility of male and female gametophytes

2.1.1 General flower characteristics and gametophyte development

Male and female flower buds were randomly collected at 8.00 - 9.00 a.m. These buds were measured and divided into 5 groups (1.0 - 1.5, 1.6 - 2.0, 2.1 - 3.0, 3.1 - 4.0 and ≥ 4.1 mm) based on diameter. For each group, morphological appearances of floral organs were recorded on at least six-sampling buds and were photographed using Olympus SZH 10 stereomicroscope joined to DP-71 digital camera. The samples were then fixed in FAA II (Appendix A) for 48 hours, dehydrated in tert-butyl alcohol series (Appendix A), embedded in Paraplast Plus and cut at 6 µm thickness using a rotary microtome. The sections were stained with hematoxylin and safranin (Appendix A) for histological features and with 0.1% (w/v) aniline blue (Appendix A) for callose wall observation (Ruzin, 1999). In the latter case, the fluorescence images were taken under excitation wavelength at 365 nm using Olympus-BX51 microscope. Pollen surface was determined using a SEM-Quanta scanning electron microscope at 20 kV. Further, ratio of female to male flowers was estimated from 40 inflorescences.

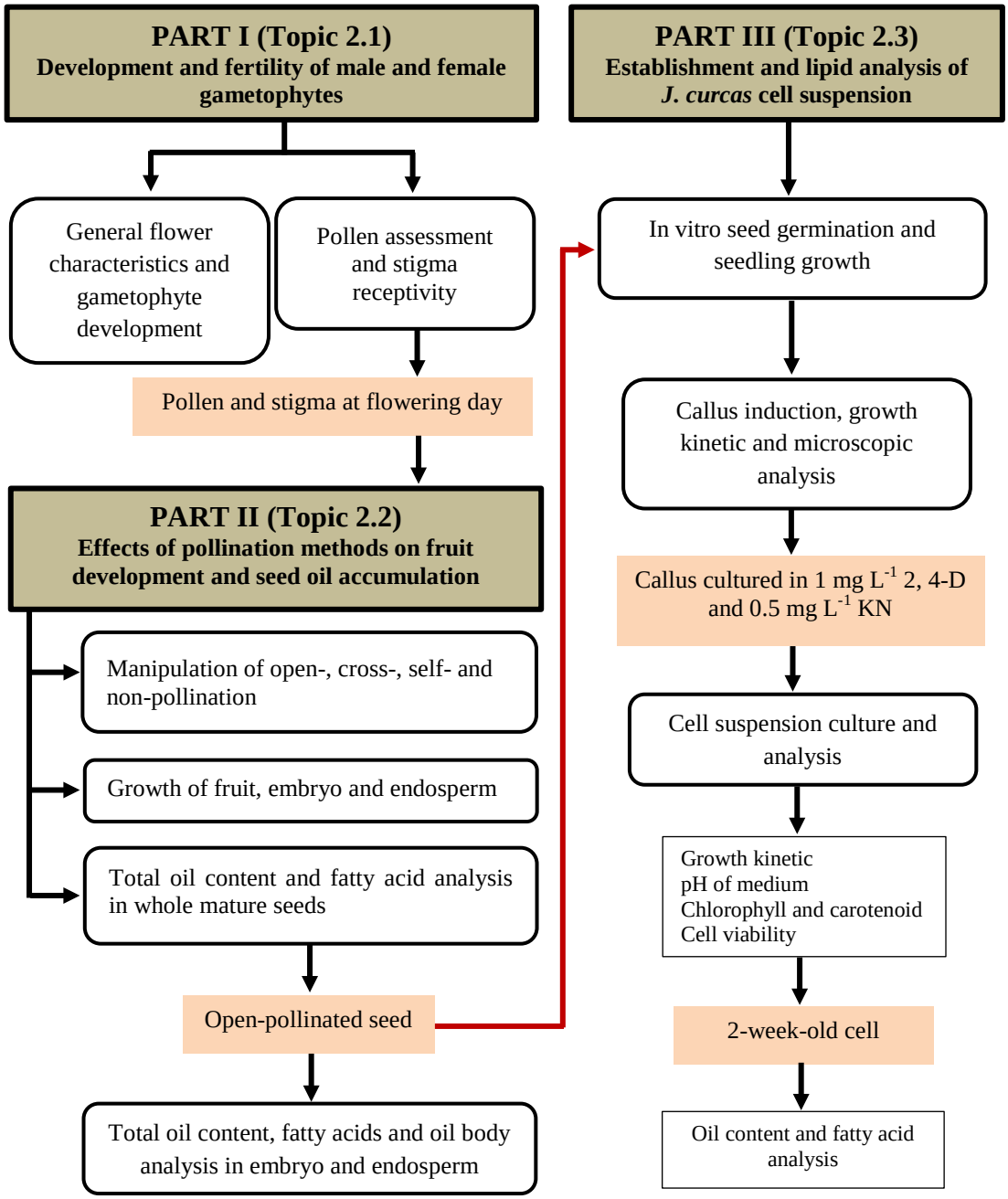

Figure 9 A whole concept of the research

2.1.2 Pollen assessment and stigma receptivity

A. Pollen assessment via FCR, TTC and germination test

The inflorescences with nearly-bloom male flowers were randomly collected, placed in 250-ml beaker filled with 200 ml tap water and maintained at room temperature (25 ± 3 °C) overnight (modified from Abdelgadir et al., 2012). Pollen viability and germination (Appendix B) were performed on pollens collected at 0 (anthesis time, 8.00 a. m.), 4, 8, 12, 24, 48, 72 and 96 hours after flowering (HAF). For fluorochromatic reaction (FCR test), the pollen grains were transferred to the mixture of 15% sucrose and fluorescein diacetate (FDA) solution followed by a 10-minute incubation in humidity chamber. Bright yellow-green pollen grains under the fluorescence microscope, with an excitation wavelength at 489 nm, were scored as viable (Ruzin, 1999). For 2, 3, 5-triphenyl tetrazolium chloride (TTC) test, pollens were stained with 1% TTC solution and kept in darkness for 24 hours, and then washed thrice with distilled water. Red-stained pollen grains were considered viable (Abdelgadir et al., 2010). In vitro germination was performed according to the published protocol (Li et al., 2010). The pollens were released into depression slide filled with 20 µl of Brewbaker and Kwack (BK) liquid medium (Brewbaker and Kwack, 1963) supplemented with 20% sucrose, 2.5% coconut water and 10% polyethylene glycol (PEG 4000) at pH 6.5. The culture media were placed in moist chamber and kept at 25 ± 3 °C in darkness for 14 hours. The pollen grains which tubes greater length than their own diameters were considered germinated. For all experiments, the pollen grains treated by autoclaving at 15 psi at 121 ºC for 20 minutes were simultaneously used as a negative control. Percentages of viability and germination were determined from 5 replicates and calculated using the following equations.

$$\text{Percentage of pollen viability}^1 = \frac{\text{Fluorescent pollens x 100}}{\text{Total number of pollens}}$$

$$\text{Percentage of pollen viability}^2 = \frac{\text{Red-stain pollens x 100}}{\text{Total number of pollens}}$$

$$\text{Percentage of pollen germination} = \frac{\text{Germinated pollens x 100}}{\text{Total number of pollens}}$$

[1] Equation for FCR test

[2] Equation for TTC test

B. Stigma receptivity

The female flowers were covered with paper bags before flowering and the receptivity of stigmata tested by 3% hydrogen peroxide solution was accomplished at 0 (at flowering time, 8.00 a. m.), 1, 2, 3, 4, 5 and 6 days after flowering (DAF). The stigmata having oxygen bubbles within 2 - 3 minutes were considered as receptive (Lankinen et al., 2007). Percentage of the stigma receptivity was calculated using 3 replications, each with 12 stigmata.

2.1.3 Statistical analysis

The percentage of pollen viability and stigma receptivity did not meet the assumption of normality by any transformations. To verify any significant differences of mean, the data were thus submitted to Kruskal-Wallis test at 5% probability level ($P \leq 0.05$) available on portable IBM SPSS statistic version 19. Correlations between pollen viability (FCR test and TTC test) and germination test were also carried out using simple linear regression analysis on the SPSS.

2.2 Effects of pollination methods on fruit development and seed oil accumulation

2.2.1 Manipulation of open-, cross-, self- and non-pollination

Open-pollination was manipulated, with modifications, according to the published method (Yan et al., 2014). Approximately 300 - 500 female flowers (newly blooming) from around 10 sampling inflorescences per tree (10 healthy plants)

were tagged in morning (7 - 9 a.m.) of anthesis day and leaved for free pollination by insects. The date in which the flowers were marked was designated as pollination day. Meanwhile, cross-, self- and non-pollination were done during 8.00 - 12.00 a. m. according to the method reported by Pranesh et al. (2010). Briefly, the entire male flowers were removed before the opening of female flowers in the same inflorescence and then the remaining female flowers were covered with paper bags. In cross-pollination, the viable pollens (pollens collected at flowering time) from different tree were transferred to the responsive stigma (stigma at flowering day), while the viable pollens from other inflorescences in the same individual plant were moved to the receptive stigma in self-pollination. For non-pollination, the emasculated flowers were covered with the paper bags without pollination. The samples were continued covering with the paper bags for 10 days.

2.2.2 Growth of fruit, embryo and endosperm

To determine the development of embryo and endosperm, fruits obtained from open-, cross-, self- and non-pollination were collected every 3 days after pollination (DAP) or days after flowering (DAF) till 48 days (at least 6 fruits/time/pollination type). The samples were prepared using paraffin method and stained according to previously provided method in 2.1.1. In order to observe the presence of lipids in mature embryo and endosperm, the fresh samples were cut into 20 µm thick with cryostat (Leica CM 1860 UV) and stained with Oil Red O (Brown, 1969) (Appendix A). Diameters of fruits, for all pollinations, were measured at 3-day intervals from 24-sampling fruits. For all treatments, percentage of fruit set and number of seeds per fruit were computed against 120 initially labeled female flowers and from 45 fruits, respectively.

2.2.3 Total oil content and fatty acid analysis in whole mature seeds

A. Oil extraction

The collected mature seeds, from all pollination methods, were clean with water, air dried for 2 days at room temperature (water content: 6.80 ± 0.14%) and stored at -20 °C for oil analysis. After dried to a constant weight at 60 °C (2 - 3 days), one gram of seeds (with seed coat) was crushed with mortar and pestle and then extracted with 250 ml *n*-hexane in a Soxhlet extractor for a period of 6 hours (Pescador et al., 2012). After oil extraction, the excess solvent was removed using a rotary evaporator (Heidolph) at 45 °C. The samples were placed in oven overnight, cooled down in desiccator, and then the oil was weighed and calculated employing the following equation. Three replicates were performed for each treatment. The oil was collected at room temperature until use.

$$\text{Percentage of oil content} = \frac{\text{Weight of oil (g) x 100}}{\text{Weight of crushed dried seeds (g)}}$$

B. Fatty acid characterization by gas chromatography (GC)

The oil was hydrolyzed in KOH/MeOH, mixed with HCl/MeOH and extracted using petroleum ether (Jham et al., 1982) (Appendix C) before subjected to biodiesel analysis. The analysis fatty acid methyl ester (FAME) was accomplished using a gas chromatograph (Hewlett-Packard 6890: GC6890), fitted with a flame ionization detector and a capillary column (30 m × 0.32 mm × 0.25 μm) of selected biodiesel for FAME. The column temperature was programmed from 210 °C to 250 °C at a linear flow rate of 20 °C/minute. The initial and final holds up time were 12 and 8 minutes, respectively. While the injector and the detector were set at 290 °C and 300 °C, respectively. One μL methyl esters was injected into the column in split mode (split ratio 50:1). The quantitative measurements were made by Chemstation software

(Agilent Technologies, Germany). The fatty acid composition was reported as a relative percentage of the total peak area from 3 replicates.

2.2.4 Total oil content, fatty acids and oil body analysis in embryo and endosperm isolated from open-pollinated seeds

A. Total oil content and fatty acid compositions

Oil content and fatty acid composition in isolated embryo and endosperm were characterized according to procedures provided in 2.2.3.

B. Oil body extraction

Physic nut oil bodies from total seed, embryo and endosperm were isolated and purified using two-layer flotation by centrifugation, detergent washing and ionic elution, with minor modification, according to published procedures (Tzen et al., 1997) (Appendix D). The oil body of sesame seed (*Sesame indicum* L.) was used as a control. Briefly, 2.5 gram of total seeds and excised endosperms and 0.7 gram embryo were firstly crushed, using mortar and pestle, in grinding buffer (Appendix D) at 4 °C (on ice) for 20 minutes. The homogenate was filtered through Miracloth (22 - 25 µm pore size, Calbiochem, EMD chemicals, Inc., USA) into 50-ml centrifuge tube. The filtrate was equally separated (1 ml) into 1.5-ml Eppendorf tube and then the grinding buffer was slowly layered on the top until reached 1.5-ml level of Eppendorf tube (2 separated layers could be seen). The sample was centrifuged at 13,200 rpm at 4 °C for 20 minutes using centrifuge machine (Eppendorf 5415D centrifuge, USA). The oil layer was again collected and extracted using detergent washing solution, flotation buffer, minimal buffer and salting buffer (Appendix D) until purified. Finally, 0.5 ml grinding buffer was added to the collected oil bodies. After centrifugation, the grinding buffer was removed until the remaining mixture of oil bodies and buffer was at 0.05 ml level of the Eppendorf tube. The purified oil bodies were stored at -20 °C.

C. Differential interference contrast (DIC) and fluorescent microscopic observation of the purified oil bodies

Oil bodies purified from total seed, embryo, and endosperm were examined with DIC and fluorescent microscopy. Two µl oil bodies were mixed with 100 µl grinding buffer and 1 µl of 1.57 mM Nile red solution (Sigma-Aldrich, USA). The samples were kept in dark condition for 20 minutes. Ten µl of samples were loaded onto glass slide and visualized using an Axioskop 2 Plus microscope (Zeiss, Germany) equipped with a charge-coupled device camera (Coolsnap-Prock, Photometrics Ltd., USA) (Lin et al., 2012). The diameters of oil bodies were measured from 100 oil body samples (from DIC photographs) using ImageJ program (1.45-free version).

D. Thin layer chromatography (TLC) analysis of neutral lipid in oil bodies

Neutral lipid in purified oil bodies was extracted and analyzed using TLC (Lin et al., 2012) (Appendix E). Oil samples were extracted with solution containing chloroform and methanol (2:1 v/v) and the chloroform layer was then collected and stored at -80 °C for the analysis. The TAG marker (5 µl) and the chloroform layer (8 µl) mixing with 20 µl of methyl chloride and methanol (2:1 v/v) were separately spotted onto a TLC plate which was previously developed to the top (R_f = 1) in hexane: diethyl ether: acetic acid (70: 30: 1 v/v/v). TLC plate with spotted samples was developed in benzene to the R_f = 1 position and followed by hexane: diethyl ether: acetic acid (70: 30: 1 v/v/v) to R_f = 0.5. The plate was stained overnight with 0.03% Coomassie brilliant blue R-250 (Sigma-Aldrich, USA) dissolved in 20% (v/v) methanol and 0.5% (v/v) acetic acid and destained in destain solution (Appendix E).

E. Sodium dodecyl sulfate-polyacrylamide gel electrophoresis (SDS-PAGE) and Western blotting of oil body protein

This experiment was performed following the previous methods (Lin et al., 2012). Oil body proteins from sesame and physic nut seed, previously extracted with 4× sample buffer, were resolved by glycine SDS-PAGE using 15% polyacrylamide separating gel and 4.75% polyacrylamide stacking gel (Appendix F). After electrophoresis, the gel was stained in 0.125% Coomassie brilliant blue R-250 (Sigma-Aldrich, USA) and destained with destain solution I and II (Appendix F) until the background was clear. For Western blotting, proteins were transferred from SDS-PAGE onto nitrocellulose membranes in a Trans-Blot system (Bio-Rad, USA) (Appendix G). The membranes were incubated in primary antibodies against sesame seed caleosin (27 kDa), high molecular weight oleosin (oleosin-H, 17 kDa) or low molecular weight oleosin (oleosin-L, 15 kDa) and then in the second antibodies conjugated with anti-rabbit (for caleosin) and anti-chicken alkaline phosphatase (for oleosins). The membrane color was developed in dark condition using the developmental buffer supplemented with substrates nitro blue tetrazolium chloride (NBT) (Promega, USA) and 5-bromo-4-chloro-3-indolyl phosphate (BCIP) (Promega, USA).

F. Liquid chromatography-tandem mass spectrometry (LC-MS/MS) of protein in oil body

Protein were excised from the gel and digested by trypsin (Appendix H). The resulting peptides were subjected to LC-MS/MS analysis which was performed on UltiMate 3000 RSLCnano LC Systems (Thermo Fisher Scientific) using an Acclaim PepMap C18 column (75 μm I. D. x 25 cm nanoViper, Thermo Fisher Scientific). Ten μL samples were loaded on the column which was eluted at a flow-rate of 300 nL/minute. Eluent was introduced to TripleTOF® 6600 system mass spectrometer (Applied Biosystems Sciex) operating in electrospray ionization (ESI) mode. Ion Spray voltage was set at +2500 V. Interface heater temperature and column oven temperature were arranged at 150 °C and 35 °C, respectively. Mass spectra were

acquired scanning from m/z 65 to 1800. The MS/MS data were subjected to search algorithms against the Swiss-Prot protein sequence using Mascot software (Matrix Science Ltd., London, UK).

2.2.5 Statistical analysis

The fruit set among pollination types (Result part, Table 6) as well as SFA, MUFA, PUFA and oil content among whole seed, embryo and endosperm of open-pollination (Result part, Table 7) were of normal distribution and having equal variance, mean significant differences were thus considered using an analysis of variance (ANOVA) followed by Duncan's multiple range test (DMRT). Welch was used to test the differences in oil content among pollination methods (Result part, Table 6) and oil body size among whole seed, embryo and endosperm of open-pollination (Result part, Table 7) since the data were normally distributed but lack of variance homogeneity. Kruskal-Wallis test was employed to check the differences in number of seed per fruit, fatty acid compositions as well as SFA, MUFA and PUFA among pollination types (Result part, Table 6) which cannot be transformed to meet the assumption of normality. All significant differences were calculated at $P \leq 0.05$ level and the results were reported as mean ± S.E.

Fruit diameter was fitted to the following logistic function equation modified from Wubs et al. (2012) using Excel Solver (Microsoft Excel 2010).

$$Y = \frac{A}{1+ e^{-k(x-x_m)}} \ ;$$

where Y is the fruit diameter at time after pollination, A is the highest fruit diameter, k is the constant defining the curvature of the growth feature, x is time after pollination, and x_m the position of the inflection point where the growth rate is highest.

2.3 Establishment and lipid analysis of *J. curcas* cell suspension

2.3.1 In vitro seed germination and seedling growth

Naked open-pollinated seeds were soaked in distilled water (DW) for 1 hour. The seeds were then surface-sterilized in 20% Clorox for 20 minutes. The seeds were clean with DW 3 times and the embryos were then excised and cultured on hormone-free solid MS (Murashige and Skoog, 1962) (Appendix I). This basal medium was composed of 3% sucrose and pH was adjusted to 5.8 using 1 N NaOH and 1 N HCl before autoclaving at 121 °C for 20 minutes. The cultures were maintained in culture room at 25 ± 3 °C and a photoperiod of 16/8 h light/dark regime, provided by cool daylight lamps (36 Watts, Philips, Bangkok, Thailand) at 23 µmol m^{-2} s^{-1}. After culture for 10 days, survival percentage of seedling was calculated from 5 replications, each with 14 - 20 embryo samples.

2.3.2 Callus induction, growth kinetic and microscopic observation

Hypocotyl of 10-day-old seedling which had no true leaf was transversely cut into 1 mm^2 thin cell layer (tTCL) with a thickness of 1 mm and transferred to solid MS medium added with the combination of 2, 4-D (0, 0.5 and 1 mg L^{-1}) and KN (0, 0.5 and 1 mg L^{-1}). The cultures were maintained in the same conditions to that of seedling culture as described above (Topic 2.3.1). The induction percentage, fresh weight and morphology of callus were recorded after 4 weeks of culture, from 12 replications.

Callus from medium containing 1 mg L^{-1} 2, 4-D in combination with 0.5 mg L^{-1} KN was continuously cultured and its growth kinetic, every week for 5 weeks, was monitored based on fresh and dried weight measurement using the initial fresh weight of 0.2 gram (modified from Santos et al., 2013; Benítez-García et al., 2014). The fresh weight of callus was measured and the dry weight was recorded after placing the fresh callus in oven (60 °C) for 24 hours, both with 6 replications. This callus was subcultured onto the same medium every month. The callus was observed with Olympus SZH 10 stereomicroscope joined to DP-71 digital camera and prepared

through paraffin technique (Topic 2.1.1) for morphological and histological examination, respectively.

2.3.3 Cell suspension culture and analysis

A total of 0.5 gram compact callus was gently broken with forceps and transferred to 125 ml flask containing 25 ml (modified from Soomro and Memon, 2007) of liquid MS medium supplemented with 1 mg L^{-1} 2, 4-D and 0.5 mg L^{-1} KN. The flasks were placed on shaker at 100 rpm and maintained in the culture room with the same conditions to that mentioned in topic 2.3.1. The cell suspension was observed with Olympus SZH 10 stereomicroscope joined to DP-71 digital camera for morphological analysis and prepared through paraffin technique (Topic 2.1.1) for histological examination. Fresh weight, dry weight, the medium pH, chlorophyll content, carotenoid content and viability (TTC test) were monitored as described in next topic. The cell was subcultured at 2-week intervals by transferring 5 ml culture solution to 20 ml fresh medium (modified from Soomro and Memon, 2007). In addition, 2-week-old cells were collected for the analysis of oil content and fatty acid composition.

A. Growth kinetic of cell and change of medium pH

A growth kinetic of cell was analyzed by fresh and dry weight measurement using 3 replications (3 flasks). For fresh weight, the cell suspension (from 1 flask, 25 ml) was filtered through oven dried pre-weighed filter paper (Whatman No.1) before weighing. Meanwhile, the dry weight was recorded from the cells dried for 48 hours at 60 °C. The remaining liquid media after the cell filtration were used for pH measurement. The growth and pH were monitored, without subculture, every week for five weeks.

B. Determination of chlorophyll and carotenoid content

A total of 0.01 gram fresh cells were crushed with 2.3 ml 80% acetone and centrifuged at 3,000 rpm for 5 minutes. Supernatant was collected and debris was then crushed 2 times with 2.3 ml of 80% acetone each time (6.9 ml total supernatant). The optical density of the supernatant was read with UV-visible spectrophotometer (UV-1601, Shimadzu) at 480, 510, 645 and 663 nm by using 80% acetone as a blank. Content of total chlorophyll, chlorophyll *a*, chlorophyll *b* and carotenoid were then calculated utilizing the following formulae (Misra et al., 2010). Three replications were performed for each treatment.

$$\text{Total chlorophyll (mg g}^{-1}\text{ FW)} = \frac{[20.2(A_{645}) + 8.02(A_{663})] \times V}{1000 \times FW}$$

$$\text{Chlorophyll } a \text{ (mg g}^{-1}\text{ FW)} = \frac{[12.7(A_{663}) + 2.63(A_{645})] \times V}{1000 \times FW}$$

$$\text{Chlorophyll } b \text{ (mg g}^{-1}\text{ FW)} = \frac{[22.9(A_{645}) - 4.68(A_{663})] \times V}{1000 \times FW}$$

$$\text{Carotenoid (mg g}^{-1}\text{ FW)} = \frac{[7.6\,(A_{480}) - 2.63(A_{510})] \times V}{1000 \times FW} \;;$$

where V is the volume of extracted solution (ml), FW is the fresh weight of tissue extracted (g), A_{480}, A_{510}, A_{645} and A_{663} are the absorbance values at 480, 510, 645 nm and 663 nm, respectively.

C. Cell viability by TTC test

Viability test was modified from the methods of Mikuła et al. (2006). Two ml of 0.8% TTC (dissolved in 0.05 M Na_2HPO_4-KH_2PO_4, pH 7.4) were added to 0.02 gram of the cells before incubated in dark at 25 °C for 20 hours. The samples were washed with 3 changes of DW for TTC removal. Then they were submerged in 5 ml 95% ethanol and incubated in a water bath at 85 °C for discoloration (50 minutes). Extract absorption was assessed at 530 nm (Steponkus and Lanphear, 1967)

with UV-visible spectrophotometer (UV-1601, Shimadzu) using 95% ethanol as a blank. TTC reduction was reported as absorbance 530 nm per gram of sample fresh weight (A_{530} g^{-1} FW) (Chang et al., 1999) from 3 replications.

D. Oil content and fatty acid analysis of the cells

Two-week-old cells were filtered using a mesh (280 µm pore), washed 3 times with DW and stored at -20 °C. For oil extraction, samples were incubated at 60 °C for 48 hours. The oil was extracted from 1 gram of crushed cells and analyzed for fatty acid according to the methods provided in topic 2.2.3.

2.3.4 Statistical analysis

Kruskal-Wallis was applied for testing mean differences of callus induction and fresh weight (Result part, Table 9). Independent t-test was employed for checking the differences in oil content and fatty acid composition between the cell suspension and the whole seed. All significant differences were computed at $P \leq 0.05$ and the results were represented as mean ± S.E.

CHAPTER 3
RESULTS

3.1 Development and fertility of male and female gametophytes

3.1.1 General flower characteristics and gametophyte development

A. General flower characteristics

Physic nut normally produces both male and female flowers on the same cymose inflorescence. The inner most female flower, locating at the center, is surrounded by male flowers (Figure 10A). Ratio of male to female flower is approximately 17: 1. Male flower, with round head and thin pedicel (Figure 10B), has five greenish-yellow sepals and five greenish-yellow petals enriched with hairs (Figure 10C). The male nectaries at the base of filament are globular. These nectaries are initially greenish in color and change to yellow at anthesis (Figure 10C). Male flower contains approximately 10 stamens arranging in 2 whorls; free outer and fused inner whorls (Figure 10C). The anther is bi-lobed (with four pollen sacs), extrorse type (dehisces longitudinally outward) and joins to filament by subbasifixed attachment (Figure 10D). The female flower has conical apex and thick pedicel (Figure 10E). Each female flower has five greenish-yellow sepals and five greenish-yellow petals with plentiful hairs (Figure 10F) which are similar to those of male flower. The flattened and ovate nectaries, displaying yellow in color during the anthesis period, can be found at the base of the ovary (Figure 10F). The ovary, with 3 carpels, is comprised of 3 locules, each with one ovule exhibiting apical-axial placentation (Figure 10F and G). The style is connate and stigma is of three bifurcated type (Figure 10F and H). Noticeably, the sterile stamens presenting abnormal-shaped anther and no filament can be observed at the base of ovary at both early (Figure 10H) and late (Figure 10I) stages of female flower development.

Figure 10 Floral morphology of *J. curcas* L.

(**A**) A cymose inflorescence presenting male (arrow) and female flowers (arrowhead); (**B**) Male flower showing a round head (arrowhead) with thin pedicel (arrow); (**C**) Dissected male flower showing sepal (Sp), petal (Pt) covered with hair (star), round nectary gland (Ne), filament (arrowhead), and anther (arrow); (**D**) Stamens illustrating longitudinal slits of anther (arrows) at shedding period; (**E**) Female flower with conical head (arrowhead) and thick pedicel (arrow); (**F**) Dissected female flower exhibiting sepal (Sp), petal (Pt) with hair (star), flattened and ovate nectary (Ne), ovary (Ov), style (Sty), and three bifurcate stigma (arrowhead and inset); (**G**) Ovary with an ovule (arrow) showing the apical-axial placentation; (**H**) Sterile stamens (arrows) and developing stigma (arrowhead and inset) at early development of female flower; (**I**) Sterile stamens (arrows) at nearly bloom period of female flower. Ne, nectary; Ov, ovary; Pt, petal; Sp, sepal; Sty, style

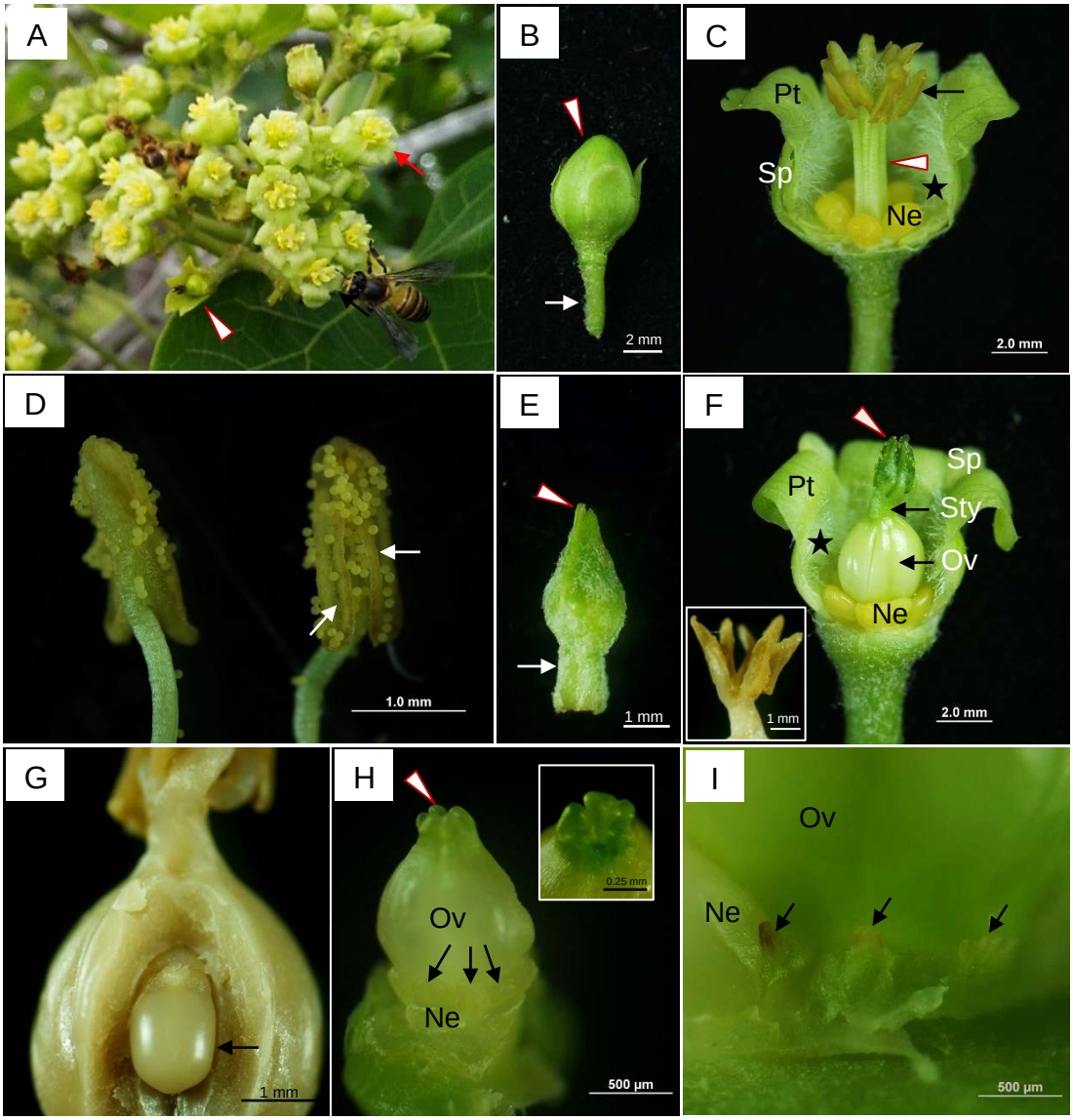

Figure 10 (see facing page for legend)

B. Male gametophyte development

Anther contains 4 locules which wall layers namely, the outermost epidermis, endothecium, middle layer and the innermost tapetum are observed. The male gametophyte development could be indicated as the stages of (a) pollen mother cell (PMC), (b) microspore tetrad, (c) uninucleate microspore, (d) early binucleate pollen with globular-shaped generative cell and (e) late binucleate pollen with spindle-shaped generative cell at the flower bud sizes of 1.0 - 1.5, 1.0 - 1.5, 1.6 - 2.0, 2.1 - 3.0 and ≥ 3.1 mm in diameter, respectively. Firstly, the flower bud (1.0 - 1.5 mm in diameter) having a clump of anthers with undeveloped filament and nectary (Table 3) displays both stages of PMC (Figure 11A) and tetrahedral tetrad (Figure 11B). At this flower size, the degrading middle layer of anther walls (Figure 11A and 11B) and the callose wall deposition around tetrad microspores (Figure 11C) could be noticed. Secondly, most of the flower buds at 1.6 - 2.0 mm are in the stage of uninucleate microspore presenting the exine layer (Figure 11D). The bud also possesses a cluster of anthers with undeveloped filament and nectary gland (Table 3). The degenerated middle layer is presented while epidermis, endothecium and tapetum are still clearly visualized (Figure 11D). Finally, the bud size of about ≥ 2.1 mm exhibits binucleate pollen stage. Flower bud (2.1 - 3.0 mm) carries the developing filament which are hidden by the presence of small greenish nectaries (Table 3). The anther wall is composed of the epidermal layer, the fibrous endothecium, the degraded middle layer and the collapsing tapetum (Figure 11E). For this bud size, the majority of flower buds were at early binucleate mature pollen grains containing the vegetative nucleus (Figure 11E, arrowhead) and the globular-shaped generative cell detached from pollen wall (Figure 11E, Gn). Then, the bud (≥ 3.1 mm until anthesis) presents a spheroidal pollen grain (76.72 ± 1.17 µm in diameter) containing the vegetative nucleus (Figure 11F, Vg) and the spindle-shaped generative cell (Figure 11F, arrowhead). At this stage, the layers of epidermal and the fibrous endothecium are still remained (Figure 11F). At anthesis, pollen grain is shed at two-celled stage (Figure 11G) and has surface clavae arranged in crotonoid pattern (polygonal alignment) (Figure 11H).

Table 3 Summarized correlation between flower bud size, bud features and developmental events of male gametophyte

	Bud diameter (mm)				
	1.0 – 1.5	**1.6 – 2.0**	**2.1 – 3.0**	**3.1 – 4.0**	**> 4.0**
Undissected flower					
Dissected flower					
Pollen stage	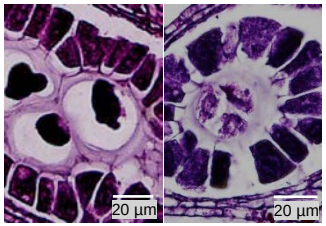	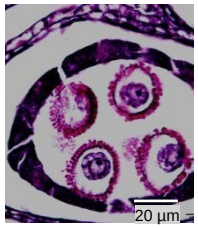	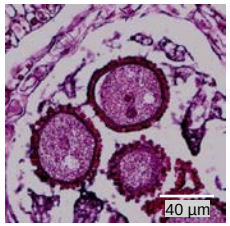	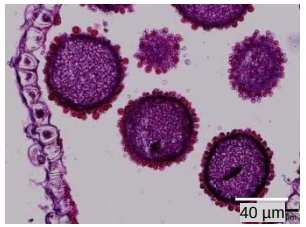	
	Pollen mother cell Tetrad	Free microspore	Binucleate pollen (globular-shape generative cell)	Binucleate pollen (spindle-shape generative cell)	
Anther wall structure	Epidermis Endothecium Middle layer Tapetum	Epidermis Endothecium Tapetum	Epidermis Thickening endothecium Collapsing tapetum	Epidermis Thickening endothecium	

Scale bars (black color) = 2 mm

Figure 11 Pollen development of *J. curcas* L.

(**A**) Pollen mother cell (PMC) stage showing a PMC with large nucleus and all anther walls including epidermis (Ep), endothecium (En), middle layer (Md) and tapetum (T); (**B**) Tetrad stage presenting a tetrad (Td) resulting from PMC meiosis including cytokinesis and exhibiting all anther wall layers; (**C**) Callose wall (arrows) surrounding the tetrad of microspores after aniline blue fluorescence; (**D**) Free microspore (Mi) displaying the exine wall (arrowhead); (**E**) Bi-nucleate pollen showing vegetative nucleus (arrowhead) and a globular-shaped generative cell (Gn). Insets illustrating the fibrous thickening of the endothecium; (**F**) Mature pollens containing the vegetative nucleus (Vg) and the spindle-shaped generative cell (arrowhead). Insets showing thicker and more fibrous wall of endothelial cells; (**G**) Pollens releasing from anther before the opening of petal (Pt); (**H**) SEM micrograph exhibiting mature pollen grain with clavae (arrow) arranging as croton pattern (circles). En, endothecium; Ep, epidermis; Gn, generative cell; Md, middle layer; Mi, microspore; PMC, pollen mother cell; Pt, petal; T, tapetum; Td, tetrad microspore; Vg, vegetative nucleus

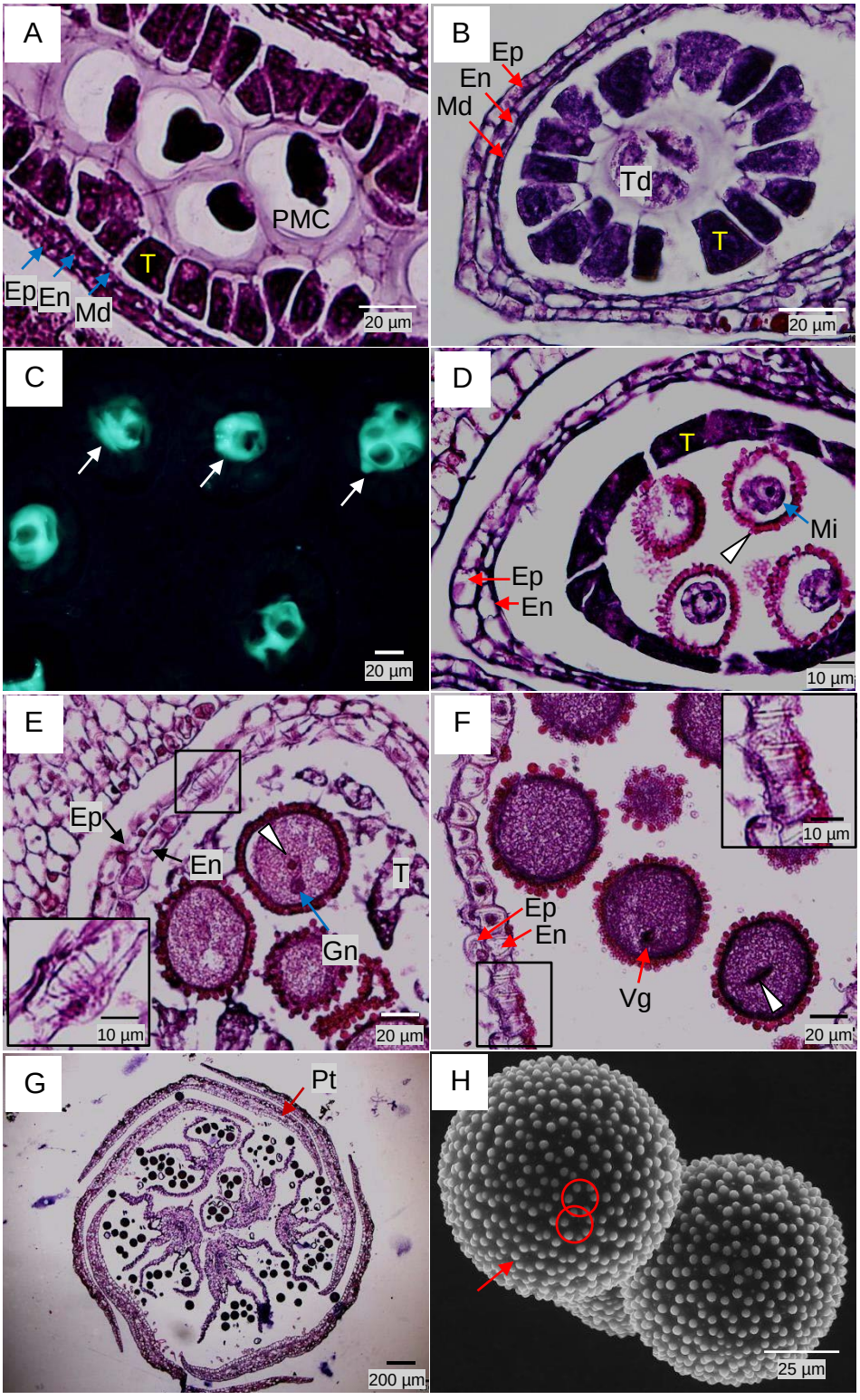

Figure 11 (see facing page for legend)

C. Female gametophyte development

The female bud (1.0 - 1.5 mm) presents the initiation of style and stigma, a large sterile stamen and a small nectary gland (Table 4). Megaspore mother cell (MMC) having a large nucleus with dense cytoplasm is deeply embedded within a massive nucellus (Figure 12A and B) which located in an anatropous bitegmic and crassinucellate ovule (Figure 12A). Remarkably, anatomical features confirmed that the stamens found in female flower are sterile by having locule shrinkage without PMC at this MMC stage (Figure 12C and D). The bud sizes of 1.6 - 2.0 mm possesses the developing style and stigma (Table 4) while the sterile stamens have remained larger than the nectaries. The linear arrangement of four haploid megaspores (Figure 12E), resulting from meiosis of MMC, was noticed at this flower size. A haploid megaspore located at chalazal end was survived while three of these megaspores at micropylar region were degenerated (Figure 12E). Afterwards, the functional megaspore (Figure 12F, inset) undergoes mitosis to produce two-nucleate embryo sac (Figure 12G) and subsequently develops to form the multinucleate immature embryo sac (Figure 12H). The stage of eight-nucleate embryo sac could mostly be found in the bud (≥ 2.1 mm) whose developed style and stigma and larger nectaries covering sterile stamens are presented (Table 4). The bud of 2.1 - 4.0 mm, displaying the white nectaries (Table 4), contains immature 8-nucleate embryo sac which the migration of two polar nuclei to the center was not completed yet (Figure 12I - K). Whereas, the buds (> 4 mm) having yellow nectaries (Table 4) possessed mature 8 nucleate embryo sac comprising of antipodal cells (Figure 12L), egg cell and synergids (Figure 12M) and two juxtaposed polar nuclei at the center (Figure 12M and N). Thus, *J. curcas* embryo sac is of polygonum type.

Table 4 Summarized correlation between flower bud, bud features and developmental events of female gametophyte

	Bud diameter (mm)				
	1.0 – 1.5	**1.6 – 2.0**	**2.1 – 3.0**	**3.1 – 4.0**	**> 4.0**
Undissected flower					
Dissected flower					
Embryo sac stage	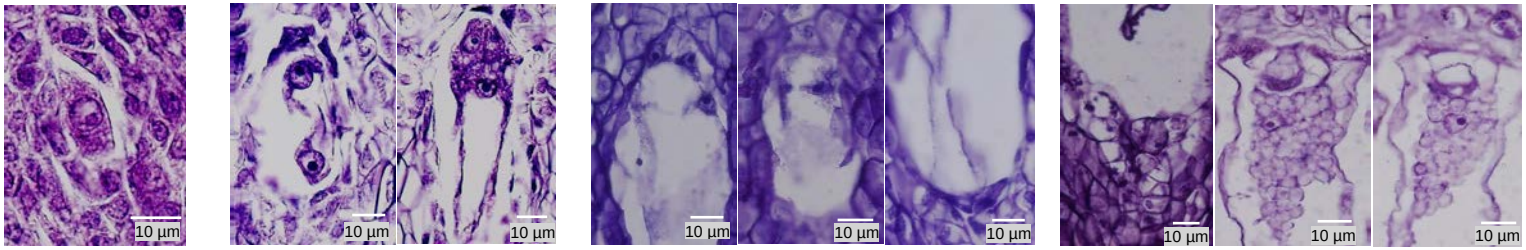				
	Megaspore mother cell	Megaspore or ≥ 2-nucleate-embryo sac		8-nucleate-embryo sac (immature)	8-nucleate-embryo sac (mature)

Scale bars (black color) = 2 mm

Figure 12 Longitudinal sections of *J. curcas* female flowers determining embryo sac development

(**A**) Anatropous ovule with MMC (arrow), nucellus (Nu), inner integument (Ii) and outer integument (Oi); (**B**) MMC; (**C**) Sterile stamens (arrows) at MMC stage; (**D**) Amplification of inset in (**C**) showing sterile stamen with shrinkage locule (arrow); (**E**) Three degenerating megaspores (arrows) at micropylar and a survival megaspore (arrowhead) at chalazal pole; (**F**) Ovule at megaspore stage presenting caruncle (Cr), nucellus (arrow), inner integument (Ii) and outer integument (Oi). Insets show the funtional megaspore; (**G**) Binucleate embryo sac; (**H**) Multinucleate embryo sac; (**I - K**) Serial sections of immature embryo sac indicating (**I**) presumptive egg apparatus (arrows) and polar nucleus (arrowhead); (**J**) The same sample as (**I**) in deeper section, showing presumptive egg apparatus (arrow); (**K**) In other section representing presumptive antipodal cells (arrows); (**L - N**) Mature embryo sac showing (**L**) antipodal cells (arrows); (**M**) Central polar nucleus (arrowhead), egg cell (arrow) and synergids (stars); (**N**) Consecutive plane of **L**, showing another polar nucleus (arrowhead) and egg cell (arrow). Cr, caruncle; Ii, inner integument; MMC, megaspore mother cell; Nu, nucellus; Ne, nectary; Oi, outer integument; Ow, ovary wall

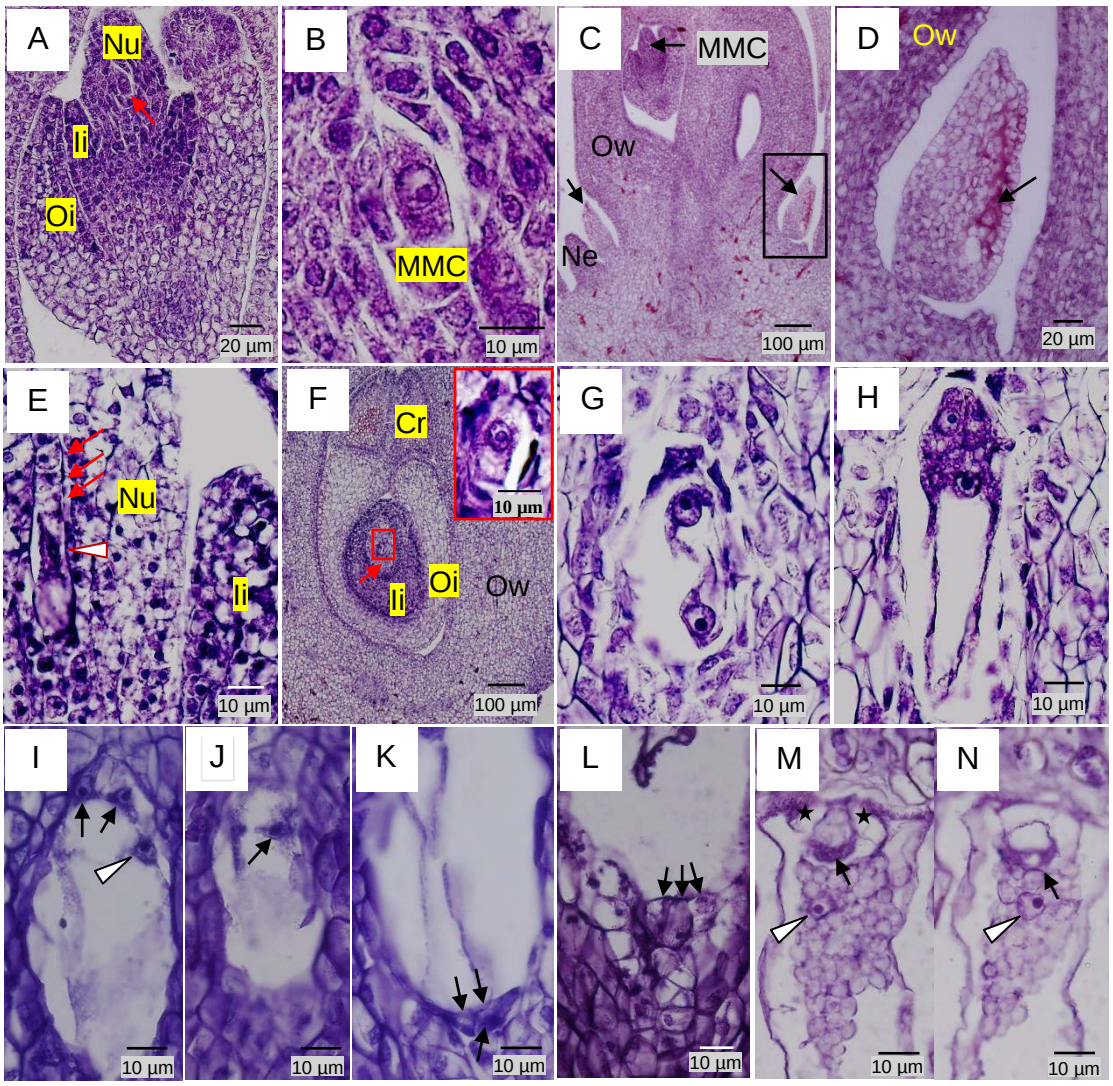

Figure 12 (see facing page for legend)

3.1.2 Pollen assessment and stigma receptivity

A. Pollen assessment via FCR, TTC and germination test

The viable pollens exhibited yellow-green fluorescence (Figure 13A, B), dark-red color (Figure 13C) and the germinated pollen tube (Figure 13D) after FCR, TTC and germination test, respectively. All techniques employed in pollen viability test, exhibiting inverse S-shape pattern, displayed the reduction of pollen viability along the time course after flowering (Figure 14A). From FCR result, the highest viability could be found at 4 HAF (98.60%) even not significantly different from 95.80% at 0 HAF and 93.20% at 8 HAF. The viability dropped sharply from 86.60% at 24 HAF to the lowest percentage (31.40%) at 96 HAF. By TTC, the maximal viability was 87.00% at flowering time (0 HAF) which was not significantly different from 4, 8 and 12 HAF. The viability decreased markedly (66.60 - 21.60%) during 24 to 48 HAF and the lowest (15%) was shown at 72 HAF. The highest germination (43.40%) was also observed at flowering time. Then, the germination frequency was exceedingly dropped to 19.60% (at 4 HAF) and to 2.20% (at 96 HAF). Even with no significant difference of determination coefficient (R square), the TTC (with slightly higher R^2, 0.62) seemed to be higher correlated with germination test than the FCR ($R^2 = 0.57$) based on linear pattern (Figure 14B).

B. Stigma receptivity

The receptive stigma presented the number of bubbles at the stigmatic apex (Figure 15, inset) and illustrated the inverse S-shape longevity (Figure 15). The stigma receptivity displayed the maximum percentage at 100 ± 0.00% during the period of 0 - 2 DAF, 97.22 ± 2.78% at the third day and it was steadily decreased to the lowest percentage of 36.11 ± 2.78% at 6 DAF.

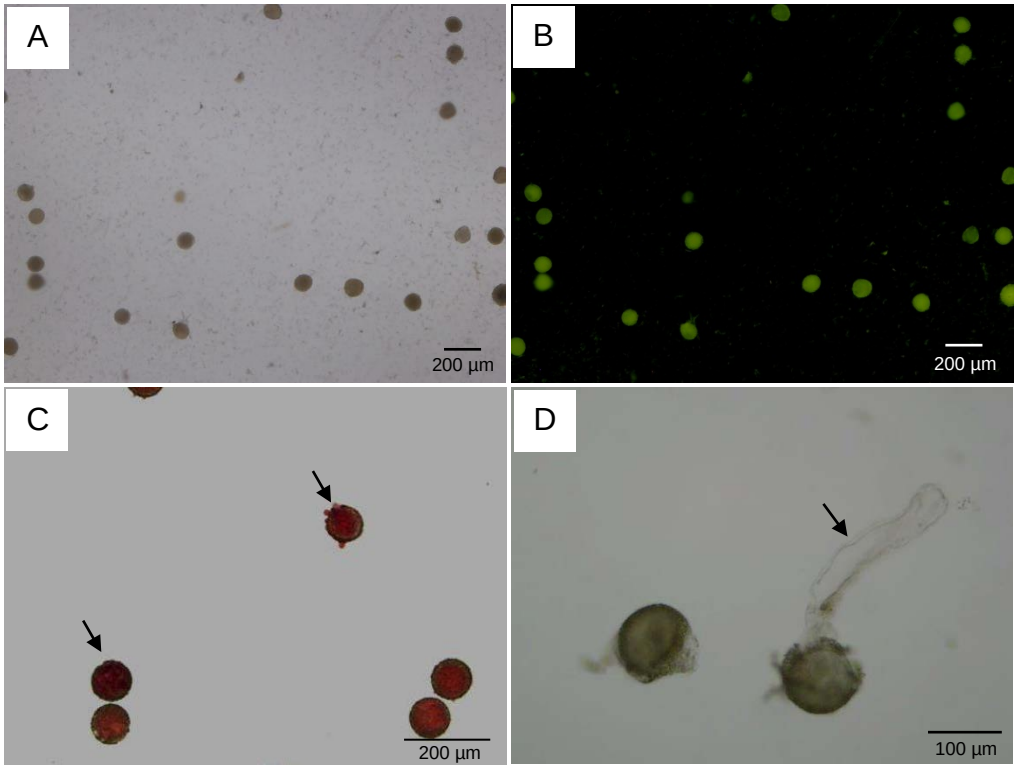

Figure 13 Features of pollen viability

(**A**) FCR-stained pollens before observed with fluorescent microscope; (**B**) Bright fluorescence of viable pollens after FCR test; (**C**) Dark-red viable pollens (arrows) after TTC test; (**D**) Germinated pollen tube (arrow) after germination test

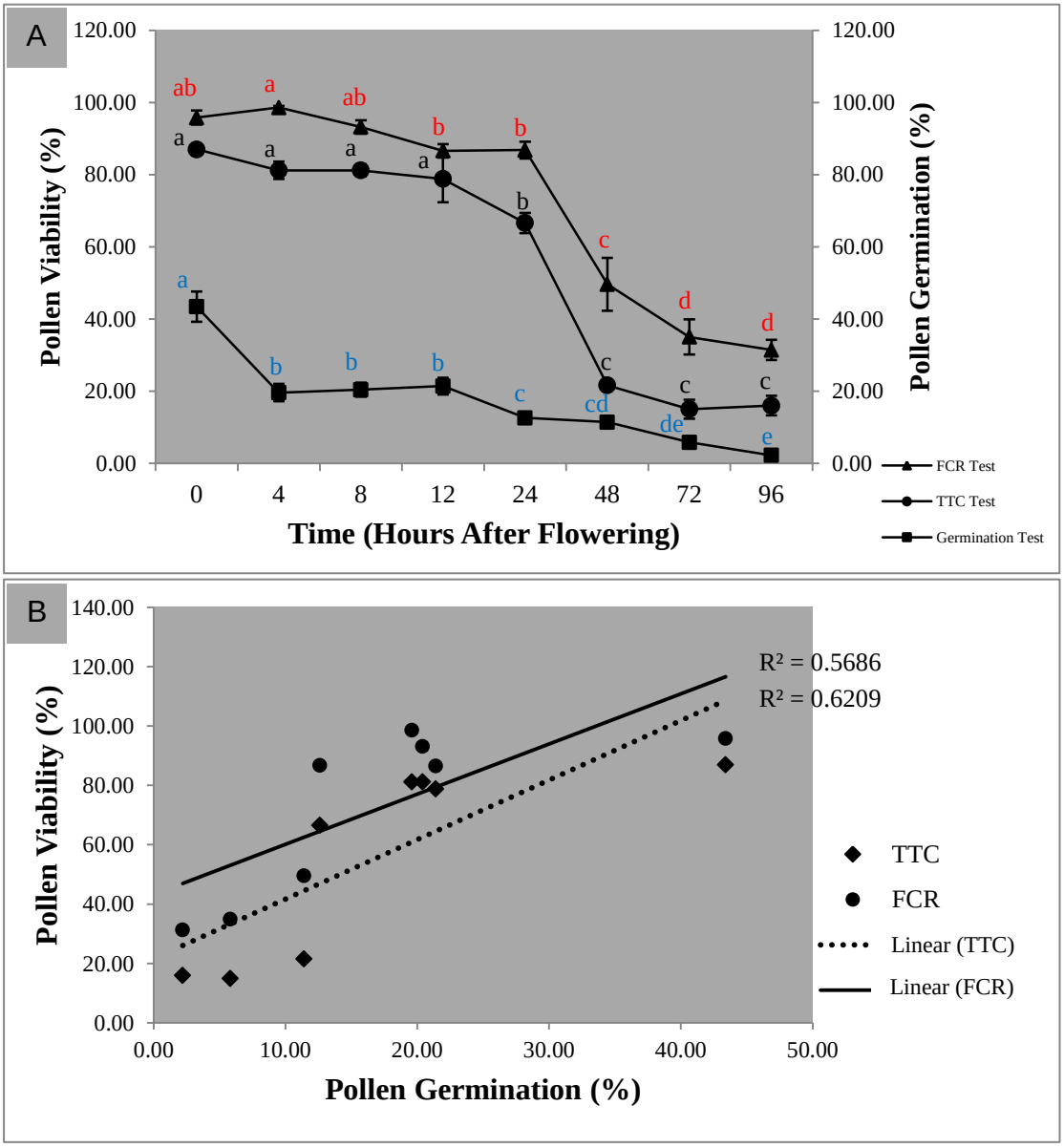

Figure 14 Pollen viability of physic nut

(**A**) Pollen viability (by TTC and FCR test) and germination percentage showing inverse S-shape pattern; (**B**) A moderate linear relationship between FCR test and germination test (R^2 = 0.57) as well as between TTC test and germination test (R^2 = 0.62). Vertical lines on the graph (A) indicate mean ± S.E. Different letters in the lines indicate significant differences at $P \leq 0.05$

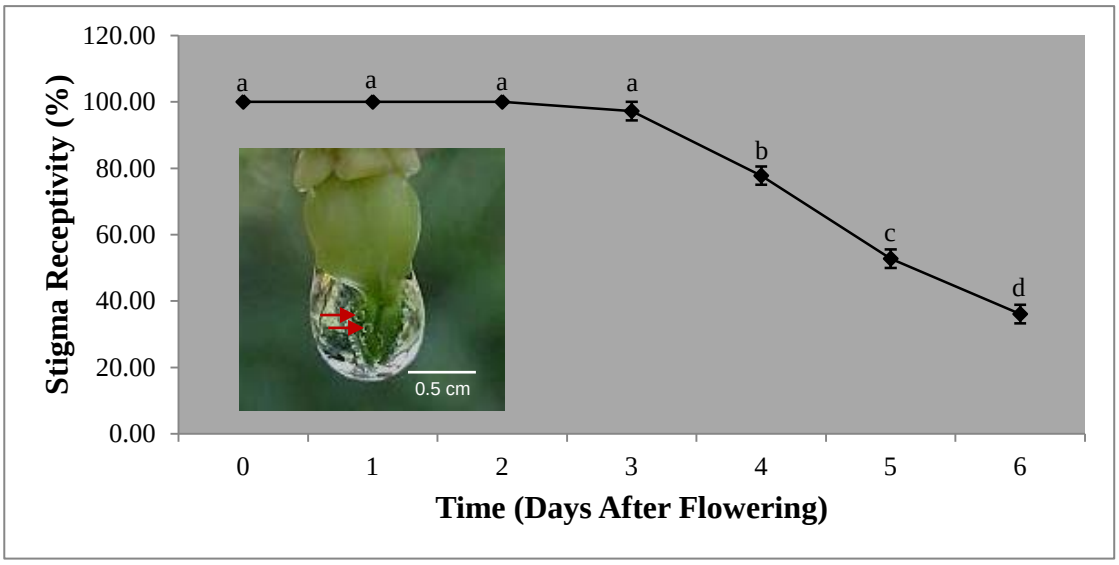

Figure 15 Stigma receptivity (hydrogen peroxide test)
The inset showing receptive stigma with released bubbles (arrows). The receptivity diminished along the increase of days after flowering (inverse S-shape). Different letters in the lines indicate significant differences at $P \leq 0.05$

3.2 Effects of pollination methods on fruit development and seed oil accumulation

3.2.1 Growth features of fruit, embryo and endosperm

Relationship of phase, time after pollination/flowering, fruit diameter size, and developmental stages of embryo and endosperm among four pollination methods was concluded in Table 5. Fruit diameter growth of all pollinations fitted to a simple sigmoid shape, with the three main stages termed the lag, log and stationary phases at approximately 0 - 9, 9 - 27 and 27 - 48 DAP/DAF, respectively (Figure 16). Open-pollination showed the highest fruit set and seed number. For open- , cross- and self-pollination, the embryo developed through stages namely globular-shaped, heart-shaped, torpedo-shaped and mature embryo at around 3 - 21, 21 - 24, 24 - 30 and 30 -

48 DAP, respectively (Figure 17 - 19). Meanwhile, an ontogeny of endosperm was of nuclear type displaying free nuclear stage at 3 - 18 DAP and cellular stage since 18 DAP forwards (Figure 17 - 19). Unfortunately, we failed to assure the developmental origin of embryo and endosperm in apomictic fruit (Figure 20). Oil droplets could be examined in both mature embryo and endosperm obtained from all pollination treatments. Details for each pollination were described on the next page.

Table 5 Relationship of phase, time after pollination/flowering, fruit diameter size, embryo and endosperm stages among the four pollination methods

Pollination methods	**Characteristics**	**Developmental phases**		
		Lag phase (0 - 9 DAP/DAF)	Log phase (9 - 27 DAP/DAF)	Stationary phase (27 - 48 DAP/DAF)
Open-pollination	Fruit diameter (mm)	2.81 - 4.16	4.16 - 28.82	28.82 - 30.30
	Embryo stage	Globular	Globular, heart and torpedo	Torpedo - mature
	Endosperm stage	Free nuclear	Free nuclear - cellular	Cellular
Cross-pollination	Fruit diameter (mm)	2.61 - 3.71	3.71 - 27.84	27.84 - 29.95
	Embryo stage	Globular	Globular, heart and torpedo	Torpedo - mature
	Endosperm stage	Free nuclear	Free nuclear - cellular	Cellular
Self-pollination	Fruit diameter (mm)	2.69 - 2.99	2.99 - 28.54	28.54 - 30.00
	Embryo stage	Globular	Globular, heart and torpedo	Torpedo - mature
	Endosperm stages	Free nuclear	Free nuclear - cellular	Cellular
Non-pollination (Apomixis)	Fruit diameter (mm)	2.78 - 3.52	3.52 - 27.29	27.29 - 28.89
	Embryo stage	–	Globular	Torpedo - mature
	Endosperm stage	–	Free nuclear - cellular	Cellular

–, not detected

A. Open-pollination

The flowers grown in the plantation were often visited by plenty of honey bees, especially around 9 - 11 a. m. The logistic equation obtained for this mode is $Y = \frac{29.97}{1+ e^{-0.27(x-15.41)}}, R^2 = 0.90$ (Figure 16A). During the lag phase (0 - 9 DAP, 2.81 - 4.16 mm fruit diameter), developing globular embryo and free nuclear stage endosperm were detected (Figure 17A). At the log phase (9 - 27 DAP, 4.16 - 28.82 mm), the embryo exhibited globular-, heart- and torpedo-shaped stage (Figure 17B - F). The open-pollinated fruit entered stationary phases at around 27 DAP which the size ranged from 28.82 to 30.30 mm and possessed mature embryo and endosperm. Reserved globules (unknown type) in endosperm could tangibly be examined (Figure 17G) at maturity. Both mature embryo and endosperm contained oil droplets (Figure 17H and I) as examined by Oil Red O staining. Furthermore, it was demonstrated that this mode exhibited the highest fruit set (74.33 ± 4.52%) and seed number (2.90 ± 0.08 seeds per fruit) (Table 6).

B. Cross-pollination

The diameter growth was fitted to $Y = \frac{29.91}{1+ e^{-0.23(x-17.77)}}, R^2 = 0.83$ (Figure 16B). During the lag phase (0 - 9 DAP), diameters of cross-pollinated fruit gradually increased from 2.61 to 3.71 mm. Similar to the open-pollination, the embryo appeared as a small globe-shaped structure and endosperm was of free nuclear stage at this period (Figure 18A and B). At the log phase (9 - 27 DAP, 3.71 - 27.84 mm), the globular (Figure 18C), heart (Figure 18E) and torpedo embryo (Figure 18G), as well as free nuclear (Figure 18D) and cellular stage endosperm (Figure 18F and H) could be detected. At the stationary phase (27.84 - 29.95 mm fruits), the mature endosperm contained many storage globules (Figure 18I). Oil was found to be accumulated compounds of embryo and endosperm as several oil droplets could be observed in both tissues (Figure 18J and K). The fruit set percentage and seed set of

this breeding were less than those of open-pollinated fruits; promoting to be 48.90 ± 4.12 percent fruit set and 2.29 ± 0.12 seeds per fruit (Table 6).

C. Self-pollination

The resemble events to those of open- and cross-pollinations were found for embryo and endosperm development in self-treatment (Figure 19A - I). Fruits diameters of this mode matched to $Y = \frac{29.69}{1+e^{-0.28(x-18.55)}}, R^2 = 0.73$ (Figure 16C). The lag, log and stationary phase were aprroximately corresponded to fruit diameter of 2.69 - 2.99, 2.99 - 28.54 and 28.54 - 30.00 mm, respectively. In average, the selfing had 31.10 ± 5.07% fruit set and 2.23 ± 0.12 seeds per fruit (Table 6).

D. Non-pollination (apomixis)

Most of unpollinated pistils were extremely dead since 12 DAF or still alive with aborted seed (Figure 20A). However, some of them could develop the apomictict fruit whose diameter growth corresponded to the sigmoid curve ($Y = \frac{28.91}{1+e^{-0.26(x-18.08)}}, R^2 = 0.80$) (Figure 16D). Origin of apomictic embryo could not be concluded in this study even if the globular embryo at micropylar region (Figure 20B), the globular embryo-like structure developing from the nucellus area (Figure 20C), the torpedo (Figure 20D) and the mature embryo (Figure 20E) were detective. Likewise, the origin of apomictic endosperm was not observed in this study. Similar to the rests, apomixis reserved oil droplets both in mature embryo (Figure 20F) and endosperm (Figure 20G). Apomixis had the least fruit set (14.04 ± 2.73%) and number of seeds per fruit (1.94 ± 0.12) (Table 6).

Figure 16 Sigmoidal pattern of fruit diameter growth
(**A**) Open-pollination; (**B**) Cross-pollination; (**C**) Self-pollination; (**D**) Non-pollination (apomixis)

●●●●●●● Measured
——— Fitted curve

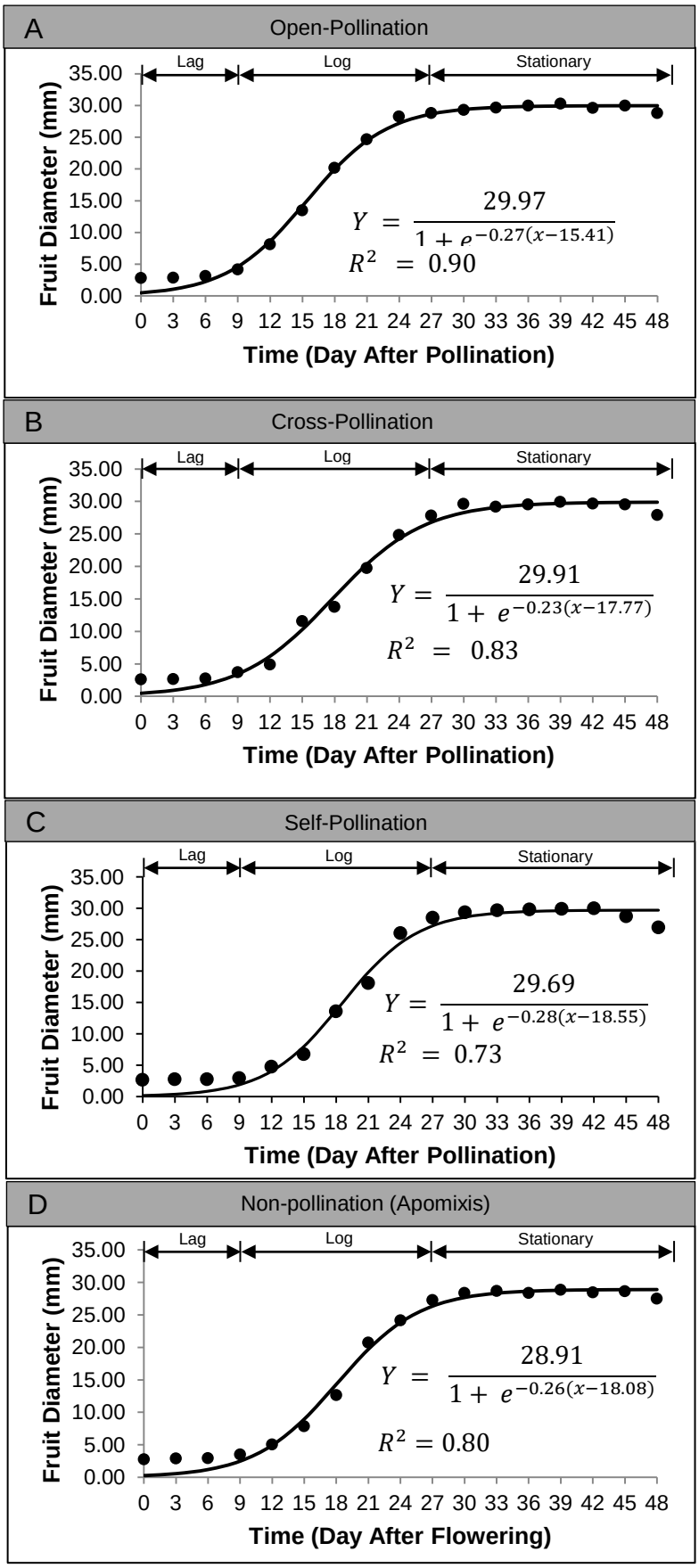

Figure 16 (see facing page for legend)

Figure 17 Embryo and endosperm development in open-pollinated physic nut (**A**) Developing globular embryo (arrowhead) and developing endosperm (arrow) at 3 DAP; (**B**) Globular embryo (arrowhead) and developing endosperm (arrow) at 18 DAP; (**C**) Magnification of endosperm (arrow) in B; (**D**) Globular embryo (arrowhead) and endosperm (En) at 21 DAP; (**E**) Heart-shaped embryo (arrowhead) and endosperm (En) at 24 DAP; (**F**) Torpedo-shaped embryo (arrowhead) and endosperm (En) at 27 DAP; (**G**) Mature endosperm with reserved globules (arrows); Oil droplets (arrows) in (**H**) mature embryo and (**I**) mature endosperm after Oil Red O staining. Ii, inner integument; En, endosperm; Mr, micropylar region

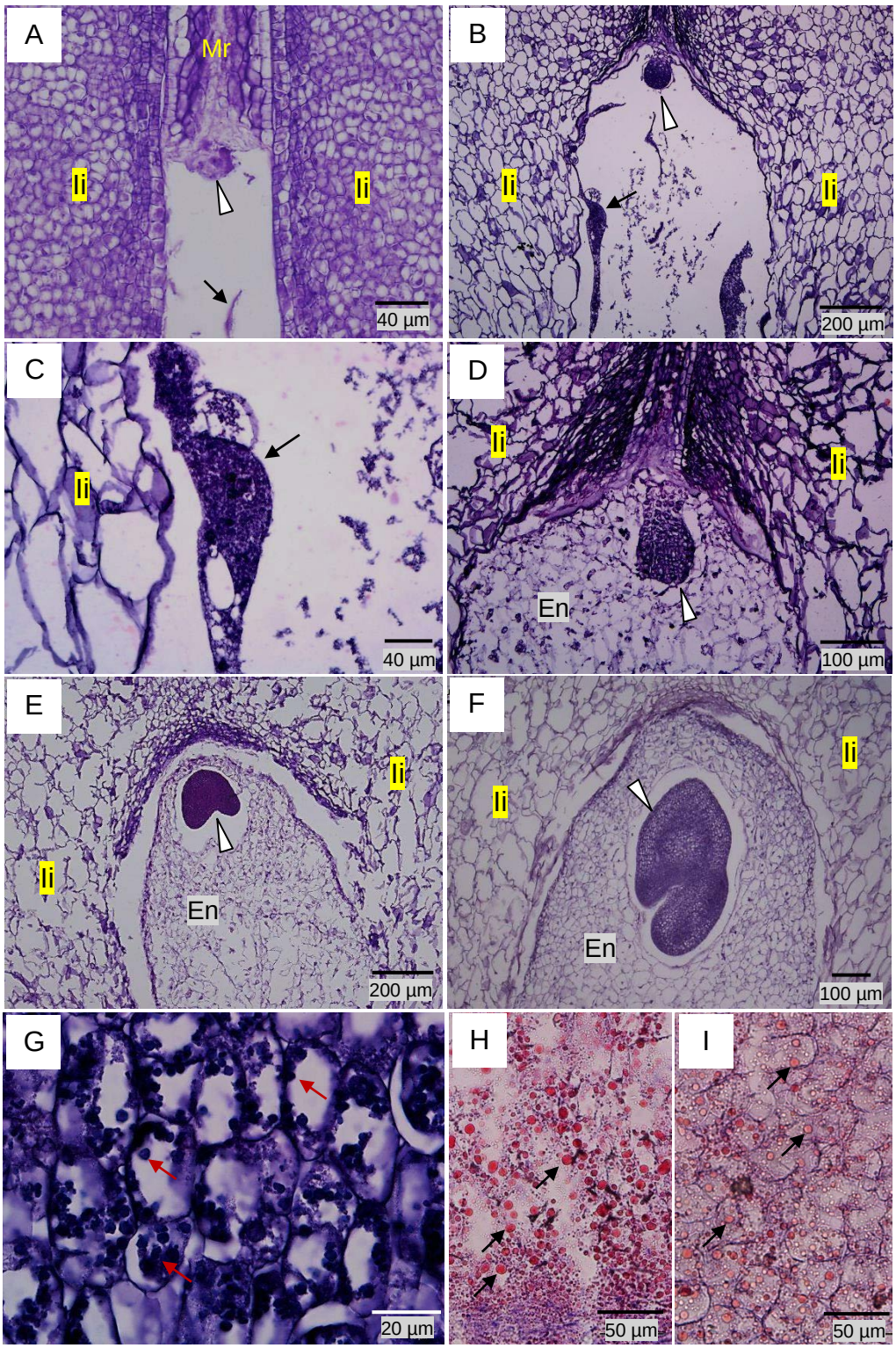

Figure 17 (see facing page for legend)

Figure 18 Embryo and endosperm development in cross-pollinated physic nut (**A**) Globular embryo (arrowheads) and endosperm (arrow) at 3 DAP; (**B**) Free nuclear-stage endosperm (arrows) at 3 DAP; (**C**) Globular embryo (arrowhead) and endosperm (En) at 18 DAP; (**D**) Cellular-stage endosperm (arrows) at 18 DAP; (**E**) Heart-shaped embryo (arrowhead) and endosperm (En) at 21 DAP; (**F**) Cellular endosperm cell at 21 DAP; (**G**) Torpedo-shaped embryo (arrowhead) and endosperm (En) at 27 DAP; (**H**) Cellular endosperm at 27 DAP; (**I**) Endosperm with storage globules (arrows); Oil droplets (arrows) in (**J**) mature embryo and (**K**) in mature endosperm. Ii, inner integument; En, endosperm; Mr, micropylar region; Nu, nucellus; Oi, outer integument; Pc, pericarp

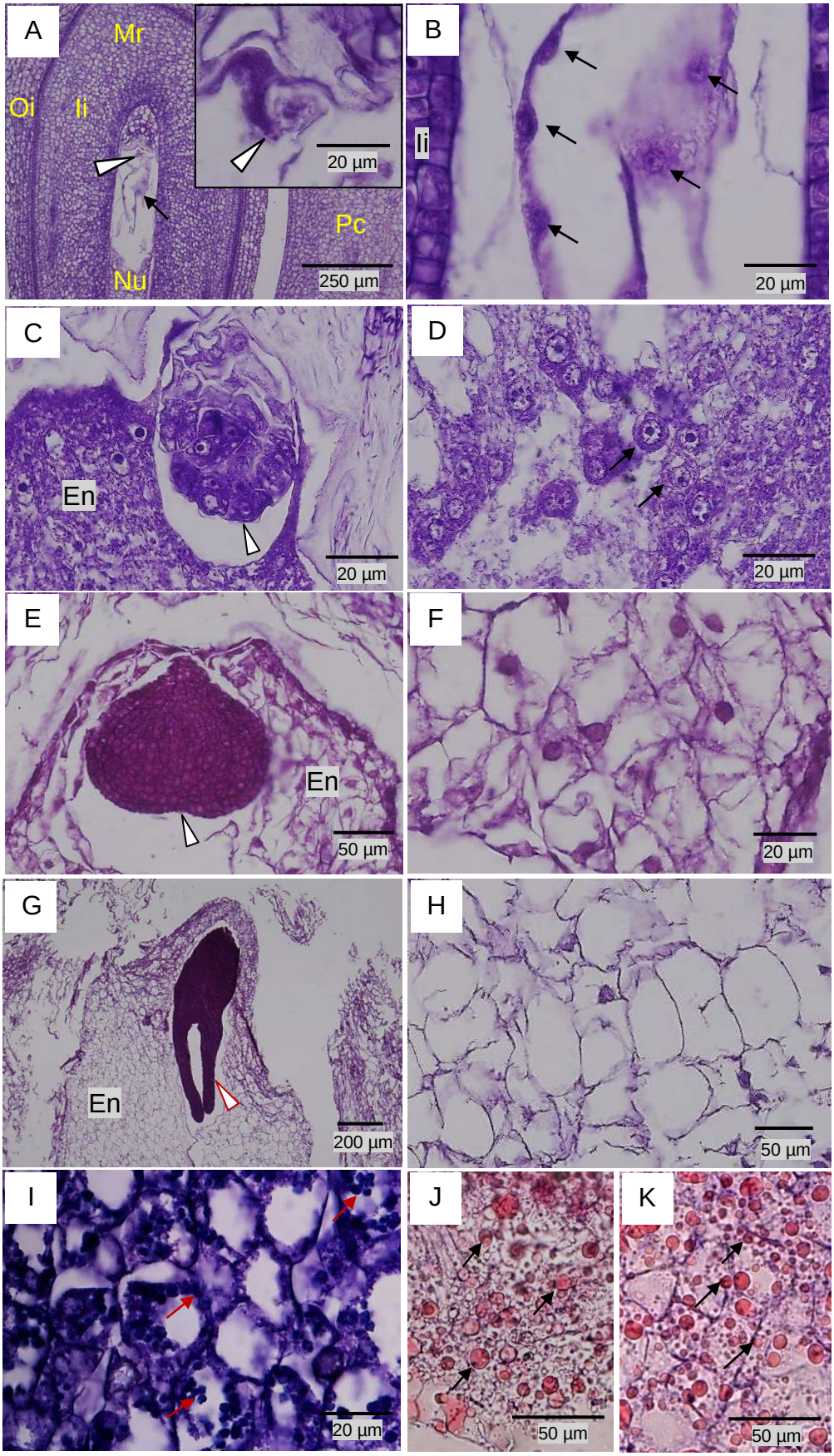

Figure 18 (see facing page for legend)

Figure 19 Embryo and endosperm development in self-pollinated physic nut

(**A**) Developing embryo (arrowhead) at 3 DAP; (**B**) Developing endosperm (arrows) at 3 DAP; (**C**) Globular embryo (arrowhead) and endosperm (En) at 21 DAP; (**D**) At 24 DAP, showing embryo at a transition between heart shape and early torpedo stage (arrowhead); (**E**) Cotyledonary-stage embryo (arrowhead) and endosperm (En) at 27 DAP; (**F**) At 27 DAP, illustrating endosperm cells with nucleus but without reserved globules; (**G**) Mature endosperm with storage compounds (arrows); Oil droplets (arrows) in (**H**) mature embryo and (**I**) mature endosperm after Oil Red O staining. En, endosperm; Ii, inner integument; Mr, micropylar region

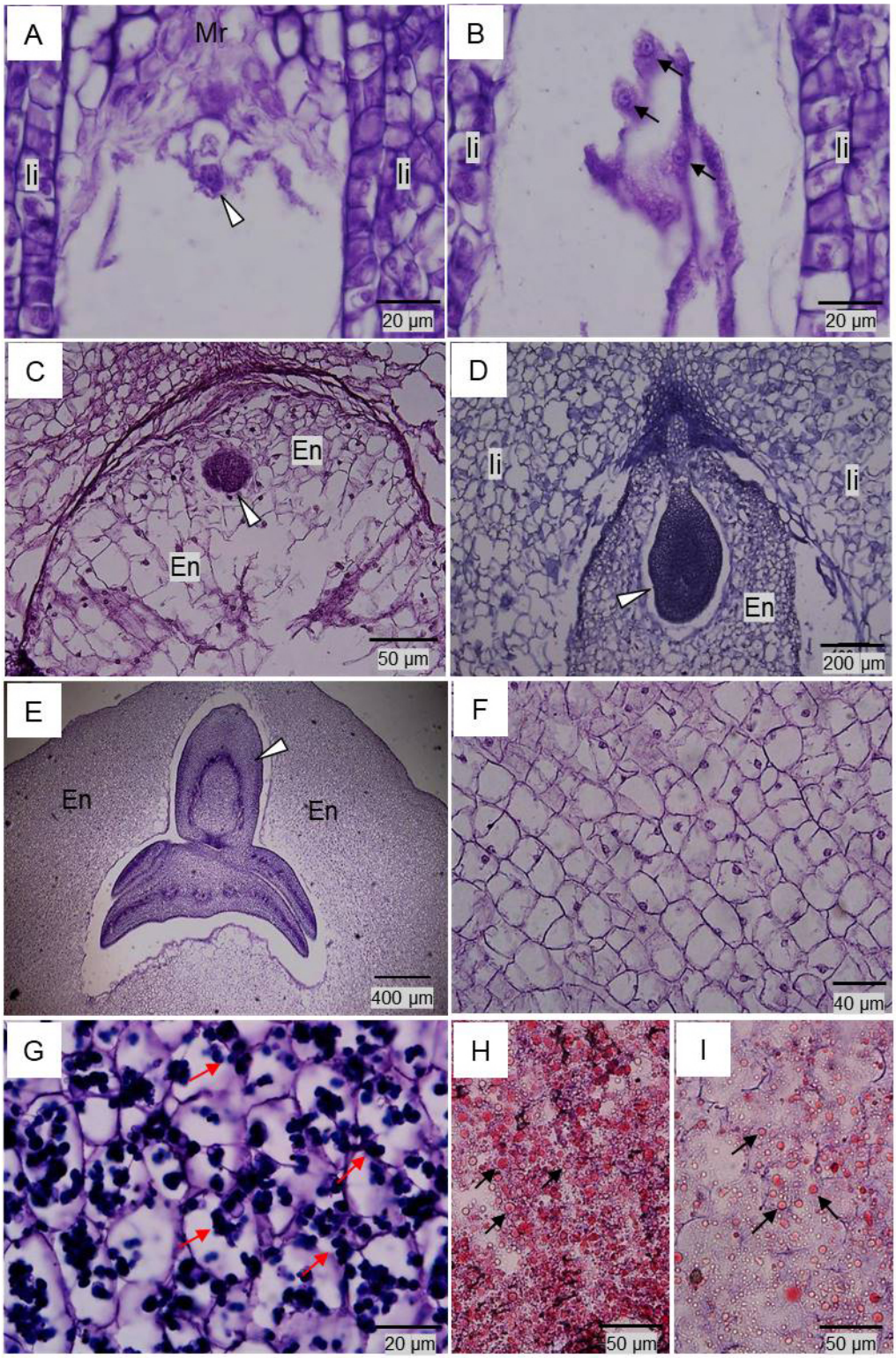

Figure 19 (see facing page for legend)

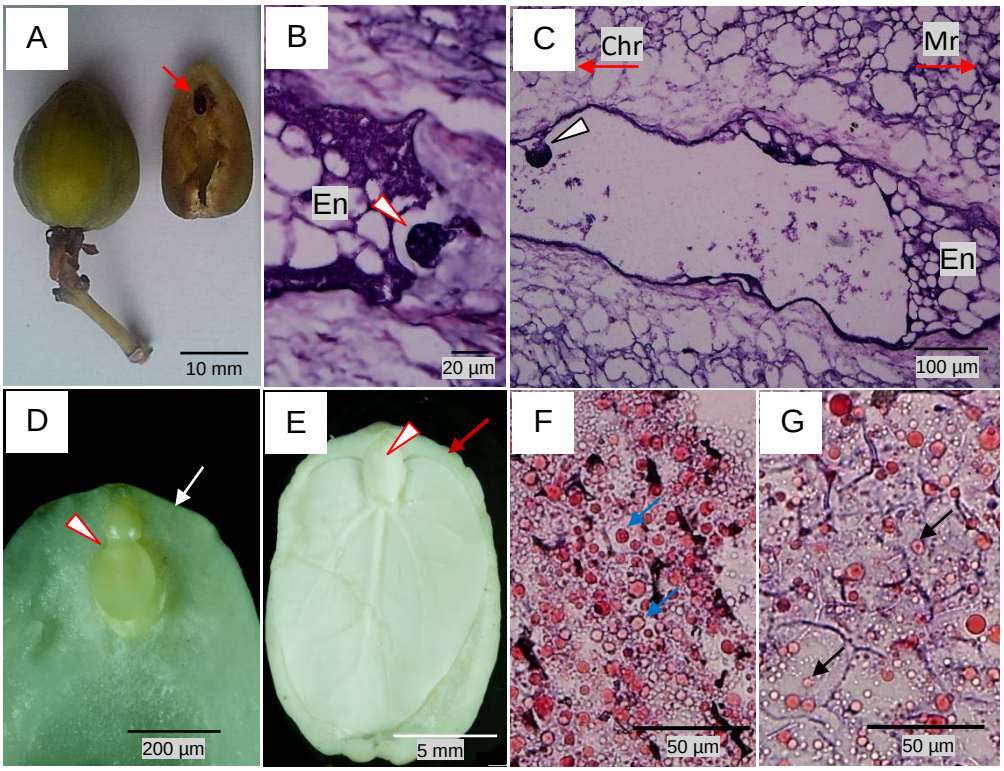

Figure 20 Fruit development of non-pollinated physic nut (apomixis)
(**A**) Abort seed (arrow) in developed fruit found at 36 DAF; (**B**) Globular embryo (arrowhead) and developing endosperm (En) at 15 DAF; (**C**) A plane towards the chalazal region of (**B**) showing globular embryo-like structure developed from nucellus area (arrowhead) at 15 DAF; (**D**) Torpedo-shape embryo (arrowhead) and endosperm (arrow) at 27 DAF; (**E**) Mature embryo (arrowhead) and thick endosperm (arrow); Oil droplets (arrows) in (**F**) mature embryo and (**G**) mature endosperm. Chr, chalazal region; En, endosperm; Mr, micropylar region

3.2.2 Total oil content and fatty acid analysis in whole mature seeds

Oil content and fatty acid profile in seeds, of all pollination types, were representing in Table 6. Percentage of oil content in open-pollinated seed (28.76 ± 1.60%) seemed to be maximal even though this was not significant different comparing with cross-pollinated seed (25.62 ± 1.05%), self-pollinated seed (22.90 ±

0.13%) and apomictic seed (23.09 ± 0.22%). For all pollinations, fourteen fatty acids could be analyzed from physic nut oil; however, the majority was oleic acid, linoleic acid, palmitic acid and stearic acid. Among these four fatty acids, oleic acid was the most predominant, existing nearly a half of all fatty acid compositions (47.16 ± 0.02 - 48.55 ± 0.02%), followed by linoleic acid (26.57 ± 0.01 - 28.64 ± 0.01%), palmitic acid (13.04 ± 0.01 - 13.50 ± 0.00%) and stearic acid (6.87 ± 0.00 - 7.65 ± 0.00%). The open-pollinated seeds contained the highest oleic acid (48.55 ± 0.02%) and MUFA content (49.45 ± 0.02%), while the non-pollination (apomixis) gave the lowest oleic acid (47.16 ± 0.02%) and MUFA (48.09 ± 0.02%).

Overall, seed oil content and fatty acid compositions were not very much different among pollination methods though some significant differences could be found (Table 6). Accordingly, the open-pollination method presenting the highest fruit set (74.33 ± 4.52%), the highest seed number (2.90 ± 0.08 seeds per fruit) and the most easiness to be manipulated in an orchard has been selected for further analysis on all following experiments (topic 3.2.3 and 3.3).

3.2.3 Lipid profiles in embryo and endosperm isolated from open-pollinated seeds

A. Total oil content and fatty acid compositions

The endosperm stored higher oil content (53.04 ± 1.43%) than the embryo (48.37 ± 0.34%) (Table 7). Ten fatty acids were discovered in isolated embryo and endosperm instead of fourteen fatty acids found in total seed; by lacking behenic acid, erucic acid, lignoceric acid and nervonic acid in embryo and endosperm (Table 7). Similar to total seed, oleic acid, linoleic acid, palmitic acid and stearic acid were dominant fatty acid in both embryo and endosperm. Endosperm reserved more oleic acid (45.95 ± 0.04%) and MUFA (46.82 ± 0.04%) than the embryo (38.41 ± 0.03% and 38.51 ± 0.03%, respectively).

Table 6 Fruit set, seed number and seed oil features of *J. curcas* among four pollination methods

	Open-pollination	**Cross-pollination**	**Self-pollination**	**Non-pollination (Apomixis)**
Fruit set (%)	74.33 ± 4.52^{a}	48.90 ± 4.12^{b}	31.10 ± 5.07^{c}	14.04 ± 2.73^{d}
Number of seed per fruit	2.90 ± 0.08^{a}	2.29 ± 0.12^{b}	2.23 ± 0.12^{bc}	1.94 ± 0.12^{c}
Oil content in seed (%)*	28.76 ± 1.60^{ns}	25.62 ± 1.05^{ns}	22.90 ± 0.13^{ns}	23.09 ± 0.22^{ns}
Fatty acid (% methyl ester)*				
Major fatty acids				
Palmitic acid (C16:0) **	13.04 ± 0.01^{d}	13.50 ± 0.00^{a}	13.33 ± 0.00^{c}	13.47 ± 0.01^{b}
Stearic acid (C18:0)	7.65 ± 0.00^{a}	7.13 ± 0.00^{b}	6.87 ± 0.00^{d}	7.10 ± 0.00^{c}
Oleic acid (C18:1)	48.55 ± 0.02^{a}	48.16 ± 0.02^{b}	47.82 ± 0.01^{c}	47.16 ± 0.02^{d}
Linoleic acid (C18:2)	26.57 ± 0.01^{d}	27.42 ± 0.01^{c}	28.33 ± 0.01^{b}	28.64 ± 0.01^{a}
Minor fatty acids				
Myristic acid (C14:0)	0.05 ± 0.00^{b}	0.05 ± 0.00^{b}	0.06 ± 0.00^{a}	0.05 ± 0.00^{b}
Pentadecanoic acid (C15:0)	0.02 ± 0.00^{ns}	0.02 ± 0.00^{ns}	0.02 ± 0.00^{ns}	0.02 ± 0.00^{ns}
Palmitoleic acid (C16:1)	0.81 ± 0.00^{d}	0.85 ± 0.00^{b}	0.88 ± 0.00^{a}	0.83 ± 0.00^{c}
Heptadecanoic acid (C17:0)	0.11 ± 0.00^{b}	0.11 ± 0.00^{b}	0.12 ± 0.00^{a}	0.11 ± 0.00^{b}
Linolenic acid (C18:3)	0.19 ± 0.00^{d}	0.25 ± 0.00^{b}	0.27 ± 0.00^{a}	0.23 ± 0.00^{c}
Arachidic acid (C20:0)	0.24 ± 0.00^{a}	0.24 ± 0.00^{a}	0.24 ± 0.00^{a}	0.23 ± 0.00^{b}
Behenic acid (C22:0)	0.05 ± 0.00^{a}	0.04 ± 0.02^{c}	0.06 ± 0.00^{a}	0.05 ± 0.00^{b}
Erucic acid (C22:1)	0.03 ± 0.00^{b}	0.04 ± 0.00^{a}	0.03 ± 0.00^{b}	0.04 ± 0.00^{a}
Lignoceric acid (C24:0)	0.07 ± 0.00^{b}	0.07 ± 0.00^{a}	0.07 ± 0.00^{a}	0.07 ± 0.00^{a}
Nervonic acid (C24:1)	0.06 ± 0.00^{ns}	0.06 ± 0.00^{ns}	0.06 ± 0.00^{ns}	0.06 ± 0.00^{ns}
SFA	21.22 ± 0.01^{a}	21.17 ± 0.03^{a}	20.77 ± 0.01^{c}	21.10 ± 0.01^{b}
MUFA	49.45 ± 0.02^{a}	49.11 ± 0.02^{b}	48.80 ± 0.02^{c}	48.09 ± 0.02^{d}
PUFA	26.76 ± 0.01^{d}	27.66 ± 0.01^{c}	28.60 ± 0.01^{b}	28.87 ± 0.01^{a}

Values are mean ± S.E. In each row, means followed by the same letter are not significantly different at the $P \leq 0.05$.

ns = no significant difference, * Extracted from total seed including seed coat

**number of carbon chain length: number of unsaturated bonds

Table 7 Characteristics of oil extracted from whole seed, embryo and endosperm of open-pollinated physic nut

	Whole seed*	**Embryo**	**Endosperm**
Oil body size (µm)	2.52 ± 0.08^{ns}	2.84 ± 0.12^{ns}	2.64 ± 0.11^{ns}
Oil content (%)	28.76 ± 1.60^{c}	48.37 ± 0.34^{b}	53.04 ± 1.43^{a}
Fatty acid (% methyl ester)			
Major fatty acids			
Palmitic acid (C16:0)	13.04 ± 0.01^{b}	10.35 ± 0.01^{c}	13.93 ± 0.01^{a}
Stearic acid (C18:0)	7.65 ± 0.00^{b}	13.57 ± 0.01^{a}	6.78 ± 0.00^{c}
Oleic acid (C18:1)	48.55 ± 0.02^{a}	38.41 ± 0.03^{c}	45.95 ± 0.04^{b}
Linoleic acid (C18:2)	26.57 ± 0.01^{c}	36.19 ± 0.03^{a}	31.84 ± 0.04^{b}
Minor fatty acids			
Myristic acid (C14:0)	0.05 ± 0.00^{c}	0.11 ± 0.00^{a}	0.06 ± 0.00^{b}
Pentadecanoic acid (C15:0)	0.02 ± 0.00^{b}	0.03 ± 0.00^{a}	0.02 ± 0.00^{b}
Palmitoleic acid (C16:1)	0.81 ± 0.00^{b}	0.10 ± 0.00^{c}	0.87 ± 0.00^{a}
Heptadecanoic acid (C17:0)	0.11 ± 0.00^{b}	0.15 ± 0.01^{a}	0.11 ± 0.00^{b}
Linolenic acid (C18:3)	0.19 ± 0.00^{b}	0.73 ± 0.02^{a}	0.16 ± 0.01^{c}
Arachidic acid (C20:0)	0.24 ± 0.00^{a}	0.23 ± 0.00^{b}	0.08 ± 0.00^{c}
Behenic acid (C22:0)	0.05 ± 0.00^{a}	0.00 ± 0.00^{b}	0.00 ± 0.00^{b}
Erucic acid (C22:1)	0.03 ± 0.00^{a}	0.00 ± 0.00^{b}	0.00 ± 0.00^{b}
Lignoceric acid (C24:0)	0.07 ± 0.00^{a}	0.00 ± 0.00^{b}	0.00 ± 0.00^{b}
Nervonic acid (C24:1)	0.06 ± 0.00^{a}	0.00 ± 0.00^{b}	0.00 ± 0.00^{b}
SFA	21.22 ± 0.01^{b}	24.44 ± 0.01^{a}	21.00 ± 0.01^{c}
MUFA	49.45 ± 0.02^{a}	38.51 ± 0.03^{c}	46.82 ± 0.04^{b}
PUFA	26.76 ± 0.01^{c}	36.92 ± 0.05^{a}	32.00 ± 0.03^{b}

Values are mean ± S.E. In each row, means followed by the same letter are not significantly different at the $P \leq 0.05$.

ns = no significant difference * With seed coat

B. Oil body characteristics

Oil bodies isolated from whole seed, embryo and endosperm formed a milky layer (Figure 21A and B, arrowheads) on the top of Eppendorf tube during extraction process. The oil body sizes, among the seed tissues, were not significant different, showing 2.52 ± 0.08, 2.84 ± 0.12 and 2.64 ± 0.11 µm in diameter for the whole seed, embryo and endosperm, respectively (Table 7). The presence of lipids in isolated oil bodies were illustrated by the red inflorescence after Nile red staining (Figure 22). The neutral lipids reserved in physic nut oil bodies were chiefly TAG after TLC analysis (Figure 23). Four bands of oil body protein (27, 17, 15 and 14 kDa) were found in the whole seed, embryo and endosperm (Figure 24A). The 27-kDa protein found in physic nut oil bodies could be cross-recognized by antibodies against sesame caleosin (Figure 24B). However, no cross-recognition was detected by antibodies against sesame oleosin-H (Figure 24C) and oleosin-L (Figure24D). LC-MS/MS analysis confirmed that 27, 17, 15 and 14 kDa protein highly matched to hypothetical protein JCGZ_02382 (caleosin), oleosin 2 (H-form), oleosin 3 (L-form) and 14.3-kDa oleosin (L-form) of *J. curcas* in database by producing 8, 5, 3 and 2 matched peptide residuals, respectively (Table 8).

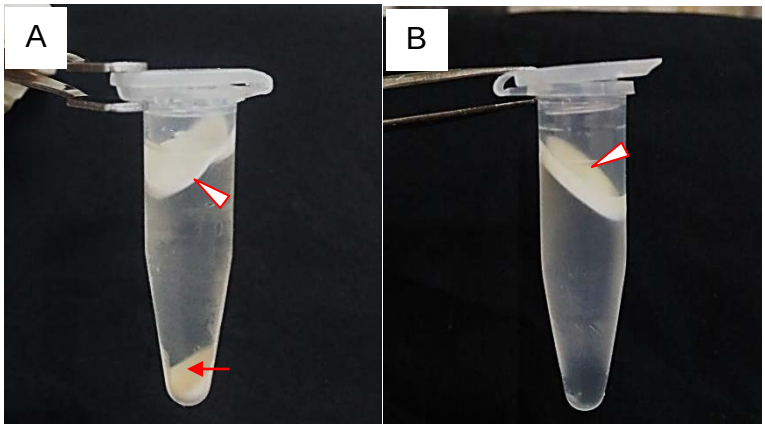

Figure 21 Isolated oil bodies forming a milky layer
(**A**) Crude oil bodies (arrowhead) and debris (arrow); (**B**) Purified oil body layer (arrowhead)

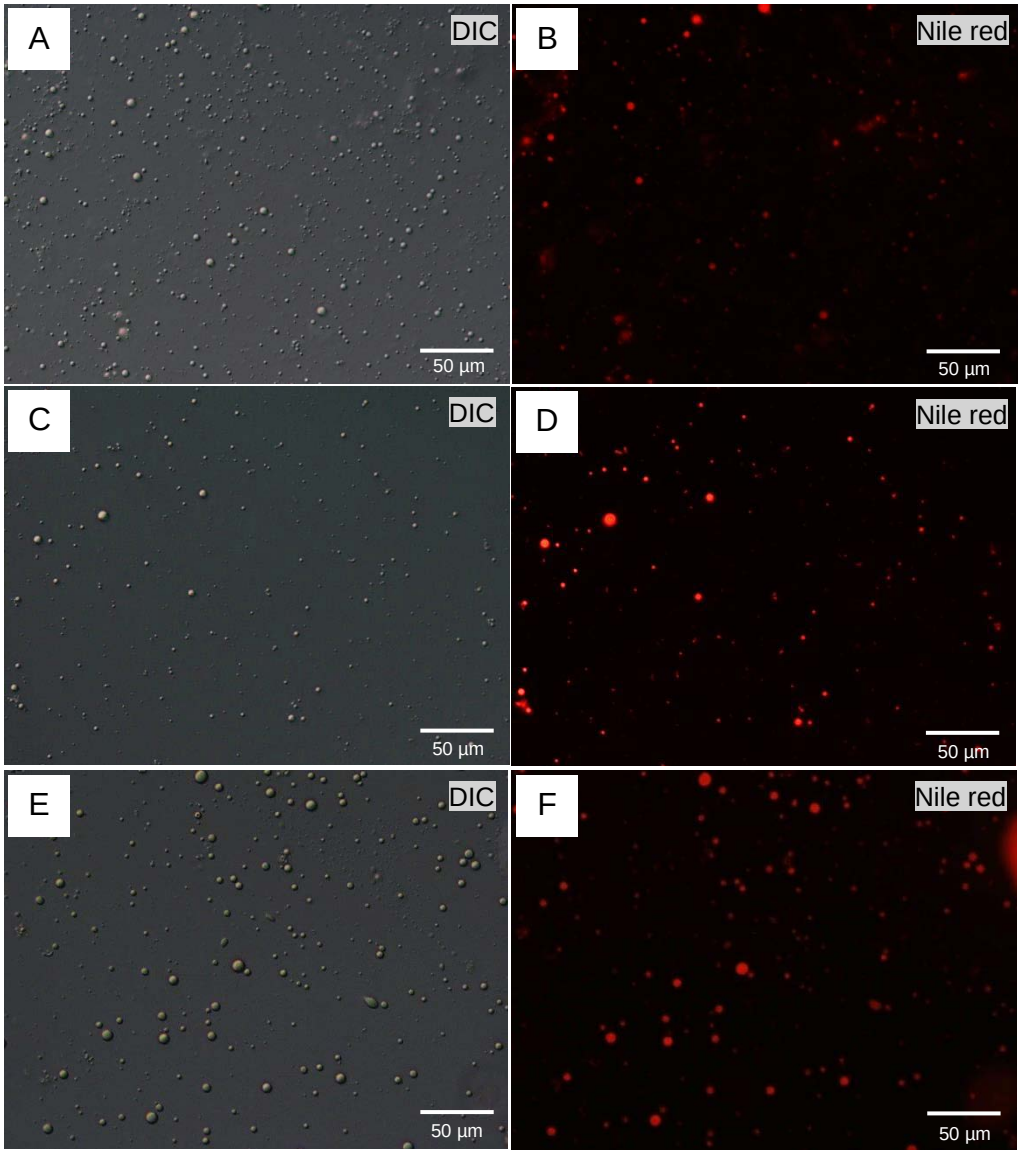

Figure 22 Neutral lipid in oil bodies by Nile red staining
Oil bodies from the whole seed observed under (**A**) DIC and (**B**) fluorescence; Oil bodies from (**C**, **D**) embryo and (**E**, **F**) endosperm

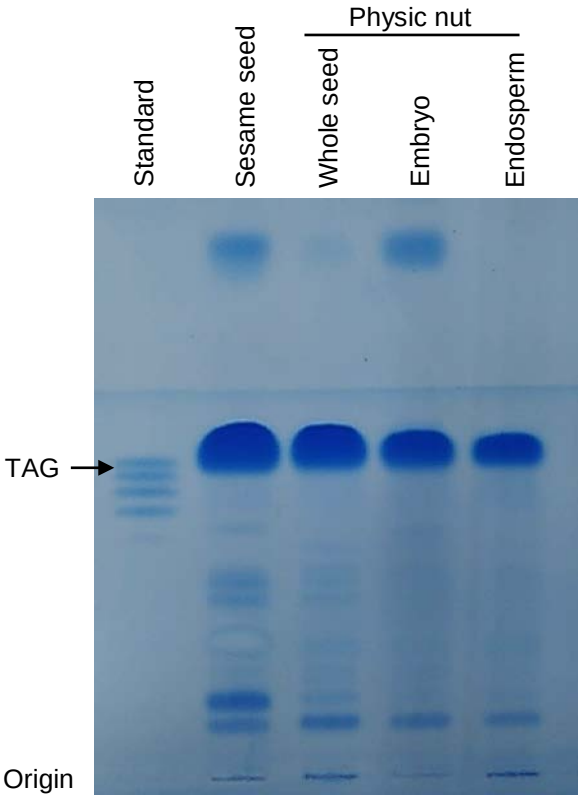

Figure 23 Neutral lipid analyses in physic nut purified oil bodies by TLC Triacyglycerol (TAG) is marked on the left edge

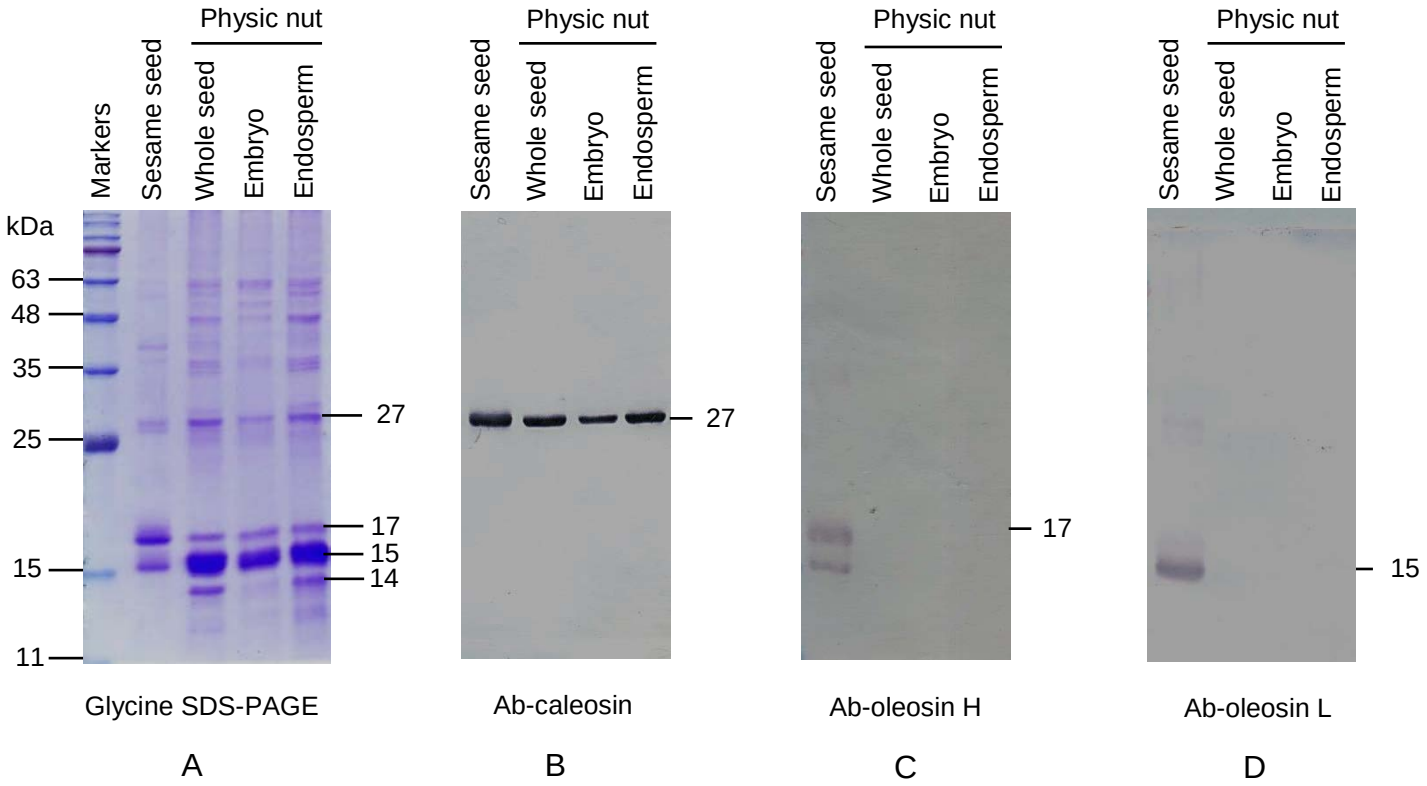

Figure 24 SDS-PAGE and Western blots of oil body protein extracted from whole seed, embryo and endosperm of open-pollinated seed

(**A**) Molecular masses of presumable caleosin (27 kDa), oleosin-H (17 kDa), oleosin-L (15 kDa) and 14-kDa protein indicating on the right. Three duplicate gels were transferred onto nitrocellulose membrane and subjected to immunodetection using antibodies against (**B**) sesame caleosin (27 kDa), (**C**) oleosin-H (17 kDa), and (**D**) oleosin-L (15 kDa). The bands marked in **A** were excised from the gel and analyzed by LC-MS/MS.

Table 8 Protein fragments found in purified oil bodies of physic nut identified by LC-MS/MS

Apparent mass (kDa)	Identified protein	Residuals	Sequences*
27	Hypothetical protein JCGZ_02382 (caleosin)	5 – 11	TDDSLDR
		12 – 39	AAPFAPVTFHRPVRDDLETTLPKPYMAR
		40 – 56	ALQAPDTEHPQGTPGHK
		132 – 146	AKHGSDSGTYDTEGR
		147 – 158	YMPVNLENIFSK
		204 – 211	DEEGFLSK
		216 – 228	RCFDGSLFEYCAK
		229 – 238	MNMGSESKMY
17	Oleosin 2 (H-form)	18 – 23	YEAAFK
		110 – 116	YLQEVTR
		118 – 126	MPEQLDIAK
		129 – 139	MQDMAGFVGQK
		140 – 149	TKEVGQEIQR
15	Oleosin 3 (L-form)	1 – 15	MAEHPQSQHVGQQPR
		100 – 111	HPPGAENLDQAR
		123 – 137	DRAEQFGQHVTGQQT
14	14.3 kDa oleosin (L-form)	1 – 15	MAEHPQSQHVGQQPR
		125 – 137	AEQFGQHVTGQQT

H-form, high molecular weight isoform

L-form, low molecular weight isoform

* see the appendix J for the full name of each amino acid

3.3 Establishment and lipid analysis of *J. curcas* cell suspension

3.3.1 Callus induction, growth features and microscopic observation

The survival rate of seedlings cultured in MS medium without PGRs was 91.13 ± 3.63%. Hypocotyls of 10-day-old seedlings presenting no true leaf were cut into tTCL explants (Figure 25) and used for callus induction. Results of callus induction and callus fresh weight at 4 weeks of culture were represented in Table 9. It illustrated that the combination of 2, 4-D and KN or 2, 4-D alone could induce the callus. While media without the PGRs (control) or with KN alone could not induce any calli and the explants turned to yellow brown color in control (Figure 26A) and in 0.5 mg L^{-1} KN and were swollen and cracked in 1 mg L^{-1} KN alone (Figure 26B). Initiation of callus could be observed at the cut end of explant since the fourth day of culture. The combination of 1 mg L^{-1} 2, 4-D and 0.5 mg L^{-1} KN promoted the best callus induction (97.22 ± 2.78%). Meanwhile, application of 0.5 mg L^{-1} 2, 4-D alone into medium could induce the minimal callus (22.20 ± 11.11%). All calli had similar yellow-green color and were compact type (Figure 26C). Among all treatments, the combination of 1 mg L^{-1} 2, 4-D and 0.5 mg L^{-1} KN seemed to stimulate the highest fresh weigh of callus (90.00 ± 24.24 mg $explant^{-1}$), while 0.5 mg L^{-1} 2, 4-D alone had the least deficiency to stimulate the callus growth (0.83 ± 0.60 mg $explant^{-1}$) (Table 9). Hence, medium supplied by 1 mg L^{-1} 2, 4-D and 0.5 mg L^{-1} KN was chosen for examining growth features of callus and using for cell suspension culture experiment based on its highest callus induction and fresh weight.

Fresh and dry weight of the compact callus showed sigmoid pattern during continuously five weeks of culture (Figure 27). Three distinct periods – lag, log and stationary phase were obtained at around week0 - week1, week1 - week3 and week3 - week5, respectively. At the third week after culture, the fresh and dry weight were maximum at 305.17 ± 42.17 and 16.08 ± 1.90 mg per 100 mg initial weight, respectively (approximately 3-fold higher than the initial week) (Figure 27).

Based on those growth patterns of fresh and dry weight, the compact callus was subcultured at 1-month intervals for maintaining. By continuity of subculture, the friable callus could occasionally be observed. The compact callus could be noticeable by more dark green color (Figure 28A), while friable callus was light green (Figure 28B). Proliferation of callus (for both compact and friable type) developed from the surface area of the original clump of callus by both periclinal and anticlinal division of cell (Figure 28C and D). Apparently, the cells of compact callus were densely aggregated and tightly packed together (Figure 28C) while those of friable callus were looser and larger as well as presenting intercellular space (Figure 28D).

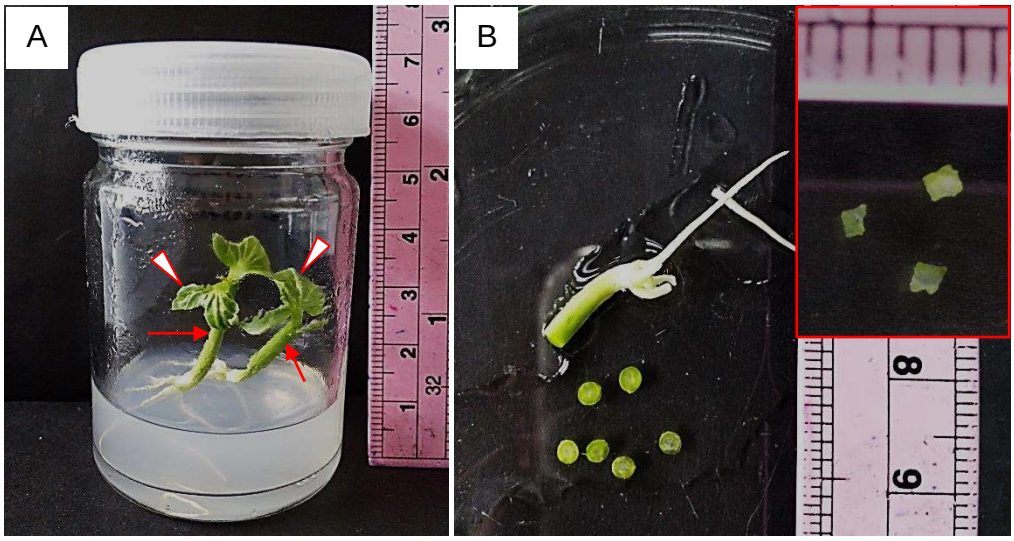

Figure 25 10-day-old seedlings cultured on MS medium without PGRs (**A**) Cotyledon (arrowheads) and hypocotyls (arrows); (**B**) Hypocotyl slices (afterwards cut into tTCL explants in the inset) used for callus induction

Table 9 Callus induction from tTCL-hypocotyls of 10-day-old seedling cultured on MS medium supplemented with various concentrations of PGRs at 4 weeks after culture

Treatment	PGRs (mg L^{-1})		Callus Induction (%)	Callus fresh weight (mg $explant^{-1}$)	Explant/Callus visual observation
	2, 4-D	KN			
1	0	0	0.00 ± 0.00[c]	–	Brown explant
2	0	0.5	0.00 ± 0.00[c]	–	Brown explant
3	0	1	0.00 ± 0.00[c]	–	Brown, swollen and crack explant
4	0.5	0	22.20 ± 11.11[c]	0.83 ± 0.60[c]	Yellow-green compact
5	0.5	0.5	63.89 ± 10.43[b]	15.97 ± 6.87[c]	Yellow-green compact
6	0.5	1	69.44 ± 11.21[b]	67.92 ± 14.80[b]	Yellow-green compact
7	1	0	61.11 ± 12.19[b]	27.22 ± 5.16[c]	Yellow-green compact
8	1	0.5	97.22 ± 2.78[a]	90.00 ± 24.24[a]	Yellow-green compact
9	1	1	94.44 ± 3.75[a]	65.69 ± 7.22[a]	Yellow-green compact

Values are mean ± S.E. In each column, means followed by the same letter are not significantly different at $P \leq 0.05$.

–, no callus formation

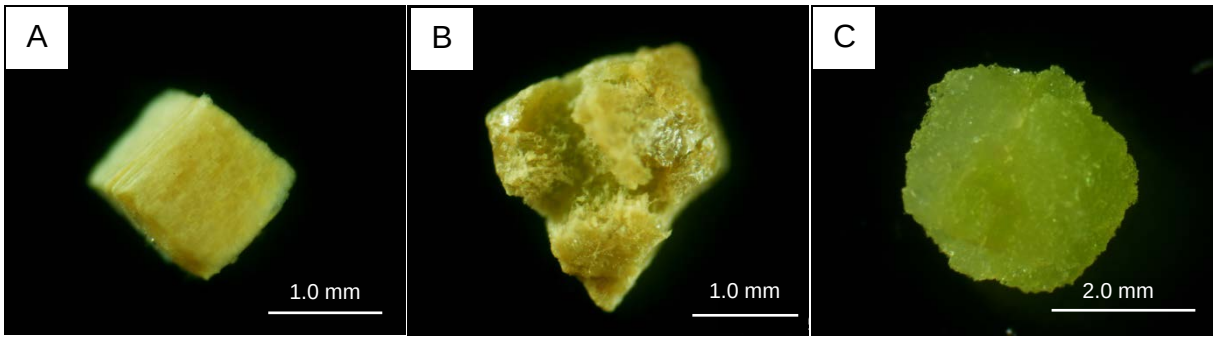

Figure 26 Morphological features of (**A-B**) explants and (**C**) callus at 4 weeks after culture

(**A**) Brown explant in control; (**B**) Crack explant after cultured on the medium containing on 1 mg L^{-1} KN alone; (**C**) Compact callus exhibiting yellow green color obtained from the treatments with a combination of 1 mg L^{-1} 2, 4-D and 0.5 mg L^{-1} KN

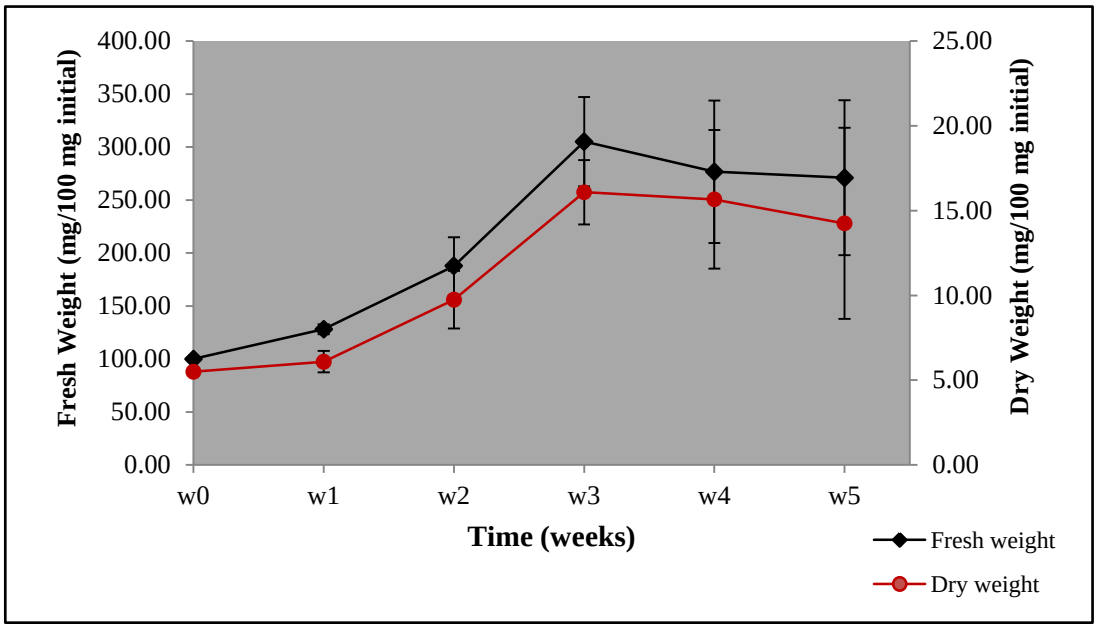

Figure 27 Fresh and dry weight of compact callus cultured on medium containing 1 mg L^{-1} 2, 4-D in combination with 0.5 mg L^{-1} KN

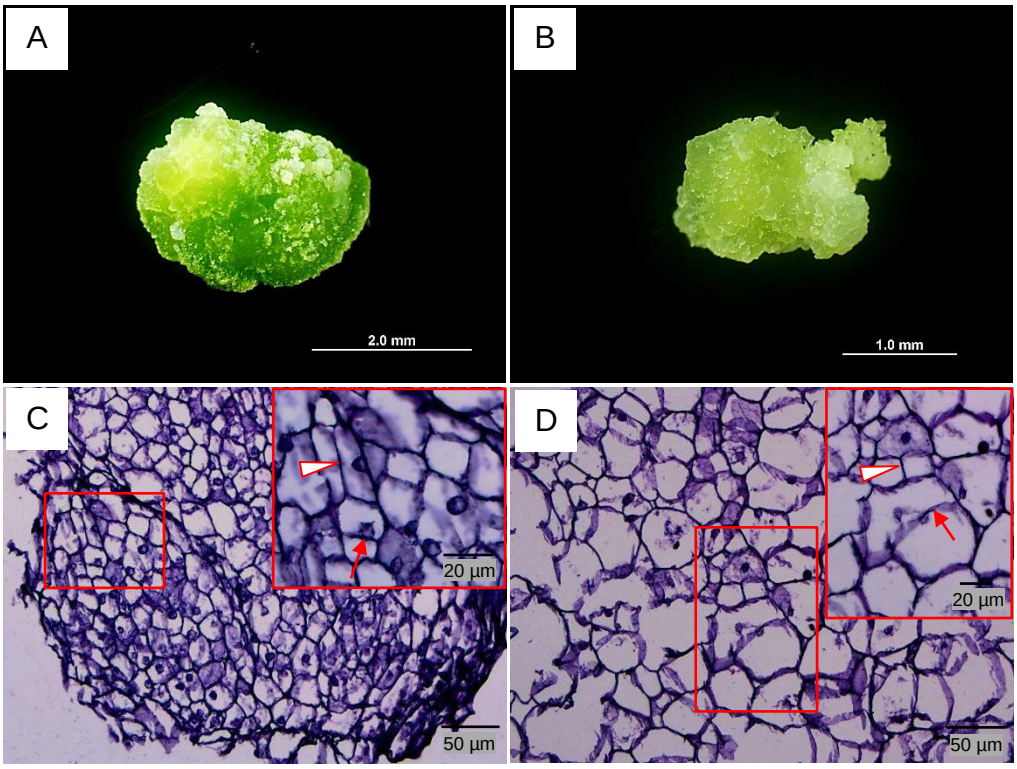

Figure 28 Morphological and histological features of compact and friable callus obtained after subculture at 1-month intervals on medium containing 1 mg L^{-1} 2, 4-D in combination with 0.5 mg L^{-1} KN

(**A**) Compact callus; (**B**) Friable callus; (**C**) Compact callus showing callus cells with periclinal (arrowhead) and anticlinal divisions (arrow); **(D**) Friable callus exhibiting periclinal (arrowhead) and anticlinal division (arrow)

3.3.2 Cell suspension culture and analysis

Cell suspension was established in liquid MS medium supplemented with 1 mg L^{-1} 2, 4-D and 0.5 mg L^{-1} KN. Similar to the callus, the fresh and dry weight of cells displayed sigmoid-shaped pattern (Figure 29A). They increased sharply during the Week1 - Week2 of culture, slightly increased at Week3 and decreased thereafter. At the third week after culture, the fresh weight reached the maximal value at 4,356.67 ± 578.72 mg (around 2-time increment compared to the initial week) as the dry weight had the peak value at 99.33 ± 11.84 mg (about 5-fold increment compared with the initial week).

It illustrated that the pH of liquid medium was reduced from 5.83 ± 0.01 (before autoclaving) to 5.36 ± 0.01 after autoclaving (Week0). The pH dropped to 4.85 ± 0.13 at the first week of culture period and then gradually increased to the maximum of 6.63 ± 0.08 at the fifth week (Figure 29B). The increment of pH medium from 4.85 to 5.75 (during Week1 - Week3) was conformed to the steep period of fresh and dry weight enlargement. Noticeably, by visual observation, the medium color became turbid within 2 weeks after culture.

Over the culture period, chlorophyll *b* was higher than chlorophyll *a* and carotenoid was the least accumulated pigment in the cell suspension (Figure 30A). Two-week-old cells had the maximal content of all pigments; 1.04 ± 0.10, 0.67 ± 0.06, 0.56 ± 0.06 and 0.19 ± 0.01 mg g^{-1} FW for total chlorophyll, chlorophyll *b*, chlorophyll *a* and carotenoid, respectively.

By using TTC reduction assay, the viable cells displayed red color (Figure 30B, inset). It revealed that the cells had supreme viability during Week1 to Week2 of culture period.

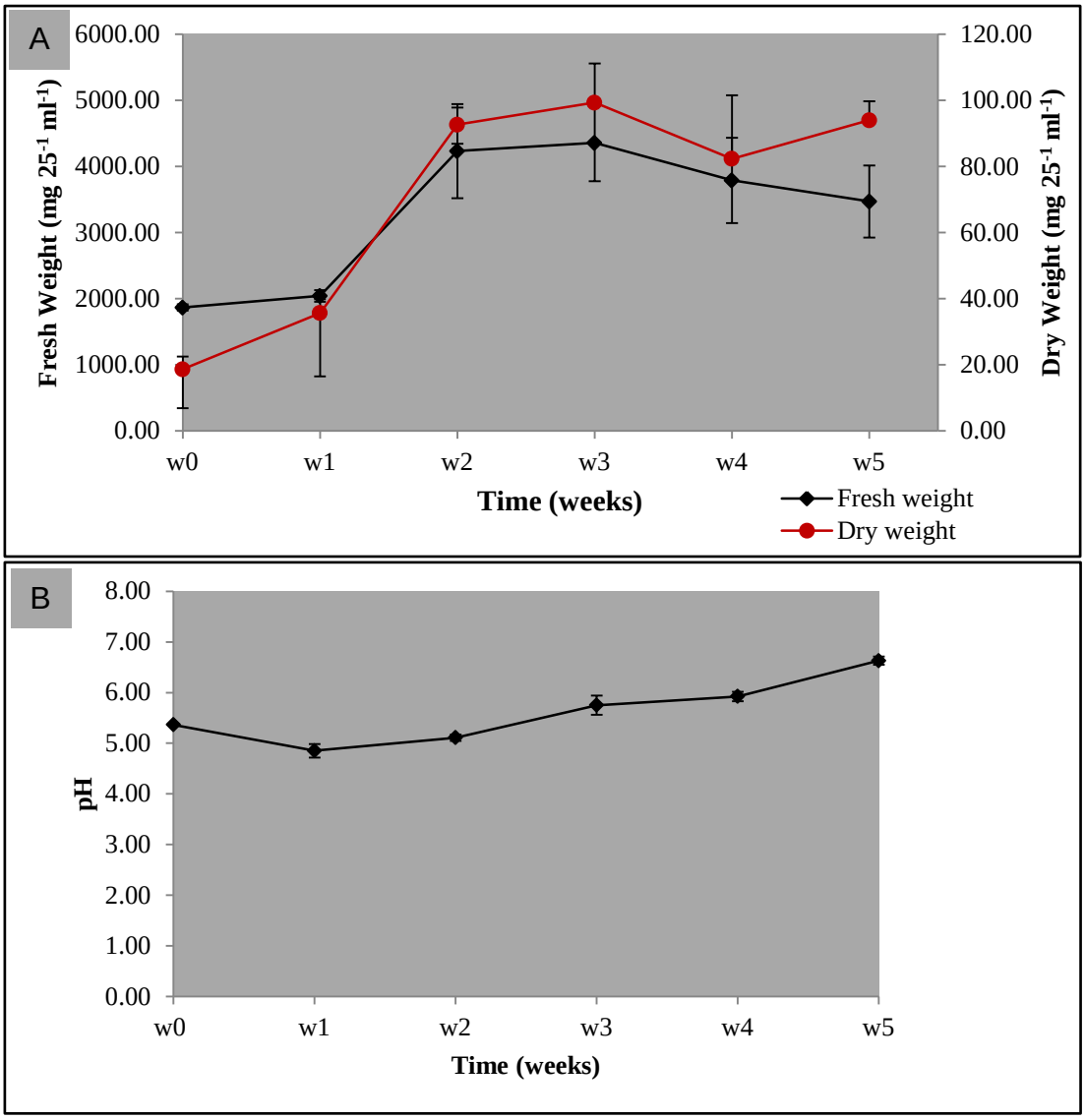

Figure 29 Growth curve of cell suspension and pH change of the cultured medium during cell culture in MS medium containing 1 mg L^{-1} 2, 4-D and 0.5 mg L^{-1} KN

(**A**) Fresh and dry weight following S-shaped pattern; (**B**) Alteration of pH in liquid medium

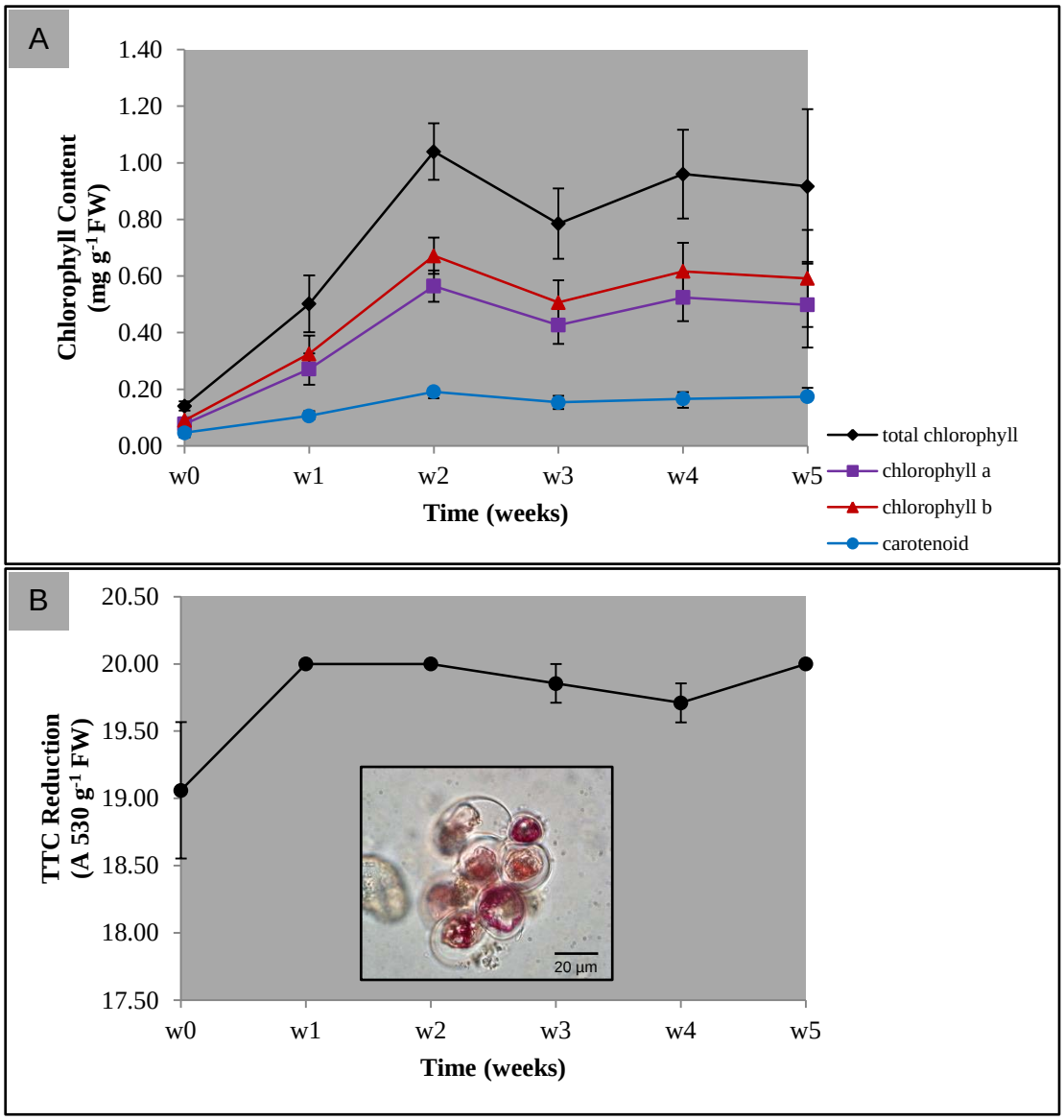

Figure 30 Pigment content and viability of cell suspension cultured in MS medium added with 1 mg L^{-1} 2, 4-D and 0.5 mg L^{-1} KN

(**A**) Total chlorophyll, chlorophyll *a*, chlorophyll *b* and carotenoid content; (**B**) Cell viability by TTC reduction assay, the inset representing viable cells with red color after stained with TTC solution

Based on those fresh weight, dry weight, viability as well as the color and pH alteration of the medium, the cells were subcultured every 2 weeks by transferring 5 ml of cell suspension culture from the old medium to 20 ml of fresh medium. At 2 weeks after subculture, most of the cells became larger aggregate (Figure 31A and B). However, the smaller or finer aggregate cells could also be observed in the liquid medium (Figure 31A, C). Anatomical observation unveiled two distinct regions for those large aggregate cells – the peripheral area and the central region (Figure 32A). The cell clump increased its mass by both periclinal and anticlinal divisions of meristematic cells (presenting obvious nucleus and dense cytoplasm) located at peripheral regions (Figure 32B). Oil droplets could be found in the cytoplasm of the aggregate cell suspension (Figure 32C).

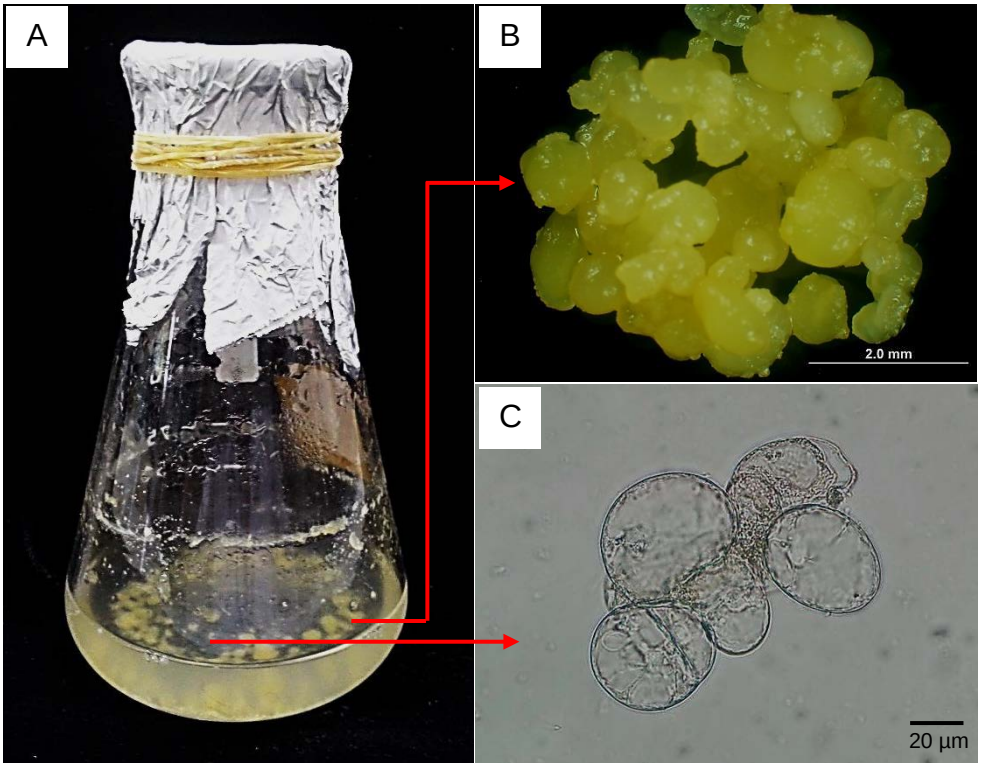

Figure 31 Cell suspension of physic nut in liquid medium added with 1 mg L^{-1} 2, 4-D and 0.5 mg L^{-1} KN

(**A**) Two-week-old cells; (**B**) Larger aggregate cells; (**C**) Smaller aggregate cells

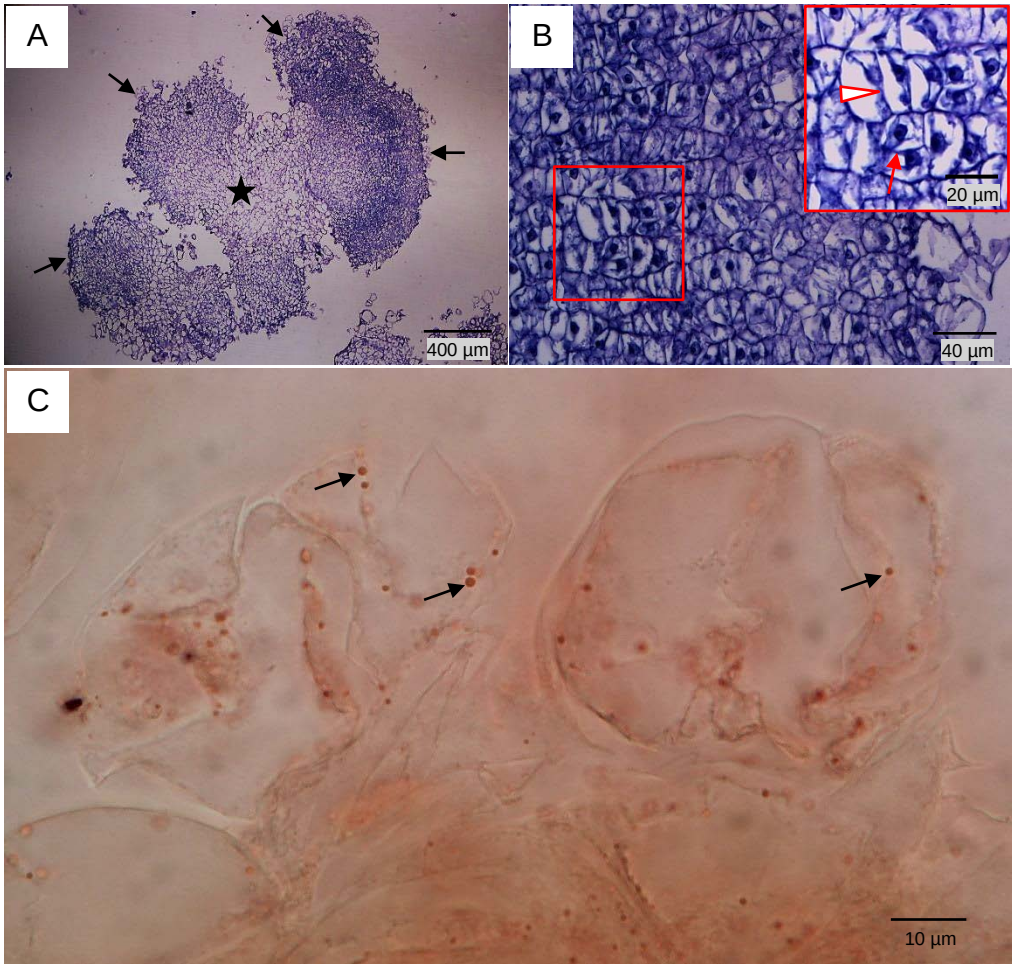

Figure 32 Histological characteristics of 2-week-old cells cultured in liquid MS medium containing 1 mg L^{-1} 2, 4-D and 0.5 mg L^{-1} KN

(**A**) Large aggregate cells showing border regions (arrows) and the central area (star); (**B**) Border region of cell cluster displaying cell with obvious nucleus and dense cytoplasm. The cells exhibiting periclinal (arrowhead) and anticlinal division (arrow); (**C**) Lipid droplets (arrows) in the cytoplasm of cell stained with Oil Red O

Total oil content extracted from 2-week-old cells was 3.84 ± 0.33% and comprised of oleic (36.13 ± 0.16%, the higest proportion), linolenic (21.45 ± 0.04%), palmitic (20.16 ± 0.08%), linoleic (11.43 ± 0.06%) and stearic acid (3.08 ± 0.01%) as the dominant types. Overall, the cells reserved more MUFA (36.87 ± 0.15%) than PUFA (32.88 ± 0.09%) and SFA (26.83 ± 0.12%) (Table 10).

The cell suspension contained significantly lower oil content, displaying approximately 7-fold reduction of oil (3.84 ± 0.33%) compared to the whole seed (28.76 ± 1.60%) (Table 10). The amount of oleic (36.13 ± 0.16%), linoleic (11.43 ± 0.06%) and stearic acid (3.08 ± 0.01%) were also lower in the cell suspension than in the seed (48.55 ± 0.02%, 26.57 ± 0.01% and 7.65 ± 0.00%, respectively). Meanwhile, the cell suspension accumulated more palmitic (20.16 ± 0.08%) and linolenic acid (21.45 ± 0.04%) than did the seed. In particular, the amount of around 113-fold increment of linolenic acid was observed in the cell suspension in comparision with the whole seed. Totally, the cell suspension stored more SFA and PUFA but less MUFA than did the seed.

Table 10 Oil content and fatty acid compositions of cell suspension in comparison with the whole seed

	Cell suspension	**Whole seed**
Oil content (%)	3.84 ± 0.33[b]	28.76 ± 1.60[a]
Fatty acid (% methyl ester)		
Caprylic acid (C8:0)	0.01 ± 0.00[ns]	0.00 ± 0.00[ns]
Nonanoic acod (C9:0)	0.03 ± 0.00[a]	0.00 ± 0.00[b]
Capric acid (C10:0)	0.03 ± 0.00[a]	0.00 ± 0.00[b]
Undecanoic acid(C11:0)	0.01 ± 0.00[ns]	0.00 ± 0.00[ns]
Lauric acid (C12:0)	0.04 ± 0.00[a]	0.00 ± 0.00[b]
Tridecanoic acid (C13:0)	0.01 ± 0.00[ns]	0.00 ± 0.00[ns]
Myristic acid (C14:0)	0.22 ± 0.00[a]	0.05 ± 0.00[b]
Pentadecanoic acid (C15:0)	0.21 ± 0.00[a]	0.02 ± 0.00[b]
Palmitic acid (C16:0)	20.16 ± 0.08[a]	13.04 ± 0.01[b]
Palmitoleic acid (C16:1)	0.51 ± 0.00[b]	0.81 ± 0.00[a]
Heptadecanoic acid (C17:0)	0.30 ± 0.00[a]	0.11 ± 0.00[b]
Stearic acid (C18:0)	3.08 ± 0.01[b]	7.65 ± 0.00[a]
Oleic acid (C18:1)	36.13 ± 0.16[b]	48.55 ± 0.02[a]
Linoleic acid (C18:2)	11.43 ± 0.06[b]	26.57 ± 0.01[a]
Linolenic acid (C18:3)	21.45 ± 0.04[a]	0.19 ± 0.00[b]
Arachidic acid (C20:0)	0.18 ± 0.00[b]	0.24 ± 0.00[a]
Gondoic acid (C20:1)	0.23 ± 0.01[a]	0.00 ± 0.00[b]
Behenic acid (C22:0)	0.79 ± 0.02[a]	0.05 ± 0.00[b]
Erucic acid (C22:1)	0.00 ± 0.00[b]	0.03 ± 0.00[a]
Lignoceric acid (C24:0)	1.76 ± 0.07[a]	0.07 ± 0.00[b]
Nervonic acid (C24:1)	0.00 ± 0.00[b]	0.06 ± 0.00[a]
SFA	26.83 ± 0.12[a]	21.22 ± 0.01[b]
MUFA	36.87 ± 0.15[b]	49.45 ± 0.02[a]
PUFA	32.88 ± 0.09[a]	26.76 ± 0.01[b]

Values are mean ± S.E.

In each row, means followed by the same letter are not significantly different at the $P \leq 0.05$ by t-test.

ns = no significant difference

CHAPTER 4
DISCUSSION

4.1 Development and fertility of male and female gametophytes

4.1.1 General flower characteristics and gametophyte development

A. Male bud features and gametophyte development

In this study, pollen development of physic nut could be categorized into 5 developmental stages; namely, pollen mother cell (PMC), tetrad microspore, uninucleate microspore, binucleate pollen with globular-shaped generative cell and binucleate pollen with spindle-shaped generative cell, which highly corresponded to flower bud sizes of 1.0 - 1.5, 1.0 - 1.5, 1.6 - 2.0, 2.1 - 3.0 and ≥ 3.1 mm, respectively. As presenting for the first time in physic nut, the occurrence of nectary and filament, in this study, could not be utilized for characterizing the stage of pollen development in detail but could be used for a rough separation of sporogenesis from gametogenesis. The bud with no appearance of filament and nectary gland (1.0 - 2.0 mm) was of sporogenesis stage, whereas the bud with visible filament and white nectary gland (≥ 2.1 mm) was in gametogenesis process. However, both sporogenesis and gametogenesis of *Arabidopsis thaliana* were observed in flower buds exhibiting visual filament (Cardarelli and Cecchetti, 2014). Besides the filament and nectary, other morphological markers such as pistil color, anther pigmentation and petal color were successfully used as the easiest and accurate criteria for identifying the stages of microsporogenesis and microgametogenesis in *Nicotiana tabacum* (Koltunow et al., 1990), *Capsicum annuum* (Vega et al., 2013) and *Malus* × *domestica* (Zhang et al., 2013).

The bud diameter correlated to the pollen stage is available for easy and fast selection of the floral bud with desired developmental stage based on the bud diameter. Using of bud which the size correlated to the suitable stage of pollen development has been one of the crucial factors determining the success of in vitro

microspore or anther culture (Lauxen et al., 2003). The stages between vacuolated microspore to early/mid-bicellular pollen were suitable for such a culture in most species because of their proliferative transcriptional status (Malik et al., 2007; Ibrahim et al., 2014). For instance, 17 - 21 mm long buds correlated with first-mitosis pollen in *Nicotiana tabacum* (Kasperbauer and Wilson, 1979) and 6 - 8 mm long buds related to uninucleate microspore in *Hibiscus cannabinus* (Ibrahim et al., 2014) were optimized for the culture. Hence, from our result, the male flower buds with ≥ 1.6 mm in diameter presenting the haploid unicellular microspore or bicellular pollen are recommended for the induction of *J. curcas* haploid plant, as a preliminary test to find the optimized stage to be induced toward androgenesis. This haploid culture, as previously established and provided the significance for breeder in other plants such as *Arachis hypogaea* (Willcox et al., 1991) and *Malus* × *domestica* (Zhang et al., 2013), will also provide the homozygous genotypes necessary for breeding program to improve the variety of physic nut.

B. Female bud features and gametophyte development

The embryo sac development of this species confirmed that the MMC underwent meiosis and produced polygonum embryo sac with eight haploid nuclei – which corresponded to the study mentioned by Krishnamurthy (2013). The bud diameters of approximately 1.0 - 1.5, 1.6 - 2.0 and ≥ 2.1 mm were highly matched to MMC stage, megaspore or ≥ 2-nucleate embryo sac and 8-nucleate embryo sac, respectively. Similarly to the physic nut, the bud diameter of onion (*Allium cepa*) was related to stage of embryo sac development. It was shown that the flower buds at 2.3 - 3.0, 3.1 - 3.7 and 3.8 - 4.4 mm were chiefly of MMC, 2 - 8 nucleate embryo sac and 8-nucleate embryo sac, respectively (Musial et al., 2005). In addition, stigmatic formation and the nectary size in comparison to that of sterile stamen could be employed to mark the stage of embryo sac in physic nut. The buds possessed non-fully developed stigma and the smaller nectary gland than the sterile stamen were of megaspore mother cell, megaspore or ≥ 2-nucleate embryo sac, whereas those with the developed bifurcated stigma and the nectary gland with the size bigger than sterile stamen tangibly contained 8-nucleate embryo sac. This is the first report that

correlated the embryo sac stage to the stigmatic formation and nectary size in plant species. Using externally floral features to classify embryo sac stage could also be observed in *Iris tenax*. The buds with perianth much shorter, slightly shorter, equal to and higher than the anther possessed megasporocyte, 2-haploid sporocyte, T-shape tetrad and 2 - 4 cell embryo sacs, respectively. Whereas, the buds which stigmatic flap was appressed to the stigma lobe contained mature 8-nucleate embryo sac (Wilson, 2001).

Haploid and dihaploid culture to obtain the homozygous genotypes for developing new *Jatropha* variety could also be performed via the process of gynogenesis. Based on information from other plants, haploid or double haploid induction of *J. curcas* would be began by using ovules from ≥ 1.6-mm buds which contained haploid megaspore to mature embryo sac – to find the most appropriate stage of female gametophyte for the haploid culture. From literature, suitable stage of ovule for the in vitro culture varied among plant species, ranging from the stage of megaspore to mature embryo sac (Chen et al., 2010). For instance, haploid plantlet of *Nicotiana tabacum* could be induced by using young uninuclear megaspore to mature embryo sacs as explants (Wu and Chen, 1982). In *Beta vulgaris*, however, only mature embryo sac was successfully employed for the production of haploid plant via gynogenesis (Ferrant and Bouharmont, 1994). Meanwhile, 2 - 4 nucleate embryo sacs could be more responsive than other stages to such a culture for *Allium cepa* (Musial et al., 2005).

Earlier notion has shown the occurrence of stamen primordial at early stage (when the ovule primordial emerged), which restrained at later period (when the stigma and nectary were formed), in physic nut female flower (Wu et al., 2011). However, the abortion time in associate to the stage of embryo sac development had never provided in that study. Thus, this study for the first time confirmed that the stamens accompanying the female flower of physic nut were sterile at very early stage of female gametophyte development (at MMC stage). Accordingly, the sterile stamens might have no impacts on any pollination sets. The sterile stamen could also be observed evidently in the female flowers of relative species such as *Jatropha podagrica, J. gossypifolia* (Liu et al., 2008), *J. multifida and J. integerrima* (Liu et al., 2015).

4.1.2 Pollen viability assessment and stigma receptivity

The results herein shown that the cytoplasmic esterase (by FCR) and dehydrogenase (By TTC) in pollen, as well as the pollen germination percentage were diminished continuously after anthesis. This reduction of pollen viability and germination with time after shedding might relate with the loss of pollen water balance causing by changeable environment condition such as temperature and humidity (Heslop-Harrison and Heslop-Harrison; 1992) as previously shown in *Cistus incanus* and *Myrtus communis* (Aronne, 1999) and *Cucurbita pepo* (Nepi et al., 2010). Even with no significant difference, the TTC was slightly closer to the germination test (which reflects a true ability of pollen to germinate under in vitro conditions) than the FCR based on linear pattern. This implied that the TTC was more effective than the FCR for pollen fertility evaluation in physic nut. This finding could be supported by the study of Abdelgadir et al. (2012) who found that TTC was more reliable than FCR for testing pollen viability of physic nut, as the TTC but not FCR could distinguish the vital pollen from the dead one. The FCR test, sometimes, gave the false negative results (predicting excessively high potential germinated ability) if the pollen was immature or was not properly rehydrated before testing (Heslop-Harrison et al., 1984). Accordingly, TTC was favorite for the evaluation of pollen viability of this physic nut (Chang-Wei et al., 2007; Kaur et al., 2011). Kaur et al. (2011) reported that pollen viability of physic nut was 71% by TTC test and these viable pollens showed the purplish pink color after staining while the dead pollens remained colorless. It was also revealed that pollen viability of physic nut, by this TTC technique, was high during the first 9 hours after anthesis and then declined since 33 hours after anthesis (Chang-Wei et al., 2007). Among several staining techniques, only TTC provided the accurate result and could differentiate the fresh and the heat-killed pollen of *Kochia scoparia* (Mulugeta et al., 1994) and *Leymus chinensis* (Huang et al., 2004). However, TTC was not effective for pollen viability test of *Festuca arundinacea* because it stained both viable and dead pollen (Wang et al., 2004). In *Prunus laurocerasus*, the TTC could be employed for only a rough evaluation of viability since this technique showed a low correlation with germination test ($R^2 = 0.06$) (Sulusoglu and Cavusoglu, 2014).

The stigma receptivity of physic nut was evaluated by detecting the peroxidase (by hydrogen peroxide test) – the enzyme that loosed the stigmatic cell wall components and aid the pollen tube to penetrate into the ovule (Mclnnis et al., 2006). The stigma had high receptive at 97.22 - 100.00% for 3 days after flowering and seemed to have receptivity lower than 50% after the fifth day. This was relatively concurred with that accounted by Chang-Wei et al. (2007) who mentioned that stigma of physic nut was receptive at the first 4 days and began to decline at the fifth day. Stigma receptivity, as important as pollen viability, played a key factor influencing the success of pollination and seed production in plant species (Pio et al., 2004; Biswas and Mohammad, 2016). Gupta et al. (2015) revealed, in cereal crops such as *Brassica juncea*, *Oryza sativa* and *Triticum aestivum*, that the pollination at high stigma receptive duration significantly gave higher seed set than low receptive period. In addition, higher seed number, fruit diameter and fruit weight of *C. pepo* were obtained when pollination was taken place at anthesis which represented high stigma receptivity (Nepi and Pacini, 2001).

Consequently, the pollen harvested at anthesis and stigma at 0 - 3 DAF presenting the highest fertility should be employed in artificial pollination and breeding program in order to increase the fruit and seed productivity in physic nut. Based on this insight information, the pollens and the stigma at flowering day were utilized for all pollination sets in this study.

4.2 Effects of pollination methods on fruit development and seed oil accumulation

4.2.1 Growth features of fruit, embryo and endosperm

This study, for the first time in *J. curcas*, illustrated for all pollinations that the fruit diameter growth, the nondestructive parameter, was substantially fit to logistic function equation (R^2 = 0.73 - 0.90) (Moore et al., 2013), indicating the efficiency of the model for describing biological incidents related to fruit growth and development (Merchán et al., 2016). The slow growth of *Jatropha* fruit size at initial stage (0 - 9 DAP) could be characterized by high cellular division, while the rapid

growth during 9 - 21 DAP corresponded to a cell elongation process (Hernández and Hernández, 2012). Since those cell division and elongation were crucial factors defining the final fruit size which strongly linked to final yield (Harada et al., 2005), sufficient managements (i.e. irrigation and fertilizer application to support cell division and elongation) during 0 - 21 DAP might improve the physic nut productivity. As demonstrated in *Prunus persica*, the shortage of water at cell division and elongation phase reduced the fruit size, pointing the necessity of proper water management during those periods of fruit development (Naor, 2006). Moreover, in *Malus domestica*, application of potassium fertilizer at elongation period could improve fruit yield and quality (Lu et al., 2015). To improve crop management and crop productivity in physic nut, further investigations of fruit diameter, fruit and seed weight, or fruit and seed composition in relation to options of crop management and environment could contribute to crop simulation models for earlier predicting crop yield and quality under certain conditions (Fernandes et al., 2017).

This investigation failed to assure the developmental origin of embryo and endosperm in apomictic fruit of *J. curcas* due to the extremely low existence of apomixis (14.04 ± 2.73% fruit set) which led us to collect almost all pistils possessing abort ovule. However, the previous review has suggested that apomixis in *J. curcas* was probably of sporophytic apomixis (adventitious embryony type) (Ambrosi et al., 2010). Therefore, the apomictic embryo of this plant might originate from the nucellus (Koltunow and Grossniklaus, 2003). Meanwhile, the endosperm might autonomously develop from polar nuclei (Bicknell and Koltunow, 2004). In addition, the majority of non-pollinated fruits began to drop prematurely since 12 DAF but some with globular, torpedo and mature embryo, as well as the mature endosperm could be found at later stages. Thus, it could be predictable that a critical period decided whether apomixis process will progress or cease happened before 12 DAF. Consequently, further analysis on early embryo and endosperm development in *J. curcas* apomict, such as by clearing and confocal microscopic technique, should be concentrated on specimens collected from the stage of gametophyte (embryo sac) development to 12 DAF.

4.2.2 Fruit and seed set

Pollination method has widely been mentioned to play a role in improving offspring quality and quantity (Mishra et al., 2011; Chautá-Mellizo et al., 2012; Blal et al., 2013). Maximal fruit set and seed number in open-pollination, in agreement with our study, has previously been mentioned in this species grown in Bengaluru and India (Pranesh et al., 2010; Kaur et al., 2011). This may reflect the role of pollinator and pollen resources on increasing fruit and seed set in open-pollination. Numerous bees (Apidae Family) found in our study field were likely to help improve fruit quality by increasing pollen deposition and competition in the naturally cross treatment (Shore and Barrett, 1984; Roldán Serrano and Guerra-Sanz, 2006). It has been established that the bees of Apidae (*Xylocopa confuse*, *Apis cerana* and *A. dorsata*) were the effective pollinator for *J. curcas* as often visited the plants and enhanced fruit and seed set (Rianti et al., 2010). The insect pollinator, feeding on pollen grains and nectar (Chang-Wei et al., 2007), also increased seed weight and germination of *J. curcas* grown in Indonesia (Rianti et al., 2010). For this plant species, the bees mostly promoted cross-pollination, whereas the ant motivated self-pollination (Samra et al., 2014). Pollinator treatment also played a role on increasing fruit equatorial diameter, fruit mass, seed set and seed mass of *Physalis peruviana* (Chautá-Mellizo et al., 2012). Lower fruit sets in response to the open-pollination than hand-cross pollination; however, were evidently observed in *J. curcas* (Raju and Ezradanam, 2002; Kaur et al., 2011). This might presumably be due to the restriction of natural pollination services in the study site (Negussie et al., 2014). Moreover, hand-pollination ensured the arrival of compatible pollen to the stigma; thus, could promote superior fruit set than the open-pollination (Guerra, 2010).

The peak of *J. curcas* seed numbers in open-pollination in our study could be supported by the earlier finding of Kaur et al. (2011) who reported the highest seed set (2.6 seeds/fruit) after open-pollination treatment in the same *Jatropha* species cultivated in India. The apomixis, in this recent study, gave the lowest number of seed per fruit. This lowest seed in the apomixis, of this biodiesel-promising species, might relate to high rate of ovule abortion taken place during fruit development (Raju and Ezradanam, 2002). The frequent rate of ovule abortion in the apomixis caused by

the failure of endosperm development due to the lack of fertilization to form two maternal and one paternal genome (2m:1p) (Koltunow and Grossniklaus, 2003).

4.2.3 Total oil content and fatty acid analysis in whole mature seeds

No significant differences on seed oil contents were found among pollination treatments, although open-pollination (28.76%) and self-pollination (22.90%) seemed to be the highest and the least, respectively. Recently, the highest oil yield was obtained in *J. curcas* grown in Zambia after open-pollination (Negussie et al., 2015). Besides to our study and that of Negussie et al. (2015), relationship between oil accumulation and breeding mode has hardly been studied in *J. curcas* – most researches restricted on oil related natural-pollinated condition only (Rao et al., 2008; Oliveira et al., 2009; Kaur et al., 2011; Pan and Xu, 2011). Equivalent 31.6% of seed oil content was reported for *J. curcas* grown in Brazil (Oliveira et al., 2009) and China (Pan and Xu, 2011) and 29.85 - 37.05% were reserved in those cultivated in India (Rao et al., 2008). Superior oil content in open-pollination treatment than other reproductive routes was accounted in other species such as *Zea mays* (Letchworth and Lambert, 1998), *Brassica campestris* (Mishra et al., 2011) and *S. indicum* (Blal et al., 2013). This situation could be due to the effect of pollinator (Mishra et al., 2011; Klatt et al., 2013) and high pollen availability (Abdelal et al., 1983; Letchworth and Lambert, 1998) in open-pollination treatment on improving fruit quality. For a better understanding in the physic nut, a direct assessment on the effect of pollinator and pollen resources on oil content should be carried out.

This study showed that the breeding mode did affect to the proportion of fatty acids but not to the type of fatty acids. Open-pollination provided the best characteristic of oil as it contained the greatest content of oleic acid (48.55%) and thus highest MUFA (49.45%), which gave the biodiesel the better on critical parameters like cetane number, cold filter plugging point and iodine value (Ramos et al., 2009). Therefore, *Jatropha* oil obtained from the open-pollinated seed will be a good source for biodiesel production. In contrast to our result, in *Prunus amygdalus*, self-pollination gave higher oleic acid than open- and cross-pollination; which might be due to the accumulation of additive genes after self-pollination (Kodad and Socias i

Company, 2008). In *B. napus*, however, pollination types had no impact on fatty acid compositions (Hua et al., 2012).

4.2.4 Lipid profiles in embryo and endosperm isolated from open-pollinated seeds

Jatropha oil was mainly reserved in endosperm tissue, in agreement with the previous report on TAG biosynthesis-related genes which were higher expressed in endosperm than in embryo for the same plant species (Sood and Chauhan, 2015). Similarly to the physic nut, *Ricinus communis* (albuminous seed) accumulated much lipid in endosperm (Joët et al., 2009). Meanwhile, in *Arabidopsis* (exalbuminous seed-produced plant), largely reserved the lipid in the embryo (Forbis et al., 2002). For fatty acid compositions, physic nut endosperm stored more oleic acid and palmitic than the embryo. Meanwhile, the embryo reserved more stearic and linoleic acid than the endosperm. This result was partially different to that found in *Argania spinosa* whose endosperm reserved higher linoleic but lower amount of oleic, palmitic and stearic acid than the embryo (Errouane et al., 2015). In *Elaeis guineensis*, nonetheless, the embryo contained superior oleic, palmitic, linoleic and stearic acid than the endosperm (Dussert et al., 2013). These differences of lipid allocation between embryo and endosperm, in diverse plant species, might correlate to tissue-specific transcriptional specialization (Dussert et al., 2013). Noticeably, both embryo and endosperm of physic nut are competent for biodiesel production since they contained higher proportion of monounsaturated oleic acid than other fatty acid types. The monounsaturated oleic acid provided the global better properties of biodiesel including cetane number, iodine value and cool filter plugging point (Ramos et al., 2009).

This study presented the behenic, erucic, lignoceric and nervonic acid in the whole seed (with all parts of seed coat) but not in isolated embryo and endosperm (without seed coat). This indicated that those minor fatty acids (just around 0.2% in total) possibly preserved in the *Jatropha* seed coat especially in the shrunken layer like tissue developed from inner integument. To support this idea, Chaitanya et al. (2015) showed that the inner integument of *J. curcas*, which is

destined for being a part of seed coat underlying the hardened seed coat derived from outer integument, could store 0.23 - 1.01% lipid throughout seed development. The inner integument of this species played an important role as a transient storage tissue proffering hydrolases to produce carbon and nitrogen sources from proteins, carbohydrates and lipids stored within the cells – to nourish the growing embryo and endosperm. Since those fatty acids could be utilized in cosmetic manufacturing (Zielińska et al., 2014), direct assessment on oil and fatty acid compositions in the inner integument during seed development should be a future project in order to estimate the feasibility of this inner integument oil for the further applications.

Oil bodies isolated from both embryo and endosperm of *J. curcas* were similar in size and nearly close to the range of 0.5 - 2.5 µm generally found in other species such as *Brassica juncea, Zea mays and S. indicum* (Tzen et al., 1993). We have confirmed by TLC analysis that the oil body from all seed tissues primarily reserved neutral lipids in a form of TAG, which corresponded to the reports in diverse species such as *Chlorella* sp. (Lin et al., 2012) and *Pinus elliottii* (Pasaribu et al, 2017). The non-cross recognition of *J. curcas* oleosins by the antibodies against sesame oleosins might be because the sequence homology of *J. curcas* and sesame oleosins is located in the central hydrophobic domain but not in the hydrophilic region including N- and C-terminal domains (Tzen et al., 1998). In rice embryo, for example, the homology of 16 and 18 kDa oleosins settled at central hydrophobic domain, thus providing deficient epitope for the antibody conjugation and resulting in non-detectable antibodies against each other (Chuang et al., 1996). Two isoforms of oleosins, the H- and the L-form, were examined and these proteins, especially oleosin 3 (L-form), were the major protein found in both embryo and endosperm of physic nut. This is concurrent with the earlier finding that oleosins were found both in embryo and endosperm of this species after two-dimensional gel electrophoresis (Liu et al., 2009) and transcriptional expression of oleosin 3 was higher than other oleosins (Popluechai et al., 2011). The oleosin 3 might have a potential for using as a codominant marker in breeding for improving seed oil characteristics in this species (Popluechai et al., 2011). Oleosin proteins played important role in preventing coalescence of lipid bodies during seed dehydration, imbibition and germination as well as they controlled the oil body size (Siloto et al., 2006). The suppression of these

proteins changed the oil body sizes, which resulted in the reduction of lipid content and modified the fatty acid components in *Arabidopsis* seed (Lu et al., 2006; Siloto et al., 2006). Another oil body protein found in *Jatropha* seed tissues, in this study, was caleosin. This protein related to mobilization of oil bodies during seed germination (Tzen, 2012).

4.3 Establishment and lipid analysis of *J. curcas* cell suspension

4.3.1 Callus induction, growth features and microscopic observation

The best callus induction and callus fresh weight were obtained from the PGR combination treatments, especially the supplementation of 2, 4-D at higher concentration (1 mg L^{-1}) and KN at lower concentration (0.5 mg L^{-1}) which was consistent with the finding of Ismidianty and Esyanti (2010) in physic nut grown in Indonesia. This indicated a requirement of auxin and cytokinin specific ratio for the formation of callus (Ikeuchi et al., 2013; Kaewubon, 2015). The auxin played a role to promote cell cycle reentry by both activating core cell cycle regulators such as those involved DNA replication and downregulating of cell cycle inhibitors; so allowed the cell to enter G1/S transition (Perrot-Rechenmann, 2010; Ikeuchi et al., 2013). Whilst, the cytokinin related to the post-translational regulation of the Cdc2MsA/B kinase complex at G1/S and G2/M transition, thus regulated mitosis and then cell proliferation (Pasternak et al., 2000; Schaller et al., 2014). In the absence of KN, the increase of callus induction percentage and fresh weight in parallel with the enhanced concentrations of 2, 4-D (from 0.5 to 1 mg L^{-1}) might associate to the possibilities that 2, 4-D fundamentally acted as auxin and secondarily stimulated cytokinin biosynthesis by repressing the cytokinin-suppressed genes named *ARR7* and *ARR15* as stated in *A. thaliana* (Zhao et al., 2010). Further, 2, 4-D may be the truly critical PGR for promoting the cell division of the callus, thus without KN the callus could develop. For this case, the effectiveness of 2, 4-D would be increased by the metabolic modifications motivated by the cytokinins (Witham, 1968). Application of 0.5 mg L^{-1} 2, 4-D alone could induce callus from hypocotyl of 4-day-old seedling of physic nut planted in Pakistan (Soomro and Memon, 2007). In similar to the previous

reports on the same species (Soomro and Memon, 2007; Mazumdar et al., 2010), we also found that all calli initiated from the cut area which assimilated greater nutrients from the medium than other sites (Ismidianty and Esyanti, 2010). Furthermore, initiation of the callus at 4 days after inoculation, in this study, was earlier than the previous observation (by 7 days) for the same species (Soomro and Memon, 2007).

Conversely, exogenous application of KN alone could not produce any calli; but, swelled the tissue and at high concentration (1 mg L^{-1}) stimulated crack formation on the explants instead. The high level of KN enhanced the amount of water uptake by stimulating membrane permeability to water (Gadallah and Sayed, 2001) and afterwards promoted the tissue swelling which resulted in the explant rupture (Tan et al., 2010). Likewise, the application of KN (2 mg L^{-1} KN) formed the crack on cotyledon explant of cashew (*Anancardium occidentale*) (Kamshananthi and Seran, 2012). Moreover, high level of kinetin could delay cell division process (Farooq et al., 2012) and activate programmed cell death as mentioned in *Vicia faba* ssp. *minor* seedlings (Kunikowska et al., 2013). The kinetin-induced programmed cell death could be characterized by nuclear degradation processes such as degradation of DNA and changes in kinase and nuclease activities (Doniak et al., 2014). Based on those negative effects of KN on the plant tissue, the medium with KN alone, thus, might stimulate the death of *Jatropha* explant rather than the dedifferentiation process.

It could also be suggested, from this study, that the levels of both endogenous auxin and cytokinin within the physic nut hypocotyl of the 10-day-old seedling were not sufficient to induce callus autonomously – as shown by no callus development found in the absence of PGRs (control). This result was resembled to those of Ramos et al. (2013) and Oliveira et al. (2017) who performed the experiment using 15-day-old hypocotyl obtained from Costa Rican physic nut and 14-day-old hypocotyl from Costa Rica and Mexico-crossed accessions, respectively. Exogenous PGRs, especially the combination of 1 mg L^{-1} NAA and 0.1 mg L^{-1} KN, were also required for callus induced from 8-day-old hypocotyl of physic nut collected from China (Li et al., 2012). Thus, exogenous hormone was essential for callus formation from *J. curcas* hypocotyl.

In order to decide management of the callus culture such as appropriate time for subculture, the growth kinetics was demanded (Costa et al., 2015). Sigmoidal curve, based on fresh and dry weight, was observed for callus growth of *J. curcas* in this study, which was in accordant with the finding of Costa et al. (2015) for the same plant species. Due to the diminution of nutrients, media drying and accumulation of toxic substances in media, the subculture should be performed at stationary phase (Silva et al., 2005). Accordingly, callus established in this study, could be subcultured at Week3 to Week4 of culture (stationary phase). For more saving cost such as medium used and time consumed during the maintenance period, callus was thus subcultured at 4-week intervals in this recent work.

In this study, all calli initially obtained from the induction treatments were compact type; however, friable callus could occasionally be obtained by a repeated subculture of the compact callus – in agreement with Correa and Atehortúa (2012) who gained the friable callus after a routine subculture for the same species. It is possible that, by the routine subculture, cell wall compositions of the callus were altered; leading to the reduction of cell to cell cohesive forces and then the increase of cell friability (Liners et al., 1994). Difference on degree of cell attachment between friable and compact callus, generally found in other species like *Rosmarinus officinalis* (Boix et al., 2013) and *Solanum tuberosum* (Boamponsem and Leung, 2017), was also detected in our calli. The looser attached cells found in friable callus resulted from more rapid cell division (George and Sherrington, 1984; Souza et al., 2011).

4.3.2 Cell suspension culture and analysis

Establishment of cell suspension culture was carried out by transferring 4-week-old compact callus belonged to the stationary phase into liquid MS medium comprising of 1 mg L^{-1} 2, 4-D and 0.5 mg L^{-1} KN. This study used the compact callus for the cell suspension induction based on the reason that this compact callus provided the cell suspension with more predominant advantage on secondary metabolite storage – due to its differentiated state (Zhao et al., 2001). The employments of the compact callus for cell suspension culture were reported in other

plant species such as *Catharanthus roseus* (Zhao et al., 2001) and *Artemisia annua* (Keng et al., 2010). The amount of 0.5 gram callus per 25 ml medium were initially used as the inoculation size for cell suspension culture in this study since the larger (1 gram/25 ml) and smaller calli (< 0.5 gram/25 ml) respectively led to the cell necrosis and the cessation of cell division and elongation for physic nut as reported by Ramos et al. (2013).

Changes of the fresh weight, dry weight, pigment content and cell viability seemed to show the similar pattern by having a rapid increase during the Week1 - Week2 of culture and displaying the slightly increase or decrease trends after Week2. The increase in cell fresh and dry weight followed the S-shape pattern; which was corresponded to those explained by Soomro and Memon (2007) and Demissie and Lele (2013) for the same species. It was observed that the *Jatropha* cell suspension moved to the exponential phase since the week1 of culture. The biomass increased till the third week (Week3) and seemed to decrease during Week3 - Week4, which might attribute to the shortage of the nutrients and oxygen in the medium. It was noticeable that the increment in the cell biomass was positively paralleled with the enhancement of pH medium (4.85 - 5.75) during Week1 - Week3. These pH values might promote the *Jatropha* cell growth by motivating the supreme solubility and absorption of the nutrients in the plant cell culture (Malik et al., 2008). Similar event was reported in the cell suspension of *Spilanthes acmella* (Singh and Chaturvedi, 2012) and *Papaver bracteatum* (Farjaminezhad et al., 2013). The alteration in pH after autoclaving is due to the high temperature during sterilization, which changes the composition of nutrients and salts of the medium (Gupta et al., 2014). Dropping of medium pH during the first week of culture may result from the cell uptake of ammonium while the increase in pH value at later stages might associate with the uptake and reduction of nitrates (formation of OH^-) (Sarasketa et al., 2016). The higher level of chlorophyll *b* than chlorophyll *a*, in our experimental condition, might be due to the function of KN, added in the culture medium, on promoting more storage of chlorophyll *b* than chlorophyll *a*. To support this concept, the application of KN into the culture medium stimulated higher accumulation of chlorophyll *b* than chlorophyll *a* in the *Tobacco* callus (Kaul and Sabharwal, 1971) and *Zea mays* seedlings (Kocot et al., 2011). This KN, the cytokinin-grouped PGR,

might increase the chlorophyll *b* content by upregulating the chlorophyll *a* oxygenase gene (*CAO*) which plays the crucial role to converse chlorophyll *a* to chlorophyll *b* (Talla et al., 2016). The high storage of chlorophyll *b* increased the photosynthetic efficiency by promoting higher solar energy capture and electron transport as previously demonstrated in *Nicotiana tabacum* (Biswal et al., 2012). From the above mentions, it could be concluded that the increase rates of the cell mass and the pigment contents was highest during the week1 to week2 of culture and it slowed down thereafter – leading to the high cell viability during this period and then reduced afterwards. Accordingly, our investigation suggested that a 2-week subculture practice may finest maintain the medium freshness, medium pH level and satisfying growth of *J. curcas* cells.

The oil amount (3.84%) gained from the *Jatropha* cells established this study needs to be intensively improved since it was very less than 30% observed by Ismidianty and Esyanti (2010) and 22 - 41% by Correa and Atehortúa (2012) from in vitro culture of the same plant species but in different variety and medium composition. Ismidianty and Esyanti (2010) did the somatic embryo culture of Indonesian-variety *Jatropha* using IG2 medium. Meanwhile, Correa and Atehortúa (2012) performed the cell culture of Brazilian physic nut (JB-1) using Lloyd and McCown medium. Moreover, the *Jatropha* cell suspension reserved significantly less oil content than the seed (around 7-fold reduction). This smaller amount of desired compound in the cell suspension than in the seed could generally be observed in other plant species such as *Bunium persicum* (Khosravinia et al., 2012) and *Capparis spinosa* (Yin et al., 2014). For the former species, around 4-fold reduction of cuminaldehyde content was detective in the cell suspension comparing to the seed. While, 52-fold diminution of alkanes in the cell suspension was observed in the latter species. The proportion of monounsaturated oleic acid in our cell (36.13 ± 0.16%) was higher than 9% reported by Ismidianty and Esyanti (2010) and was comparable to 34.36% observed by Correa and Atehortúa (2012) in in vitro culture system of the same plant species. Further, the cell suspension contained higher oleic acid than other fatty acid types. Based on the high amount of oleic acid, the cell established in this study seemed to be efficient for the use as a source of oil for producing standard-satisfied biodiesel. The very higher level of linolenic acid in *Jatropha* cell suspension

(around 113-fold enlargement) in comparison to the seed, in this study, might ascribe to the effect of 2, 4-D in the medium on promoting the activity of desaturation-related processes which converses linoleic to linolenic acid as previously demonstrated in cotyledons of *Glycine max* cultured on MS0 medium added with 2, 4-D. Nevertheless, the mechanism by which 2, 4-D influences the desaturation-related processes was not understandable (Liu et al., 1995).

An intensive research to increase the biomass and oil content of *Jatropha* cell suspension should be a future subject, in particular by applying a two-stage culture system in air-lift bioreactor. This two-stage culture is a technique in which the cell suspension are firstly cultured in a nutrient-rich medium appropriate for growth (phase I) and are afterwards moved to a second metabolite production medium containing elicitors, precursors or stress-inducing ingredients (phase II) (Malik et al., 2013). This system, for example, was successfully employed for the induction of napthoquinone metabolite in *Arnebia* sp. (Gupta et al., 2014) and TAG content in *Chlorella vulgaris* (Santos et al., 2015).

CHAPTER 5
CONCLUSIONS

This present work is the first report describing the correlation between flower bud diameter and developmental stages of both male gametophyte (pollen) and female gametophyte (embryo sac) in physic nut. The floral buds of 1.6 mm in diameter onwards, which highly related to the stage of haploid microspore - binucleated pollen (for the male flowers) and haploid megaspore - mature embryo sac (for the female flowers), would be employed for haploid production to generate homozygous genotype for variety improvement program. Pollens collected at blooming and stigmata at 0 - 3 DAF, representing high fertility, should be applied in artificial pollination and breeding program to enhance the fruit and seed set.

Open-pollination proved to be the best pollination method for physic nut as provided maximal fruit set (74.33%), number of seeds per fruit (2.90) and monounsaturated oleic acid (48.55%). Oil storage in endosperm (53.04%) was greater than embryo (48.37%). Moreover, the endosperm reserved more oleic acid (45.95%) than embryo (38.41%). The isolated seed oil bodies were mainly composed of TAG enclosed by integral proteins termed caleosin, high molecular weight oleosin and low molecular weight oleosin.

The cell suspension established from the compact callus, in the liquid MS medium supplemented with 1 mg L^{-1} 2, 4-D and 0.5 mg L^{-1} KN, was aggregate and was subcultured at 2-week intervals based on the features of fresh weight, dry weight, medium pH, pigment content and viability. This study indicated that the contents of oil (3.84%), oleic acid (36.12%) and MUFA (36.87%) in the cultured cells were lower than those of the whole seed (28.76%, 48.55% and 49.45%, respectively). This cell suspension, nonetheless, contained the highest proportion of monounsaturated oleic acid comparing with other fatty acids found within the cell, pointing its competent use as a source of standard-reached biodiesel. The increment of cell biomass and oil content should be intensively carried out in the near future in order to achieving the mercantile demand.

REFERENCES

Abdelal, A. F., Mahmoud, H. M. and El-Agamy, S. Z. 1983. The effect of pollen source on fruit characteristics of Zaghloul dates. (*Phoenix dactylifera* L.). *Assiut Journal of Agricultural Sciences.* 14: 347 - 355.

Abdelgadir, H. A., Jäger, A. K., Johnson, S. D. and Staden, J. V. 2010. Influence of plant growth regulators on flowering, fruiting, seed oil content, and oil quality of *Jatropha curcas*. *South African Journal of Botany*. 76: 440 - 446.

Abdelgadir, H. A., Johnson, S. D. and Staden, J. V. 2012. Pollen viability, pollen germination and pollen tube growth in the biofuel seed crop *Jatropha curcas* (Euphorbiaceae). *South African Journal of Botany*. 79: 132 - 139.

Achten, W. M. J, Verchot, L. and Franken, Y. J. 2008. *Jatropha* biodiesel production and use. *Biomass and Bioenergy.* 32: 1063 - 1084.

Akbar, E., Yaakob, Z., Kamarudin, S. K., Ismail, M. and Salimon, J. 2009. Characteristic and composition of *Jatropha curcas* oil seed from Malaysia and its potential as biodiesel feedstock. *European Journal of Scientific Research*. 29: 396 - 403.

Aly, M. A. M., Amer, E. A., Al-Zayadneh, W. A. and Eldin, A. E. N. 2008. Growth regulators influence the fatty acid profiles of in vitro induced jojoba somatic embryos. *Plant Cell, Tissue and Organ Culture*. 93: 107 - 114.

Ambrosi, D. G., Galla, G., Purelli, M., Barbi, T., Fabbri, A., Lucretti, S., Sharbel, T. F. and Barcaccia, G. 2010. DNA markers and FCSS analyses shed light on the genetic diversity and reproductive strategy of *Jatropha curcas* L. *Diversity*. 2: 810 - 836.

Aronne, G. 1999. Effects of relative humidity and temperature stress on pollen viability of *Cistus incanus* and *Myrtus communis*. *Grana*. 38: 364 - 367.

Baraki, Y. and Kenji, K. 2001. Application of image analysis to plant cell suspension cultures. *Computers and Electronics in Agriculture*. 30: 193 - 203.

Baud, S. and Lepiniec, L. 2010. Physiological and developmental regulation of seed oil production. *Progress in Lipid Research*. 49: 235 - 249.

Baydar, H. 2000. Effects of gibberellic acid on male sterility, seed yield and oil and fatty acid syntheses of safflower (*Carthamus tinctorius* L.). *Turkish Journal of Biology*. 24: 159 - 168.

Benítez-García, I., Vanegas-Espinoza, P. E., Meléndez-Martínez, A. J., Heredia, F. J., Paredes-López, O. and Villar-Martínez, A. A. D. 2014. Callus culture development of two varieties of *Tagetes erecta* and carotenoid production. *Electronic Journal of Biotechnology*. 17: 107 - 113.

Bicknell, R. A. and Koltunow, A. M. 2004. Understanding apomixis: recent advances and remaining conundrums. *The Plant Cell*. 16, S228 - S245.

Biswal, A. K., Pattanayak, G. K., Pandey, S. S., Leelavathi, S., Reddy, V. S., Govindjee and Tripathy, B. C. 2012. Light intensity-dependent modulation of chlorophyll b biosynthesis and photosynthesis by overexpression of Chlorophyllide a Oxygenase in Tobacco. *Plant Physiology*. 159: 433 - 449.

Biswas, P. and Mohammad, J. 2016**.** Studies on esterase and peroxidase activity of *Clerodendrum inerme* (linn.) Gaertn. in relation to stigma receptivity. *International Journal of Advanced Biotechnology and Research*. 6: 386-389.

Blal, A. E. H., Kamel, S. M., Mahfouz, H. M. and Said, M. 2013. Impact of opened, non opened pollination and nitrogen fertilizer on sesame production in the reclaimed lands, Ismailia Governorate, Egypt. *Cercetări Agronomice în Moldova*. 3: 57 - 68.

Boamponsem, G. A. and Leung, D. W. M. 2017. Use of compact and friable callus cultures to study adaptive morphological and biochemical responses of potato (*Solanum tuberosum*) to iron supply. *Scientia Horticulturae*. 219: 161 - 172.

Boix, Y. F., Arruda, R. C. O., Defaveri, A. C. A., Sato, A., Lage, C. L. S. and Victorio, C. P. 2013. Callus in *Rosmarinus officinalis* L. (Lamiaceae): A morphoanatomical, histochemical and volatile analysis, plant biosystems – an international journal dealing with all aspects of plant biology. *Official Journal of the Societa Botanica Italiana*. 147: 751 - 757.

Brewbaker, J. L. and Kwack, B. H. 1963. The essential role of calcium ion in pollen germination and pollen tube growth. *American Journal of Botany*. 50: 859-865.

Brown, G. G. 1969. *Primer of Histopathologic Technique*., New York: Appleton-Century-Crofts Educational Division.

Cai, L., Fu, L. and Ji, L. 2011. Regeneration of *Jatropha curcas* through efficient somatic embryogenesis and suspension culture. *GM Crops*. 2: 110 - 117.

Cao, Y. Z. and Huang, A. H. C. 1986. Diacylglycerol acyltransferase in maturing oil seeds of maize and other species. *Plant Physiology*. 82: 813 - 820.

Cardarelli, M. and Cecchetti, V. 2014. Auxin polar transport in stamen formation and development: how many actors?. *Frontiers in Plant Science*. 5: 1 - 13.

Carvalho, C. R., Clarindo, W. R., Prac, M. M., Arau' jo, F. S. and Carels, N. 2008. Genome size, base composition and karyotype of *Jatropha curcas* L., an important biofuel plant. *Plant Science*. 174 : 613 - 617.

Chaitanya, B. S. K., Kumar, S., Anjaneyulu, E., Prasad, R. B. N., Sastry, P. S. and Reddy, A. R. 2015. Pivotal role of sugar fluxes between the inner integument and endosperm in lipid synthesis during seed ontogeny in *Jatropha curcas* L. *Industrial Crops and Products*. 76: 1106 - 1113.

Chang, W. C., Chen, M. H. and Lee, T. M. 1999. 2, 3, 5-Triphenyltetrazolium reductions in the viability assay of *Ulva fasciata* (Chlorophyta) in response to salinity stress. *Botanical Bulletin of Academia Sinica*. 40: 207 - 212.

Chang-Wei, L., Kun, L., You, C. and Yong-Yu, S. 2007. Floral display and breeding system of *Jatropha curcas* L. *Forestry Studies in China*. 9: 114 - 119.

Chaudhury, A. M., Craig, S., Dennis, E. S. and Peacock, W. J. 1998. Ovule and embryo development, apomixis and fertilization. *Current Opinion in Plant Biology*. 1: 26 - 31.

Chautá-Mellizo, A., Campbell, S. A., Bonilla, M. A., Thaler, J. S. and Poveda, K. 2012. Effects of natural and artificial pollination on fruit and offspring quality. *Basic and Applied Ecology*. 13: 524 - 532.

Chawla, H.S. 2003. *Plant Biotechnology Laboratory Manual for Plant Biotechnology.* New Delhi: Oxford and IBH Publishing.

Chen, J. F., Cui, L., Malik, A. A. and Mbira, K. G. 2010. In vitro haploid and dihaploid production via unfertilized ovule culture. *Plant Cell, Tissue and Organ Culture*, doi: 10.1007/s11240-010-9874-6.

Chuang, R. L. C., Chen, J. C. F., Chu, J. and Tzen, J. T. C. 1996. Characterization of seed oil bodies and their surface oleosin isoforms from rice embryos. *The Journal of Biochemistry*. 120: 74 - 81.

Correa, S. M. and Atehortúa, L. 2012. Lipid profile of in vitro oil produced through cell culture of *Jatropha curcas. Journal of AOAC International*. 95: 1161-1169.

Costa, J. L., Silva, A. L. L., Bier, M. C. J., Brondani, G. E., Gollo, A. L., Letti, L. A. J., Erasmo, E. A. L. and Soccol, C. R. 2015. Callus growth kinetics of physic nut (*Jatropha curcas* L.) and content of fatty acids from crude oil obtained in vitro. *Applied Biochemistry and Biotechnology*. 176: 892 - 902.

Currais, L. M., Canhoto, J. M. and Linde, P. V. D. 2012. Microsporogenesis in *Jatropha curcas* L. *Acta Horticulturae*. 935: 113 - 120.

Demirbas, A. 2003. Biodiesel fuels from vegetable oils via catalytic and non-catalytic supercritical alcohol transesterifications and other methods: a survey. *Energy Conversion and Management*. 44: 2093 - 2109.

Demissie, A. G. and Lele, S. S. 2013. In vitro cultivation of *Jatropha curcas* L. cells for growth kinetic and total fatty acid determination. *Advances in Bioresearch*. 4: 64 - 72.

Divakara, B. N., Upadhyaya, H. D., Wani, S. P. and Gowda, C. L. L. 2009. Biology and genetic improvement of *Jatropha curcas* L.: a review. *Applied Energy*. doi: 10.1016/j.apenergy.2009.07.013.

Doniak, M., Barciszewska, M. Z., Kaz´mierczak, J. and Kaz´mierczak, A. 2014. The crucial elements of the ‘last step’ of programmed cell death induced by kinetin in root cortex of *V. faba* ssp. *minor* seedlings. *Plant Cell Reports*. 33: 2063 - 2076.

Dunham, R. S. 1951. Chemical Control of Grass Weeds in Flax. Proc. Flax Institute of the United States, Minneapolis.

Dunn, R. O. and Bagby, M. O. 1996. Low-temperature filterability properties of alternative diesel fuels from vegetable oils. Liquid fuel and industrial product from renewable resources. In: Proc. Third Liquid Fuel Conference, ASAE, 95 - 103.

Dussert, S., Guerin, C., Andersson, M., Joët, T., Tranbarger, T. J., Pizot, M., Sarah, G., Omore, A., Gasselin, T. D. and Morcillo, F. 2013. Comparative transcriptome analysis of three oil palm fruit and seed tissues that differ in oil content and fatty acid composition. *Plant Physiology*. 162: 1337 - 1358.

Errouane, K., Doulbeau, S., Vaissayre, V., Leblanc, O., Collin, M., Harche, M. K. and Dussert, S. 2015. The embryo and the endosperm contribute equally to argan seed oil yield but confer distinct lipid features to argan oil. *Food Chemistry*. 181: 270 - 276.

Faizanullah, A. B., Bano, A. and Nosheen, A. 2010. Role of plant growth regulators on oil yield and biodiesel production of Linseed (*Linum usitatissimum* L.). *Journal of Chemical Society of Pakistan*. 32: 668 - 671.

Farjaminezhad, R., Zare, N., Asghari-zakaria, R. and Farjaminezhad, M. 2013. Establishment and optimization of cell growth in suspension culture of *Papaver bracteatum*: a biotechnology approach for thebaine production. *Turkish Journal of Biology*. 37: 689 - 697.

Farooq, M., Hussain, M., Wahid, A. and Siddique, K. H. M. 2012. Drought stress in plants: an overview. In *Plant responses to drought stress from morphological to molecular features*, Aroca R., editor. p. 1 - 33. Berlin: Springer.

Farooqi, A. H. A., Fatima, S., Khan, A. and Sharma, S. 2005. Ameliorative effect of chlormequat chloride and IAA on drought stressed plants of *Cymbopogon martinii* and *C. winterianus*. *Plant Growth Regulation*. 46: 277 - 284.

Fernandes, T. J., Pereira, A. A. and Muniz, J. A. 2017. Double sigmoidal models describing the growth of coffee berries. *Ciência Rural*. 47: 1 - 7.

Ferrant, V. and Bouharmont, J. 1994. Origin of gynogenetic embryos of *Beta vulgaris* L. *Sexual Plant Reproduction*. 7: 12 - 16.

Figueiredo, A. C., Salomé, M., Pais, S. and Scheffer, J. J. C. 1995. Composition of the essential oil from cell suspension cultures of *Achillea millefolium* ssp. *millefolium*. *Plant Cell, Tissue and Organ Culture*. 40: 113 - 118.

Forbis, T. A., Floyd, S. K. and Queiroz, A. 2002. The evolution of embryo size in angiosperms and other seed plants: implications for the evolution of seed dormancy. *Evolution*. 56: 2112 - 2125.

Gadallah, M. A. A. and Sayed, S. A. 2001. The impact of kinetin application on water relations, leaf osmotic potential and soluble carbon and nitrogen compound contents in *Sorghum bicolor* plants growing at varying levels of soil acidity. *Pakistan Journal of Biological Sciences*. 4: 10 - 16.

Gaur, D. 2017. Endosperm and types of endosperm. DRGP biology (online study center). http://www.drgpbiology.com/types-of-endosperm. (accessed January 27, 2018).

George, E. F. and Sherrington, P. D. 1984. *Plant Propagation by Tissue Culture: Handbook and Directory of Commercial Laboratories*. Basingstoke, England: Exegetics.

González, M., Baeza, E., Lao, J. L. and Cuevas, J. 2006. Pollen load affects fruit set, size, and shape in cherimoya. *Scientia Horticulturae*. 110: 51 - 56.

Gu, K., Yi, C., Tian, D., Singh, J. S., Hong, Y. and Yin, Z. 2012. Expression of fatty acid and lipid biosynthetic genes in developing endosperm of *Jatropha curcas*. *Biotechnology for Biofuels*. 5. doi: 10.1186/1754-6834-5-47.

Guerra, M. E., Wunsch, A., Corrales, M. L. and Rodrigo, J. 2010. Flower emasculation as the cause for lack of fruit set in Japanese plum crosses. *Journal of the American Society for Horticultural Science*. 135: 556 - 562.

Gupta, K., Garg, S., Singh, J. and Kumar, M. 2014. Enhanced production of napthoquinone metabolite (shikonin) from cell suspension culture of *Arnebia* sp. and its up-scaling through bioreactor. *3 Biotech*. 4: 263 - 273.

Gupta, R., Sutradhar, H., Chakrabarty, S. K., Ansari, M. W. and Singh, Y. 2015. Stigmatic receptivity determines the seed set in Indian mustard, rice and wheat crops. *Communicative and Integrative Biology*. 8: 1 - 4.

Harada, T., Kurahashi, W., Yanai, M., Wakasa, Y. and Satoh, T. 2005. Involvement of cell proliferation and cell enlargement in increasing the fruit size of *Malus* species. *Scientia Horticulturae*. 105: 447 - 456.

Hedhly, A., Hormaza, J. I. and Herrero, M. 2003. The effect of temperature on stigmatic receptivity in sweet cherry (*Prunus avium* L.). *Plant, Cell and Environment*. 26: 1673 - 1680.

Hernández, C. L. and Hernández, M. S. G. 2012. Growth and development of the cupuaçu fruit (*Theobroma grandiflorum* [Willd. Ex Spreng.] Schum.) in the western Colombian Amazon. *Agronomía Colombiana*. 30: 95 - 102.

Heslop-Harrison, J. and Heslop-Harrison, Y. 1992. Cyclical transformation of the actin cytoskeleton of hyacinth pollen subjected to recurrent vapour-phase hydration and dehydration. *Biology of the Cell*. 75: 245 - 252.

Heslop-Harrison, J., Heslop-Harrison, Y. and Shivanna, K. R. 1984. The evaluation of pollen quality, and a further appraisal of the fluorochromatic (FCR) test procedure. *Theoretical and Applied Genetics*. 67: 367 - 375.

Hua, W., Li, R. J., Zhan, G. M., Liu, J., Li, J., Wang, X. F., Liu, G. H. and Wang, H. Z. 2012. Maternal control of seed oil content in *Brassica napus*: the role of silique wall photosynthesis. *The Plant Journal*. 69: 432 - 444.

Huang, A. H. C. 1992. Oil bodies and oleosins in seeds. *Annual Review of Plant Physiology and Plant Molecular Biology*. 43: 177 - 200.

Huang, Z., Zhu, J., Mu, X. and Lin, J. 2004. Pollen dispersion, pollen viability and pistil receptivity in *Leymus chinensis*. *Annals of Botany*. 93: 295 - 301.

Ibrahim, A. M., Kayat, F .B., Hussin, Z. E. S. M., Susanto, D. and Ariffulah, M. 2014. Determination of suitable microspore stage and callus induction from anthers of kenaf (*Hibiscus cannabinus* L.). *The Scientific World Journal*, doi: 10.1155/2014/284342.

Ikeuchi, M., Sugimoto, K. and Iwase, A. 2013. Plant callus: mechanisms of induction and repression**.** *The Plant Cell*. 25: 3159 - 3173.

Ismidianty, D. and Esyanti, R. R. 2010. Fatty acid composition induced in somatic embryo of *Jatropha curcas* in bioreactor. Proceedings of the Third International Conference on Mathematics and Natural Sciences (ICMNS 2010).

Jham, G. N., Teles, F. F. F. and Campos, L. G. 1982. Use of aqueous HCI/MeOH as esterification reagent for analysis of fatty acids derived from soybean lipids. *Journal of the American Oil Chemists Society*. 59: 132 - 133.

Jiang, P. L., Chen, J. C., Chiu, S. T. and Tzen, J. T. C. 2009. Stable oil bodies sheltered by a unique caleosin in cycad megagametophytes. *Plant Physiology and Biochemistry*. 47: 1009 - 1016.

Joët, T., Laffargue, A., Salmona, J., Doulbeau, S., Descroix, F., Bertrand, B., Kochko, A. D. and Dussert, S. 2009. Metabolic pathways in tropical dicotyledonous albuminous seeds: *Coffea arabica* as a case study. *New Phytologist*. 182: 146 - 162.

Kaewpoo, M. 2010. Micropropagation of *Jatropha curcas* Linn. and chromosome duplication by colchicine and oryzalin treatment. Doctor of Philosophy in Plant Science, Faculty of Natural Resources, Prince of Songkla University.

Kaewubon, P. 2015. Inhibition of browning agents in bisected protocorm-derived callus of pigeon orchid (*Dendrobium crumenatum* Swartz). Doctor of Philosophy in Biology, Faculty of Science, Prince of Songkla University.

Kamshananthi, T. and Seran, T. H. 2012. Induction of somatic embryogenesis from cotyledon explants of cashew (*Anancardium occidentale* L.). *Journal of Agricultural Technology*. 8: 2089 - 2099.

Kasperbauer, M. J. and Wilson, H. M. 1979. Haploid plant production and use. In *Nicotiana: Procedures for Experimental Use,* Durbin, R. D., Editor. p. 33-39. Washington, DC: USDA Technical Bulletin 1586.

Kaul, K. and Sabharwal, P. S. 1971. Effects of sucrose and kinetin on growth and chlorophyll synthesis in *Tobacco* tissue cultures. *Plant Physiology*. 47: 691 - 695.

Kaur, K., Dhillon, G. P. S. and Gill, R. 2011. Floral biology and breeding system of *Jatropha curcas* in North-western India. *Journal of Tropical Forest Science.* 23: 4 - 9.

Kawashima, T. and Berger, F. 2014. Epigenetic reprogramming in plant sexual reproduction. *Nature Reviews Genetics*. 15: 613 - 624.

Keng, C. L., Singaram, N. and Lim, B. P. 2010. Production of artemisinin from cell suspension culture of *Artemisia annua* L. *Asia-Pacific Journal of Molecular Biology and Biotechnology.* 18: 139 - 141.

Khan, A. F., Mujeeb, F., Aha, F. and Farooqui, A., 2015. Effect of plant growth regulators on growth and essential oil content in palmarosa *(Cymbopogon martinii). Asian Journal of Pharmaceutical and Clinical Research.* 8: 373 - 376.

Khanpour-Ardestani, N., Sharifi, M. and Behmanesh, M. 2015. Establishment of callus and cell suspension culture of *Scrophularia striata* Boiss.: an in vitro approach for acteoside production. *Cytotechnology*. 67: 475 - 485.

Kharenko, O. A., Zaharia, L. I., Giblin, M., Ekic, V. C., Taylor, D. C., Palmer, C. D., Abrams, S. R. and Loewen, M. C. 2011. Abscisic acid metabolism and lipid accumulation of a cell suspension culture of *Lesquerella fendleri*. *Plant Cell, Tissue and Organ Culture*. 105: 415 - 422.

Khosravinia, S., Ziaratnia, S. M., Bagheri, A., Rajabzadeh, G. and Marashi, S. H. 2012. Comparison of cuminaldehyde contents from cell suspension cultures and seeds of [*Bunium persicum* (Boiss.) B. Fedtsch.]. *Notulae Scientia Biologicae*. 4: 49 - 54.

Klatt, B. K., Holzschuh, A., Westphal, C., Clough, Y., Smit, I., Pawelzik, E. and Tscharntke, T. 2014. Bee pollination improves crop quality, shelf life and commercial value. *Proceedings of the Royal Society B*. 281: 1 - 8.

Kocot, K. P., Kita, A. and Haduch, A. 2011. The effect of kinetin on the chlorophyll pigments content in leaves of *Zea mays* L. seedlings and accumulation of some metal ions. *Inżynieria i Ochrona Środowiska*. 14: 397 - 409.

Kodad, O. and Socias i Company, R. 2008. Fruit quality in almond as related to the type of pollination in self-compatible genotypes. *Journal of the American Society for Horticultural Science.*133: 320 - 326.

Koltunow, A. M. 1993. Apomixis: embryo sacs and embryos formed without meiosis or fertilization in ovules. *Plant Cell*. 5: 1425 - 1437.

Koltunow, A. M. and Grossniklaus, U. 2003. Apomixis: a developmental perspective. *Annual Review of Plant Biology*. 54: 547 - 574.

Koltunow, A. M., Bicknell, R. A. and Chaudhury, A. M. 1995. Apomixis: molecular strategies for the generation of genetically identical seeds without fertilization. *Plant Physiology*. 108: 1345 - 1352.

Koltunow, A. M., Truettner, J., Cox, K. H., Wallroth, M. and Goldberg, R. B. 1990. Different temporal and spatial gene expression patterns occur during anther development. *The Plant Cell*. 2: 1201 - 1224.

Krishnamurthy, K. V. 2013. Embryology of *Jatropha*: A Review. In *Jatropha*, Challenges for a New Energy Crop: Volume 2: Genetic Improvement and Biotechnology, Bahadur et al., Editor. p. 75 - 86. New York: Springer Science+Business Media.

Kumar, A. and Sharma, S. 2008. An evaluation of multipurpose oil seed crop for industrial uses (*Jatropha curcas* L.): a review. *Industrial Crops and Products*. 28: 1 - 10.

Kunikowska, A., Byczkowska, A. and Kaźmierczak, A. 2013. Kinetin induces cell death in root cortex cells of *Vicia faba* ssp. *minor* seedlings. *Protoplasma*. 250: 851 - 861.

Lankinen, A., Armbruster, W. S. and Antonsen, L. 2007. Delayed stigma receptivity in *Collinsia heterophylla* (Plantaginaceae): genetic variation and adaptive significance in relation to pollen competition, delayed self-pollination, and mating-system evolution. *American Journal of Botany*. 94: 1183 - 1192.

Lauxen, M. D. S., Santos, E. K., Hu, C. Y., Jacques, S. M. C. and Zanettini, M. H. B. 2003. Association between floral bud size and developmental stage in soybean microspores. *Brazilian Archives of Biology and Technology*. 46: 515 - 520.

Le, B. H., Cheng, C., Bui, A. Q., Wagmaister, J. A., Henry, K. F., Pelletier, J., Kwong, L., Belmonte, M., Kirkbride, R., Horvath, S., Drews, G. N., Fischer, R. L., Okamuro, J. K., Harada, J. J. and Goldberg, R. B. 2010. Global analysis of gene activity during *Arabidopsis* seed development and identification of seed-specific transcription factors. *Proceedings of the National Academy of Sciences*. 107: 8063 - 8070.

Letchworth, M. B. and Lambert, R. J. 1998. Pollen parent effects on oil, protein, and starch concentration in maize kernels. *Crop Science*. 38: 363 - 367.

Li, C., Yu, M., Chen, F. and Wang, S. 2010. In vitro maturation and germination of *Jatropha curcas* microspores. *International Journal of Agriculture and Biology*. 12: 541 - 546.

Li, Z. G., Gong, M., Yang, S. Z. and Long, W. B. 2012. Efficient callus induction and indirect plant regeneration from various tissues of *Jatropha curcas*. *African Journal of Biotechnology*. 11: 7843 - 7849.

Lin, I. P., Jiang, P. L., Chen, C. S. and Tzen, J. T. C. 2012. A unique caleosin serving as the major protein in oil bodies isolated from *Chlorella* sp. cells cultured with limited nitrogen. *Plant Physiology and Biochemistry*. 61: 80 - 87.

Lin, L. J., Tai, S. S. K., Peng, C. C. and Tzen, J. T. C. 2002. Steroleosin, a sterol-binding dehydrogenase in seed oil bodies. *Plant Physiology*. 128: 1200 - 1211.

Liners, F., Gaspar, T. and Cutsem, P. V. 1994. Acetyl- and methyl-esterification of pectins of friable and compact sugar-beet calli: consequences for intercellular adhesion. *Planta*. 192: 545 - 556.

Liu, H. F., Deng, Y. F. and Liao, J. P. 2008. Floral organogenesis of three species of *Jatropha* (Euphorbiaceae). *Journal of Systematics and Evolution*. 46: 71 - 79.

Liu, H., Kirchoff, B. K., Wu, G. and Liao, J. 2007. Microsporogenesis and male gametogenesis in *Jatropha curcas* L. (Euphorbiaceae). *The Journal of the Torrey Botanical Society*. 134: 335 - 343.

Liu, H., Lin, S. and Liao, J. 2015. Floral ontogeny of two *Jatropha* species (Euphorbiaceae S.S) and its systematic implications. *Pakistan Journal of Botany*. 47: 959 - 965.

Liu, H., Liu, Y. J., Yang, M. F. and Shen, S. H. 2009. A comparative analysis of embryo and endosperm proteome from seeds of *Jatropha curcas*. *Journal of Integrative Plant Biology*. 51: 850 - 857.

Liu, W., Hildebrand, D. F., and Collins, G. B. 1995. Auxin-regulated changes of fatty acid content and composition in soybean zygotic embryo cotyledons. *Plant Science*. 106: 31 - 42.

Lora, J., Herrero, M. and Hormaza, J. I. 2009. The coexistence of bicellular and tricellular pollen in *Annona cherimola* (Annonaceae): implications for pollen evolution. *American Journal of Botany*. 96: 802 - 808.

Lu, C., Fulda, M., Wallis, J. G. and Browse, J. 2006. A high-throughput screen for genes from castor that boost hydroxy fatty acid accumulation in seed oils of transgenic *Arabidopsis*. *The Plant Journal*. 45: 847 - 856.

Lu, Y. L., Yang, X. L., Li, R., Li, S. L. and Tong, Y. A. 2015. Effects of different potassium fertilizer application periods on the yield and quality of Fuji apple. *The Journal of Applied Ecology*. 26: 1179 - 1185.

Lyra, D. H., Sampaio, L. S., Pereira, D. A., Silva, A. P. and Amaral, C. L. F. 2011. Pollen viability and germination in *Jatropha ribifolia* and *Jatropha mollissima* (Euphorbiaceae): species with potential for biofuel production. *African Journal of Biotechnol*ogy. 10: 368 - 374.

Ma, J., Skibbe, D. S., Fernandes, J. and Walbot, V. 2008. Male reproductive development: gene expression profiling of maize anther and pollen ontogeny. *Genome Biology*. 9: 1 - 17.

Malik, M. R., Wang, F., Dirpaul, J. M., Zhou, N., Polowick, P. L., Ferrie, A. M. R. and Krochko, J. E. 2007. Transcript profiling and identification of molecular markers for early microspore embryogenesis in *Brassica napus*. *Plant Physiol*ogy. 144: 134 - 154.

Malik, S., Bhushan, S., Verma, S. C., Sharma, N., Sinha, A. K., Sharma, M. and Ahuja, P. S. 2008. Production of naphthoquinone pigments in cell suspension cultures of *Arnebia euchroma* (Royle) Johnston: Influence of pH on growth kinetics and acetylshikonin. *Medicinal and Aromatic Plant Science and Biotechnology*. 2: 43 - 49.

Malik, S., Mirjalili, M. H., Fett-Neto, A. G., Mazzafera, P. and Bonfill, M. 2013. Living between two worlds: two-phase culture systems for producing plant secondary metabolites. *Critical Reviews in Biotechnology*. 33: 1 - 22.

Mazumdar, P., Basu, A., Paul, A., Mahanta, C. and Sahoo, L. 2010. Age and orientation of the cotyledonary leaf explants determine the efficiency of *de novo* plant regeneration and *Agrobacterium tumefaciens*-mediated transformation in *Jatropha curcas* L. *South African Journal of Botany*. 76: 337 - 344.

Mazumdar, P., Borugadda, V. B., Goud, V. V. and Sahoo, L. 2012. Physico-chemical characteristics of *Jatropha curcas* L. of North East India for exploration of biodiesel. *Biomass and bioenergy*. http://dx.doi.org/10.1016/j. biombioe.2012.07.005.

McInnis, S. M., Emery, D. C., Porter, R., Desikan, R., Hancock, J. T. and Hiscock, S. J. 2006. The role of stigma peroxidases in flowering plants: insights from further characterization of a stigma-specific peroxidase (SSP) from *Senecio squalidus* (Asteraceae). *Journal of Experimental Botany*. 57: 1835 - 1846.

Meher, L. C., Vidya Sagar, D. and Naik, S. N. 2006. Technical aspects of biodiesel production by transesterification – a review. *Renewable and Sustainable Energy Reviews*. 10: 248 - 268.

Merchán, P. J. A., Arévalo, Y. A., Cely, G. E. R., Pinzón, E. H. and Serrano, P. A. C. 2016. Fruit growth characterization of the tomato (*Solanum lycopersicum* L.) hybrid 'Ichiban' grown under cover. *Agronomía Colombiana*. 34: 155 - 162.

Mikuła, A., Niedzielski, M. and Rybczynski, J. J. 2006. The use of TTC reduction assay for assessment of *Gentiana* spp. cell suspension viability after cryopreservation. *Acta Physiologiae Plantarum*. 28: 315 - 324.

Mishra, R. C., Kumar, J. and Gupta, J. K. 2011. The effect of mode of pollination on yield and oil potential of *Brassica campestris* L. var. *sarson* with observations on insect pollinators. *Journal of Apicultural Research*. 27: 186 - 189.

Misra, P., Toppo, D. D., Gupta, N., Chakrabarty, D. and Tuli, R. 2010. Effect of antioxidants and associate changes in antioxidant enzymes in controlling browning and necrosis of proliferating shoots of elite *Jatropha curcas* L. *Biomass and Bioenergy*. 34: 1861 - 1869.

Mittelbach, M., 1996. Diesel fuel derived from vegetable oils, VI: specifications and quality control of biodiesel. *Bioresource Technology*. 56: 7 - 11.

Mohan, N., Nikdad, S. and Singh, G. 2011. Studied on seed germination and embryo culture of *Jatropha curcas* L. under in vitro conditions. *Biotechnology, Bioinformatics and Bioengineering*. 1: 187 - 194.

Moore, D. S., Notz, W. I. and Flinger, M. A. 2013. *The Basic Practice of Statistics*. New York: W. H. Freeman and Company.

Moore, G., Goldman, D., Garland, M. and Anderson, K. 2017. The plants database. Natural resources conservation service, United States Department of Agriculture. https://plants.usda.gov/java/ClassificationServlet?source=display &classid=JACU2 (accessed January 4, 2018).

Mulugeta, D., Maxwell, B. D., Fay, P. K. and Dyer, W. E. 1994. Kochia (*Kochia scoparia*) pollen dispersion, viability and germination. *Weed Science*. 42: 548 - 552.

Murashige, T. and Skoog, F. 1962. A revised medium for rapid growth and bioassays with tobacco tissue cultures. *Physiologia Plantarum*. 15: 473 - 497.

Musial, K., Bohanec, B., Jakše, M. and Przywara, L. 2005. The development of onion (*Allium cepa* L.) embryo sacs in vitro and gynogenesis induction in relation to flower size. *In Vitro Cellular and Developmental Biology*. 41: 446 - 452.

Naor, A. 2006. Irrigation scheduling of peach-deficit irrigation at different phenological stages and water stress assessment. *ISHS Acta Horticulturae*. 713, doi: 10.17660/ActaHortic.2006.713.49.

Negussie, A., Achten, W. M. J., Verboven, H. A. F., Aerts, R., Sloan, R., Hermy, M. and Muys, B. 2015. Conserving open natural pollination safeguards *Jatropha* oil yield and oil quality. *Bioenergy Research*. 8: 340 - 349.

Negussie, A., Achten, W. M. J., Verboven, H. A. F., Hermy, M. and Muys, B. 2014. Floral display and effects of natural and artificial pollination on fruiting and seed yield of the tropical biofuel crop *Jatropha curcas* L. *Global Change Biology Bioenergy*. 6: 210 - 218.

Nepi, M. and Pacini, E. 2001. Effect of pistil age on pollen tube growth, fruit development and seed set in *Cucurbita pepo* L. *Acta Societatis Botanicorum Poloniae*. 70: 165 - 172.

Nepi, M., Cresti, L., Guarnieri, M. and Pacini, E. 2010. Effect of relative humidity on water content, viability and carbohydrate profile of *Petunia hybrid* and *Cucurbita pepo* pollen. *Plant Systematics and Evolution*. 284: 57 - 64.

Oliveira, A. B., Vendrame, W. A., Londe, L. C. N. and Sanaey, M. 2017. Induction of different types of *callus* in *Jatropha curcas* L. hybrid accession at in vitro condition. *Australian Journal of Crop Science*. 11: 874 - 879.

Oliveira, J. S., Leite, P. M., Souza, L. B., Mello, V. M., Silva, E. C., Rubim, J. C., Meneghetti, S. M. P. and Suarez, P. A. Z. 2009. Characteristics and composition of *Jatropha gossypiifolia* and *Jatropha curcas* L. oils and application for biodiesel production. *Biomass and Bioenergy*. 33: 449 - 453.

Olsen, O. A. 2004. Nuclear endosperm development in cereals and *Arabidopsis thaliana*. *The Plant Cell*. 16: S214 - S227.

Ong, H. C., Silitonga, A. S., Masjuki, H. H., Mahlia, T. M. I., Chong, W. T. and Boosroh, M. H. 2013. Production and comparative fuel properties of biodiesel from non-edible oils: *Jatropha curcas, Sterculia foetida* and *Ceiba pentandra*. *Energy Conversion and Management.* 73: 245 - 255.

Pan, B. Z. and Xu, Z. F. 2011. Benzyladenine treatment significantly increases the seed yield of the biofuel plant *Jatropha curcas*. *Journal of Plant Growth Regulation*. 30: 166 - 174.

Parthiban, K. T., Kumar, R. S., Thiyagarajan, P., Subbulakshmi, V., Vennila, S. and Rao, M. G. 2009. Hybrid progenies in *Jatropha* – a new development. *Current Science*. 96: 815 - 23.

Pasaribu, B., Chen, C. S., Liao, Y. K., Jiang, P. L. and Tzen, J. T. C. 2017. Identification of caleosin and oleosin in oil bodies of pine pollen. *Plant Physiology and Biochemistry*. 111: 20 - 29.

Pasternak, T., Miskolczi, P., Ayaydin, F., Meszaros, T., Dudits, D. and Feher, A. 2000. Exogenous auxin and cytokinin dependent activation of CDKs and cell division in leaf protoplast-derived cells of alfalfa. *Plant Growth Regulation.* 32: 129 - 141.

Perrot-Rechenmann, C. 2010. Cellular responses to auxin: division versus expansion. *Cold Spring Harbor Perspectives in Biology*. 2: 1 - 15.

Pescador, R., Kerbauy, G. B., Santos, Y. A. C., Vesco, L. D, Fraga, H. P. F. and Guerra, M. P. 2012. Comparative study of reserve lipid accumulation during somatic and zygotic *Acca sellowiana* (O. Berg.) Burret embryogenesis. *Acta Physiologiae Plantarum*. 34: 771 - 778.

Pio, L. A. S., Ramos, J. D., Pasqual, M., Santos, F. C. and Junqueira, K. P. 2004. Receptiveness of the stigma and in vitro germination of orange pollen, submitted to different temperatures. *Ciência Agrotecnologia*. 28: 1087 - 1091.

Pires, N. D. 2014. Seed evolution: parental conflicts in a multi-generational household. *Biomolecular Concepts*. 5: 71 - 86.

Popluechai, S., Froissard, M., Jolivet, P., Breviario, D., Gatehouse, A. M. R., O'Donnell, A. G., Chardot, T. and Kohli, A. 2011. *Jatropha curcas* oil body proteome and oleosins: L-form *JcOle3* as a potential phylogenetic marker. *Plant Physiology and Biochemistry*. 49: 352 - 356.

Pranesh, K. J., Rao, M. R. G., Sowmya, H. C., Gowda, B., Savithramma, D. L. and Naveen, N. L. 2010. Studies on floral display and mode of reproduction in *Jatropha* (*Jatropha curcas* L.). *Electronic Journal of Plant Breeding*. 1: 832 - 838.

Pullen, J. and Saeed, K. 2012. An overview of biodiesel oxidation stability. *Renewable and Sustainable Energy Reviews*. 16: 5924 - 5950.

Raju, A. J. S. and Ezradanam, V. 2002. Pollination ecology and fruiting behavior in a monoecious species, *Jatropha curcas* L. (Euphorbiaceae). *Current Science*. 83: 1395 - 1398.

Ramos, L. Y. S., Carballo, L. M. and Melara, M. V. 2013. Establishment of cell suspension cultures of two Costa Rican *Jatropha* species (Euphorbiaceae). *Revista De Biologia Tropical*. 61: 1095 - 1107.

Ramos, M. J., Fernandez, C. M., Casas, A., Rodriguez, L. and Perez, A. 2009. Influence of fatty acid composition of raw materials on biodiesel properties. *Bioresource Technology*. 100: 261 - 268.

Ramrao, K. R., Kokiladevi, E., Aishwarya, V., Sudhakar, D., Arul, L. and Balasubramanian, P. 2016. Plant regeneration from leaf and petiole explants of *jatropha curcas* L.: a biofuel plant. *Global Journal of Bio-Science and Biotechnology*. 5: 26 - 30.

Rao, G. R., Korwar, G. R., Shanker, A. K. and Ramakrishna, Y. S. 2008. Genetic associations, variability and diversity in seed characters, growth, reproductive phenology and yield in *Jatropha curcas* (L.) accessions. *Trees*. 22: 697 - 709.

Rashid, U., Anwar, F., Jamil, A. and Bhatti, H. N. 2010. *Jatropha curcas* seed oil as a viable source for biodiesel. *Pakistan Journal of Botany*. 42: 575 - 582.

Reale, L., Ricci, A., Ferranti, F., Torricelli, R., Venanzoni, R. and Falcinelli, M. 2012. Cytohistological analysis and mobilization of reserves in *Jatropha curcas* L. seed. *Crop Science*. 52: 830 - 835.

Reece, J. B., Urry, L. A., Cain, M. L., Wasserman, S. A., Minorsky, P. V. and Jackson, R. B. 2011. *Campbell Biology*. Ninth edition. Boston: Pearson Education, Incorporated.

Rianti, P., Suryobroto, B. and Atmowidi, T. 2010. Diversity and effectiveness of insect pollinators of *Jatropha curcas* L. (Euphorbiaceae). *HAYATI Journal of Biosciences*. 17: 38 - 42.

Roldan-Serrano, A. and Guerra-Sanz, J. M. 2006. Quality fruit improvement in sweet pepper culture by bumblebee pollination. *Scientia Horticulturae*. 110: 160 - 166.

Ruzin, S. 1999. *Plant Microtechnique and Microscopy*. New York: Oxford University Press, Incorporated.

Samra, S., Samocha, Y., Eisikowitch, D. and Vaknin, Y. 2014. Can ants equal honeybees as effective pollinators of the energy crop *Jatropha curcas* L. under Mediterranean conditions?. *GCB Bioenergy*. 6: 756 - 767.

Santos, D. N., Nunes, C. F., Soares, J. D. R., Valente, T. C. T., Alves, E., Labory, C. R. G. and Pasqual, M. 2013. Cytological characterization of *Jatropha curcas* callus in different periods of cultivation. *Crop Breeding and Applied Biotechnology*. 13: 228 - 233.

Santos, R. R., Kunigami, C. N., Aranda, D. A. G. and Teixeira, C. M. L. L. 2015. Assessment of triacylglycerol content in *Chlorella vulgaris* cultivated in a two-stage process. *Journal of Biotechnology and Biomaterials*. 5. doi: 10.4172 /2155-952X.1000212.

Sarasketa, A., González-Moro, M. B., González-Murua, C. and Marino, D. 2016. Nitrogen source and external medium pH interaction differentially affects root and shoot metabolism in *Arabidopsis*. *Frontiers in Plant Science*. 7: 1 - 12.

Sauerwein, M., Yoshimatsu, K. and Shimomura, K. 1992. Further approaches in the production of secondary metabolites by plant tissue cultures. *Plant Tissue Culture Letters*. 9: 1 - 9.

Saygideger, S. D. and Okkay, O. 2008. Effect of 2, 4-dichlorophenoxyacetic acid on growth, protein and chlorophyll-*a* content of *Chlorella vulgaris* and *Spirulina platensis* cells. *Journal of Environmental Biology*. 29: 175 - 178.

Schaller, G. E., Street, I. H. and Kieber, J. J. 2014. Cytokinin and the cell cycle. *Current Opinion in Plant Biology*. 21: 7 - 15.

Schuchardt, U., Serchelia, R. and Vargas, R. M. 1998. Transesterification of vegetable oils: a review. *Journal of the Brazilian Chemical Society*. 9: 199 - 210.

Sharma, N., Nehal, N., Singh, M., Singh, P., Rajpoot, P., Pandey, A. K., Khan, A. H., Singh, A. K. and Yadav, R. K. 2017. Effect of plant growth regulators on growth, biochemical changes and yield of mustard [*Brassica juncea* (L.) Czern. & Coss.]. *Plant Archives.*17: 33 - 38.

Shockey, J. M., Gidda, S. K., Chapital, D. C., Kuan, J. C., Dhanoa, P. K., Bland, J. M., Rothstein, S. J., Mullen, R. T. and Dyer, J. M. 2006. Tung tree DGAT1 and DGAT2 have nonredundant functions in triacylglycerol biosynthesis and are localized to different subdomains of the endoplasmic reticulum. *Plant Cell*. 18: 2294 - 2313.

Shore, J. and Barreit, S. H. 1984. The effect of pollination intensity and incompatible pollen on seed set in *Turnera ulmifolia* (Tusnesaceae). *Canadian Journal of Botany*. 62: 1298 - 1303.

Siang, T. C., Soong, S. T. and Yien, A. T. S. 2012. Plant regeneration studies of *Jatropha curcas* using induced embryogenic callus from cotyledon explants. *African Journal of Biotechnology*. 11: 8022 - 8031.

Silitonga, A. S., Masjuki, H. H., Mahlia, T. M. I., Ong, H. C., Atabani, A. E. and Chong, W. T. 2013. A global comparative review of biodiesel production from *Jatropha curcas* using different homogeneous acid and alkaline catalysts: study of physical and chemical properties. *Renewable and Sustainable Energy Reviews*. 24: 514 - 533.

Siloto, R. M. P., Findlay, K., Villalobos, A. L., Yeung, E. C., Nykiforuk, C. L. and Moloney, M. M. 2006. The accumulation of oleosins determines the size of seed oilbodies in *Arabidopsis*. *The Plant Cell*. 18: 1961 - 1974.

Silva, A. L. C., Caruso, C. S., Moreira, R. A. and Horta, A. C. G. 2005. Growth characteristics and dynamics of protein synthesis in callus cultures from *Glycine wightii* (Wight & Arn.) Verdc. *Ciência Agrotecnologia*. 29: 1161 - 1166.

Singh, M. and Chaturvedi, R. 2012. Evaluation of nutrient uptake and physical parameters on cell biomass growth and production of spilanthol in suspension cultures of *Spilanthes acmella* Murr. *Bioprocess and Biosystems Engineering*. 35: 943 - 951.

Skoog, F. and Miller, C. O. 1957. Chemical regulation of growth and organ formation in plant tissues cultured in vitro. *Symposia of the Society for Experimental Biology*. 11: 118 - 130.

Soares, E. L., Lima, M. L. B., Nascimento, J. R. S., Soares, A. A., Coutinho, I. A. C. and Campos, F. A. P. 2017. Seed development of *Jatropha curcas* L. (Euphorbiaceae): integrating anatomical, ultrastructural and molecular studies. *Plant Cell Reports*. 36: 1707 - 1716.

Sood, A. and Chauhan, R. S. 2015. Regulation of FA and TAG biosynthesis pathway genes in endosperms and embryos of high and low oil content genotypes of *Jatropha curcas* L. *Plant Physiology and Biochemistry*. 94: 253 - 267.

Soomro, R. and Memon, R. A. 2007. Establishment of callus and suspension culture in *Jatropha curcas*. *Pakistan Journal of Botany*. 39: 2431 - 2441.

Souza, J. M. M., Berkov, S. and Santos, A. S. 2014. Improvement of friable callus production of *Boerhaavia paniculata* Rich and the investigation of its lipid profile by GC/MS. *Annals of the Brazilian Academy of Sciences*. 86: 1015 - 1027.

Souza, J. M. M., Tomaz, M. L., Arruda, S. C. C., Demétrio, C. G. B., Venables, W. N. and Martinelli, A. P. 2011. Callus sieving is effective in improving synchronization and frequency of somatic embryogenesis in *Citrus sinensis*. *Biologia Plantarum*. 55: 703 - 707.

Staubmann, R., Ncube, I., Gubitz, G. M., Steiner, W. and Read, J. S. 1999. Esterase and lipase activity in *Jatropha curcas* L. seeds. *Journal of Biotechnology*. 75: 117 - 126.

Steponkus, P. L. and Lanphear, F. O. 1967. Refinement of the triphenyl tetrazolium chloride method of determining cold injury. *Plant Physiology*. 42: 1423 - 1426.

Stone, J. L., Thomson, J. D. and Acosta, S. J. D. 1995. Assessment of pollen viability in hand-pollination experiments: a review. *American Journal of Botany*. 82: 1186 - 1197.

Sulusoglu, M. and Cavusoglu, A. 2014. In vitro pollen viability and pollen germination in cherry laurel (*Prunus laurocerasus* L.). *Scientific World Journal*. 2014: 1 - 7.

Taha, R. A. 2014. Effect of growth regulators and salinity levels on in vitro cultures of jojoba plants. *World Applied Sciences Journal*. 31: 751 - 758.

Taiz, L., Zeiger, E., Moller, L. M. and Murphy, A. 2015. *Plant physiology and development*. Sixth edition. Oxford: Sinauer Associates, Incorporated.

Takeda, Y. 1982. Development study on *Jatropha curcas* (sabudum) oil as a substitute for diesel engine oil in Thailand. Interim Report of the Ministry of Agriculture, Thailand.

Talla, S. K., Panigrahy, M., Kappara, S., Nirosha, P., Neelamraju, S. and Ramanan, R. 2016. Cytokinin delays dark-induced senescence in rice by maintaining the chlorophyll cycle and photosynthetic complexes. *Journal of Experimental Botany*. 67: 1839 - 1851.

Tan, S. H., Musa, R., Ariff, A. and Maziah, M. 2010. Effect of plant growth regulators on callus, cell suspension and cell line selection for flavonoid production from pegaga (*Centella asiatica* L. urban). *American Journal of Biochemistry and Biotechnology*. 6: 284 - 299.

Thepsamran, N., Thepsithar, C. and Thongpukdee, A. 2006. *In vitro multiple shoot induction of physic nut* (*Jatropha curcas*). Nakhon Pathom: Department of Biology, Faculty of Science, Silpakorn University, Thailand.

Townsley, P. M. 1974. Production of coffee from plant cell suspension cultures. *Canadian Institute of Food Science and Technology Journal*. 7: 79 - 81.

Tzen, J. T. C, Lai, Y. K., Chan, K. L. and Huang, A. H. C. 1990. Oleosin isoforms of high and low molecular weights are present in the oil bodies of diverse seed species. *Plant Physiology*. 94: 1282 - 1289.

Tzen, J. T. C. 2012. Integral proteins in plant oil bodies. *ISRN Botany*. 2012: 263 - 270.

Tzen, J. T. C. and Huang, A. H. C. 1992. Surface structure and properties of plant seed oil bodies. *Journal of Cell Biology*. 117: 327 - 335.

Tzen, J. T. C., Cao, Y. Z., Laurent, P., Ratnayake, C. and Huang, A. H. C. 1993. Lipids, proteins, and structure of seed oil bodies from diverse species. *Plant Physiology*. 101: 67 - 276.

Tzen, J. T. C., Chuang, R. L. C., Chen, J. C. F. and Wu, L. S. H. 1998. Coexistence of both oleosin isoforms on the surface of seed oil bodies and their individual stabilization to the organelles. *Journal of Biochemistry*. 123: 318 - 323.

Tzen, J. T. C., Peng, C. C., Cheng, D. J., Chen, E. C. F. and Chiu, J. M. H. 1997. A new method for seed oil body purification and examination of oil body integrity following germination. *The Journal of Biochemistry*. 121: 762 - 768.

Ullah, F. and Bano, A. 2011. Effect of plant growth regulators on oil yield and biodiesel production of safflower (*Carthamus tinctorius* L.). *Brazilian Society of Plant Physiology*. 23: 27 - 31.

Ullah, F., Bano, A. and Nosheen, A. 2012. Effects of plant growth regulators on growth and oil quality of canola (*Brassica napus* L.) under drought stress. *Pakistan Journal of Botany*. 44: 1873 - 1880.

Vega, V. P., Garcia, B. G. and Simarro, J. M. 2013. Morphological markers to correlate bud and anther development with microsporogenesis and microgametogenesis in pepper (*Capsicum annuum* L.) *Acta Physiologiae Plantarum*. 35: 627 - 633.

Verma, P., Sharma, M. P. and Dwivedi, G. 2015. Operational and environmental impact of biodiesel on engine performance: a review of literature. *International Journal of Renewable Energy Research*. 5: 961 - 970.

Vinkenoog, R. and Scott, R. J. 2001. Autonomous endosperm development in flowering plants: how to overcome the imprinting problem?. *Sexual Plant Reproduction*. 14: 189 - 194.

Wang, Y., Ou, S. Y., Liu, P. Z. and Tang, S. Z. 2006. Comparison of two different processes to synthesize biodiesel by waste cooking oil. *Journal of Molecular Catalysis A: Chemical*. 252: 107 - 112.

Wang, Z. Y., Ge, Y., Scott, M. and Spangenberg, G. 2004. Viability and longevity of pollen from transgenic and nontransgenic tall fescue (*festuca arundinacea*) (Poaceae) plants. *American Journal of Botany*. 91: 523 - 530.

Widholm, J. M. 1992. Properties and uses of phytoautotrophic plant cell cultures. *International Review of Cytology*. 132: 109 - 175.

Willcox, M. C., Reed, S. M., Burns, J. A. and Wynne, J. C. 1991. Effect of microspore stage and media on anther culture of peanut (*A. hypogaea* L.). *Plant Cell, Tissue and Organ Culture*. 24: 25 - 28.

Wilson, C. A. 2001. Floral stages, ovule development, and ovule and fruit success in *Iris tenax*, focusing on var. *gormanii*, a taxon with low seed set. *American Journal of Botany*. 88: 2221 - 2231.

Witham, F. H. 1968. Effect of 2, 4-dichlorophenoxyacetic acid on the cytokinin requirement of soybean cotyledon and tobacco stem pith callus tissues. *Plant Physiology*. 43: 1455 - 1457.

Wu, B. J. and Chen, K. C. 1982. Cytological and embryological studies on haploid plant production from cultured unpollinated ovaries of *Nicotiana tabacum* L. *Acta Botanica Sinica*. 24: 125 - 129.

Wu, J., Liu, Y., Tang, L., Zhang, F. and Chen, F. 2011. A study on structural features in early flower development of *Jatropha curcas* L. and the classification of its inflorescences. *African Journal of Agricultural Research*. 6: 275 - 284.

Wu, L. S. H., Wang, L. D., Chen, P. W., Chen, L. J. and Tzen, J. T. C. 1998. Genomic cloning of 18 kDa oleosin and detection of triacylglycerols and oleosin isoforms in maturing rice and postgerminative seedlings. *Journal of Biochemistry*. 123: 386 - 391.

Wubs, A. M., Ma, Y. T., Heuvelink, E., Hemerik, L. and Marcelis, L. F. M. 2012. Model selection for nondestructive quantification of fruit growth in pepper. *Journal of the American Society for Horticultural Science*. 137: 71 - 79.

Yan, H., Lu, L., Alzate, A., Ceballos, H., Hershey, C., Chen, S. and Li, K. 2014. Fruit, seed and embryo development of different cassava (*Manihot esculenta* Crantz) genotypes and embryo rescues. *African Journal of Biotechnology*. 13: 1524 - 1528.

Yin, Y., He, Y., Liu, W., Gan, L., Fu, C., Jia, H. and Li, M. 2014. The durative use of suspension cells and callus for volatile oil by comparative with seeds and fruits in *Capparis spinosa* L. Plos One. 9: 1 - 19.

Zhang, C., Tsukuni, T., Ikeda, M., Sato, M., Okada, H., Ohashi, Y., Matsuno, H., Yamamoto, T., Wada, M., Yoshikawa, N., Matsumoto, S., Li, J., Mimida, N., Watanabe, M., Suzuki, A. and Komori, S. 2013. Effects of the microspore development stage and cold pre-treatment of flower buds on embryo induction in apple (*Malus* × *domestica* Borkh.) anther culture. *Journal of the Japanese Society for Horticultural Science*. 82: 114 - 124.

Zhao, J., Zhu, W. H., Hu, Q. and Guo, Y. Q. 2001. Compact callus cluster suspension cultures of *Catharanthus roseus* with enhanced indole alkaloid biosynthesis. *In Vitro Cellular and Developmental Biology-Plant*. 37: 68 - 72.

Zhao, Z., Andersen, S. U., Ljung, K., Dolezal, K., Miotk, A., Schultheiss, S. J. and Lohmann, J. U. 2010. Hormonal control of the shoot stem-cell niche. Nature. 465: 1089 - 1092.

Zhong, J. J., Bai, Y. and Wang, S. J. 1996. Effects of plant growth regulators on cell growth and ginsenoside saponin production by suspension cultures of *Panax quinquefolium*. *Journal of Biotechnology*. 45: 227 - 234.

Zielińska, A. and Nowak, I. 2014. Fatty acids in vegetable oils and their importance in cosmetic industry. Chemik. 68: 103 - 110.

APPENDICES

APPENDIX A
MICROTECHNIQUE PROCESS AND STAINING

1. FAA II solution

Formaldehyde	5% (v/v)
Glacial acetic acid	5% (v/v)
70 % alcohol	90% (v/v)

2. Dehydration solution

No.	Total alcohol (%)	Composition (ml)				
		TBA	Ethanol		Water	Other
			95%	100%		
1	5	-	5	-	95	-
2	10	-	10	-	90	-
3	20	-	20	-	80	-
4	30	-	30	-	70	-
5	50	10	40	-	50	-
6	70	20	50	-	30	-
7	85	35	50	-	15	-
8	95	55	40	-	5	-
9	100	75	-	25	-	-
10	-	100	-	-	-	Eosin
11	-	100	-	-	-	-
12	-	100	-	-	-	Paraffin oil 100

TBA, tert-butyl alcohol

3. Hematoxylin and safranin staining for histological observation (Ruzin, 1999)

3.1 Deparaffinization and place the paraffin-prepared sample in DW 2 minutes

3.2 Place sample slides in Delafield's hematoxylin 30 minutes

3.3 Wash with tap water 2 minutes

3.4 Dip the slide in acidulate water 8 times

3.5 Dip the slide in tap water 2 times

3.6 Place the slide in 0.1% lithium carbonate 2 minutes

3.7 Dip the slide in tap water 2 times

3.8 Place the slide in safranin solution 5 seconds

3.9 Wash with tap water

3.10 Dip the slide in acidulate water 2 times

3.11 Dip the slide in 0.1% lithium carbonate 1 time

3.12 Dehydrate with 70%, 95% and 100% alcohol

3.13 Place the slide in absolute alcohol: xylene 2 minutes

3.14 Place the slide in xylene 2 times (each 5 minutes)

3.15 Mount the slide using Hi-MO

* Nucleus is stained blue-purple, cytoplasm is in pink color.

4. Aniline blue staining for callose wall observation (Ruzin, 1999)

4.1 Place the paraffin-prepared sample in xylene substitute solution 2 times (each 10 minutes)

4.2 Place sample slides in absolute alcohol: xylene substitute solution 2 minutes

4.3 Place sample slides in absolute alcohol 2 times (each 2 minutes)

4.4 Place sample slides in 95% alcohol 2 times (each 2 minutes)

4.5 Place sample slides in 70% alcohol 2 times (each 2 minutes)

4.6 Place sample slides in distilled water 2 minutes

4.7 Place sample slides in 1.5 M K_2HPO_4, pH 9.2 solution 2 minutes

4.8 Stain the samples in 0.1% (w/v) aniline blue solution 30 minutes

4.9 Wash sample with phosphate buffer

4.10 Mount the slide using glycerin jelly

4.11 Viewed with fluorescent microscope using 365 nm excitation wavelength

* Callose wall represents as yellow-green fluorescence.

5. Oil Red O staining for lipid droplet observation (Brown, 1969)

5.1 Place the fresh-cut samples (cryostat, 20 µm) in distilled water for 1 minute

5.2 Drop 100% propylene glycol onto the samples, keep 2 minutes

5.3 Drop 0.5% Oil Red O onto the samples, keep 25 minutes

5.4 Drop 85% propylene glycol onto the samples, keep 1 minute

5.5 Drop distilled water onto the samples, keep 1 minute

5.6 Drop Harris's hematoxylin onto the samples, keep 30 seconds

5.7 Drop distilled water onto the samples, keep 2 minutes

5.8 Mount with glycerin jelly

* Lipid droplets are in orange-red color.

APPENDIX B
POLLEN VIABILITY AND GERMINATION

1. Tetrazolium salt (TTC-test)

Colorless tetrazolium salt $\xrightarrow{\text{Dehydrogenase}}$ Reddish insoluble formazan

1.1 Stock solution (2% TTC)

Dissolve 2 grams tetrazolium salt using distilled water, adjust total volume to 100 ml by distilled water and store the solution in refrigerator in dark condition

1.2 Working solution (1% TTC in sucrose solution)

Mix the TTC stock solution with 30% sucrose solution (stock TTC: sucrose = 1:1)

1.3 Staining procedures

1.3.1 Load pollen grains into the test tube

1.3.2 Add TTC working solution to the tube (pollen grain: TTC =1:1)

1.3.3 Wrap the tube with foil paper

1.3.4 Store the tube in humid area for 24 hours

1.3.5 Wash pollen grains 3 times with distilled water and observe with light microscope

* Red pollen grains are viable.

2. Fluorochromatic Reaction (FCR-Test)

Fluorescein diacetate $\xrightarrow[\text{hydrolyzed}]{\text{Esterase (cytoplasm)}}$ Fluorescein (fluorescent)

2.1 Solutions

FDA solution (2 mg ml^{-1}, solvent: acetone)

15% sucrose solution mixed with 300 mg ml^{-1} calcium nitrate

2.2 Staining procedures

2.2.1 Drop 2 - 5 ml sucrose solution into tube

2.2.2 Add FDA solution to the tube until the mixed solution become turbid (within 30 minutes)

2.2.3 Drop the above solution onto glass slide

2.2.4 Load pollen grains to the solution on the slide

2.2.5 Place the samples in humidity chamber 10 minutes

2.2.6 Observe with fluorescent microscope (489 nm excitation wavelength)

* Yellow-green fluorescent grains are viable.

3. Pollen germination (Li et al., 2010)

3.1 Medium composition

Sucrose	20%
Calcium nitrate [$Ca(NO_3)_2$. $4H_2O$]	400 mg L^{-1}
Magnesium sulfate ($MgSO_4$. $7H_2O$)	200 mg L^{-1}
Boric acid (H_3BO_3)	100 mg L^{-1}
Potassium nitrate (KNO_3)	100 mg L^{-1}
Coconut water	2.5%
Polyethylene glycol (PEG 4000)	10%
pH	6.5

3.2 Procedure

3.2.1 Drop 20 µl of liquid media into depression slide

3.2.2 Release pollens to the media

3.2.3 Place in moisture chamber in dark condition, 25 ± 3 ºC for 14 h

* The pollen grains whose tubes reached the same or greater length than their own diameters were considered germinated.

APPENDIX C
FATTY ACID CHARACTERIZATION BY GAS CHROMATOGRAPHY

Hydrolysis of extracted oil (Jham et al., 1982)

1. Adding 1 ml of KOH/MeOH (0.5 M) to 50 µl of oil
2. Heating at 100 °C for 10 minutes
3. Adding 400 µl HCl/MeOH (4:1, % v/v) into the hydrolysis mixture
4. Heating at 100 °C for 15 minutes
5. Cooling
6. Adding 2 ml water to the sample solution
7. Extracting with 3 ml petroleum ether for 2 times
8. Separating the organic phase
9. Drying using Na_2SO_4 (anhydrous)
10. Filtering the mixture through filter paper Whatman No.1
11. Evaporating and redissolving in 500 µl $CHCl_3$

APPENDIX D
OIL BODY EXTRACTION SOLUTIONS

1. Stock solution

1.1 <u>0.5 M Na-phosphate, pH 7.5 (50× stock) (store at 4 ºC)</u>

Phosphoric acid (H_3PO_4)	16.9 ml
ddH_2O	400 ml
NaOH	10 g
NaOH (2 N) to	pH 7.5
ddH_2O to	500 ml (final volume)

1.2 <u>10% Tween 20 (v/v) (Tween 20, CMC = 0.059%)</u>

Tween 20 (100%)	1 ml
ddH_2O (about 9 ml) to	10 ml (final volume)

2. Working reagents (store at 4 ºC)

Grinding buffer (buffer A) (10 mM Na-Pi, pH 7.5 and 0.6 M sucrose)

Floation buffer (buffer B) (10 mM Na-Pi, pH 7.5 and 0.4 M sucrose)

Salting buffer (buffer C) (10 mM Na-Pi, pH 7.5, 2 M NaCl and 0.6 M sucrose)

Floating buffer (buffer D) (10 mM Na-Pi, pH 7.5, 2 M NaCl and 0.25 M sucrose)

	Buffer A	**Buffer B**	**Buffer C**	**Buffer D**
50× Na-Pi	10 ml	10 ml	4 ml	4 ml
Sucrose	102.7 g	68.46 g	41.1 g	17.1 g
NaCl	0	0	23.4 g	23.4 g
Add ddH_2O to (final volume)	500 ml	500 ml	200 ml	200 ml

Detergent washing solution (0.1 Tween 20, ½ Buffer B)

10% Tween 20	0.4 ml
Buffer B	20 ml
ddH_2O to	40 ml (final volume)

Minimal Buffer (10 mM Na-Pi)

0.5 M Na-Pi (50×stock)	2 ml
ddH_2O to	100 ml (final volume)

3. Procedure (Tzen et al., 1997)

3.1 2.5 grams of samples were crushed using mortar and pestle, in 11 ml grinding buffer at 4 °C (on ice) for 20 minutes.

3.2 The homogenate was filtered through Miracloth (CALBIOCHEM, EMD chemicals, Inc., USA) into 50 ml centrifuge tube.

3.3 The filtrate was separated equally (1 ml) into 1.5-ml Eppendorf tube and then the grinding buffer was slowly layered on the top until reached 1.5-ml level by using plastic dropper (2 separated layers could be observed).

3.4 The sample was centrifuged at 13,200 rpm at 4 °C for 20 minutes using centrifuge machine (Eppendorf 5415D centrifuge, USA).

3.5 The oil layer on the top of Eppendorf tube was collected into 50 ml centrifuge tube using spatula and then by 20 - 200 µl auto-pipette (Gilson, Inc., USA).

3.6 4 ml detergent washing solution was added to the oil (oil: detergent washing solution = 1:1), the sample was mixed using vortex mixer (Scientific industries, Inc., USA) and then homogenized using glass homogenizer for 20 minutes.

3.7 The homogenate was equally transferred to Eppendorf tubes and centrifuged at 13,200 rpm at 4 °C for 20 minutes.

3.8 The oil bodies were collected, resuspended in 3 ml flotation buffer (oil: flotation buffer = 1:1), separated to Eppendorf tube and again centrifuged.

3.9 The oil bodies were purified in flotation buffer for the second time.

3.10 The oil bodies were mixed with 3 ml minimal buffer and centrifuged.

3.11 The oil bodies were collected and again washed with 3 ml detergent washing solution and centrifuged.

3.12 The oil bodies were resuspended to salting buffer and then flotation buffer.

3.13 0.5 ml grinding buffer was added to the oil bodies and then centrifugated.

3.14 The grinding buffer was sucked out until the remaining mixture of oil bodies and buffer was at 0.05-ml level of Eppendorf tube.

3.15 The purified oil bodies were stored at -20 °C.

APPENDIX E
THIN LAYER CHROMATOGRAPHY

1. TLC Staining

Coomassie blue R-250	0.15 g
Methanol	100 ml
Acetic acid	2.5 ml
Distilled water	400 ml

* Store at room temperature

2. Destain solution

Distilled water	400 ml
Methanol	100 ml

* Store at room temperature

3. Procedure (Lin et al., 2012)

3.1 25 µl of oil samples was extracted with 200 µl chloroform/methanol (2/1 v/v) in 1.5-ml Eppendorf tube.

3.2 50 µl distilled water was added in the tube, for better separation of two layers, and then mixed by vertical mixture.

3.3 The mixture was centrifuged at 12,000 rpm for 4 minutes to separate chloroform layer (lower part) and methanol/water layer (upper part).

3.4 The chloroform layer was collected and stored at -80 °C for TLC analysis.

3.5 8 µl of chloroform layer was mixed with 20 µl CH_3Cl: CH_3OH (2:1 v/v).

3.6 20 µl of the samples and 5 µl TAG marker were spotted onto TLC plate which was previously developed to the top (R_f = 1) in hexane: diethyl ether: acetic acid (70: 30: 1 v/v/v).

3.7 TLC plate with spotted samples was air-dried at room temperature for 10 minutes and then developed in benzene to the R_f = 1 position.

3.8 After air-dried, the plate was developed to R_f = 0.5 in hexane: diethyl ether: acetic acid (70: 30: 1 v/v/v).

3.9 The plate, after drying, was stained overnight with 0.03% Coomassie blue R-250 (Sigma, USA) dissolved in 20% (v/v) methanol and 0.5% (v/v) acetic acid and destained for 20 minutes in destain solution.

APPENDIX F
GLYCINE SDS-PAGE

1. Stock solution

10 X Tank buffer (keep at room temperature)

Tris	15.14 g	30.28 g
Glycine	72.06 g	144.12 g
SDS	5 g	10 g
ddH_2O to	500 ml	1000 ml (final volume)

0.1% Bromophenol Blue (BPB)

BPB	0.1 g
ddH_2O to	100 ml (final volume)

1.25 M Tris-HCl, pH 6.8 (keep at room temperature)

Tris	15.14 g
ddH_2O	80 ml
HCl (conc.) to	pH 6.8
ddH_2O to	100 ml (final volume)

2. Working reagents

30% Acrylamide: Bis-acrylamide (30%, 0.8%) (keep at 4 ºC)

Acrylamide	30 g	75 g
Bis-acrylamide	0.8 g	2 g
ddH_2O to	100 ml	250 ml (final volume)

1.5 M Tris-HCl, pH 8.8 (keep at room temperature)

Tris	90.83 g
ddH_2O	400 ml
HCl (conc.) to	pH 8.8
ddH_2O to	500 ml (final volume)

0.5 M Tris-HCl, pH 6.8 (keep at room temperature)

Tris	6.06 g
ddH_2O	80 ml
HCl (conc.) to	pH 6.8
ddH_2O to	100 ml (final volume)

10% SDS (keep at room temperature)

SDS	10 g
ddH_2O to	100 ml (final volume)

10% Ammonium Persulfate (APS)

APS	0.5 g
ddH_2O	5 ml

Aliquot to 200 µl per tube (0.5 ml Eppendorf tube) and freeze at -20 ºC

TEMED (keep at room temperature)

4× Sample Buffer

[final conc. of sample treatment (1×) = 62.5 mM Tris-HCl, pH 6.8, 2% SDS, 5% 2-ME, 0.004% BPB and 10% glycerol]

SDS	0.8 g	3.2 g
2-mercaptoethanol	0.2 ml	0.8 ml
0.1% Bromophenol Blue	1.6 ml	6.4 ml
Glycerol	4 ml	16 ml
1.25 M Tris-HCl, pH 6.8	2 ml	8 ml
ddH_2O to	10 ml	40 ml (final volume)

* keep at room temperature, cover with aluminum foil to protect from light

Running Buffer (1× Tank buffer) (keep at room temperature)

10× Tank buffer	100 ml
ddH_2O to	1000 ml

Stain solution, 0.125% Coomassie blue in 50% methanol and 10% acetic acid (keep at room temperature)

Methanol	500 ml
Acetic acid	100 ml
ddH_2O	400 ml
Coomasie Blue	1.25 g

* Dissolve Coomasie Blue in methanol, then add acetic acid, shaking on stirrer for 1 hour before adding ddH_2O
* This stain can be reused several times, filter through Whatman # 1 between uses.

Destain solution I, 50% methanol and 10% acetic acid

Methanol	500 ml
Acetic acid	100 ml
ddH_2O	400 ml

* keep at room temperature

Destain solution II, 5% methanol and 7% acetic acid

Methanol	50 ml
Acetic acid	70 ml
ddH_2O	880 ml

* or Destain solution II = 50% diluted destain solution I
* keep at room temperature

3. Gel compositions

Separating gel (lower gel) (15% acrylamide, for 10 kDa)

Solutions	**Amount for 2 baby gels**
1.5 M Tris, pH 8.8	2.5 ml
ddH_2O	2.37 ml
30% Acrylamide: Bis	5 ml
10% SDS	0.1 ml
Total volume	10 ml
10% APS	100 µl
TEMED	10 µl

Stacking gel (upper gel) (4.75% acrylamide)

Solutions	**Amount for 2 baby gels**
0.5 M Tris, pH 8.8	1 ml
ddH_2O	2.3 ml
30% Acrylamide: Bis	0.63 ml
10% SDS	40 µl
Total volume	4 ml
10% APS	100 µl
TEMED	10 µl

* Continuously and gently shaking after adding 30% Acrylamide: Bis to the solution

APPENDIX G

WESTERN BLOTTING

1. Stock solution

1 M Tris-HCl, pH 7.5

Tris	60.55 g
ddH_2O	400 ml
HCl to	pH 7.5
ddH_2O to	500 ml

2. Working solution

Equilibration/Blotting solution, 25 mM Tris, 192 mM Glycine, 20% methanol (prepare ahead and store at 4 ºC)

Tris	12.11 g	3.03 g
Glycine	57.65 g	14.41 g
Methanol	800 ml	200 ml
ddH_2O to	4000 ml	1000 ml

Tris Buffer Saline (TBS), 20 mM Tris-HCl, 0.5 M NaCl, pH 7.5 (keep at 4 ºC)

1 M Tris-HCl, pH 7.5	80 ml
NaCl	116.9 g
ddH_2O to	4000 ml

Blocking solution, 3% gelatin in TBS

Gelatin	4.5 g	3 g
TBS	150 ml	100 ml

Antibody solution, 1% gelatin in TBS

Gelatin	2 g	1 g
TBS	200 ml	100 ml

TTBS, 0.05% Tween 20 in TBS

TBS	4 L
Tween 20	2 ml

Ponceau S solution, 0.1% in ddH_2O

Ponceau S	0.1 g
ddH_2O to	100 ml

Development buffer, 0.1 $NaHCO_3$ - 1 mM $MgCl_2$, pH 9.8

$NaHCO_3$	8.4 g
$MgCl_2$. $6H_2O$	0.2033 g
ddH_2O	800 ml
NaOH to	pH 9.8
ddH_2O to	1000 ml (final volume)

Color development solution

BCIP	16.5 µl
NBT	33 µl
Development buffer	5 ml

3. Procedure

3.1 Proteins were transferred from SDS-PAGE onto a nitrocellulose membrane in a Trans-Blot system (Bio-Rad, USA).

3.2 The system was run using voltage of 100 and current of 400 mA (Electrophoresis power supply-EPS 301, Amersham Biosciences, UK) at 4 °C.

3.3 The membrane was stained with Ponceau S solution (Sigma-Aldrich), on orbital shaker, for a while and washed with distilled water for around 10 minutes.

3.4 The membrane was transferred to blocking solution and shaken for 30 minutes.

3.5 After pouring the blocking solution out, 6 ml antibody solution and 3 µl primary antibodies (antibodies against sesame seed 27-kDa caleosin, 17- kDa oleosin, or 15-kDa oleosin) were subjected to the membrane, then shaking for 1.5 hours at room temperature.

3.6 The membrane was washed with TTBS solution 3 times, each with 10 minutes and then shaken in TTBS at 4 °C overnight.

3.7 The membrane was washed with TTBS 3 times, each with 10 minutes.

3.8 The membrane was incubated in 6 ml of TTBS and 3 µl secondary antibodies for one hour, on a shaker at room temperature. Secondary antibodies conjugated with anti-rabbit alkaline phosphatase and conjugated with anti-chicken alkaline phosphatase were used for immune detection of caleosin and oleosins, respectively.

3.9 After washing with TTBS for 1 hour (the solution was changed every 15 minutes), color of membrane was developed in dark condition, on a shaker for 30 minutes, using the mixture of developmental buffer, substrates nitro blue tetrazolium chloride (NBT) (Promega, USA) and 5-bromo-4 –chloro-3-indolyl phosphate (BCIP) (Promega, USA).

APPENDIX H

LC-MS/MS

1. Solutions

Acetonitrile (ACN, J.T. Baker)

Ammonium bicarbonate (NH_4HCO_3, ABC, Fluka)

Iodoacetamide (IAA, sigma)

Dithioerythreitol (DTT, sigma)

Formic acid (FA, Fluka)

ddH_2O (J.T. Baker)

Trypsin (Promega)

2. Destain

Add 50 mM ABC/50% ACN to gel. Incubate for 30 minutes at room temperature, repeat as necessary until color is gone. Dehydrate the gel pieces with 100% ACN.

3. Reduction and alkylation

Add 10 mM DTT in 50 mM ABC to gel. Incubate for 60 minutes at 56 ºC to reduce proteins. Discard solution and then add 55 mM iodoacetamide in 50 mM ABC, incubate for 45 minutes in dark place at room temperature. Discard solution and dehydrate the gel pieces with 100% ACN.

4. Trypsin Digestion

Rehydrate the gel pieces at 4 °C for 30 minutes in buffer containing 50 mM ABC and trypsin. Digest overnight at 37 °C.

5. Peptide extraction

Add 50% ACN / 1% FA to gel. Sonicate sample gel for 10 seconds, and then stop for 10 seconds. Repeat sonication 10 times. Repeat step to give a combine peptide extract. Speed Vac to dry the combined solution.

6. Desalting ((Millipore Ziptip C18)

6.1 Dissolve dried peptide mixtures in 10 µl of ddH_2O containing 0.1% FA.

6.2 Prepare Zip-tip C18 (Millipore). Activate Zip-tip by rinsing 3 times with 10 µl 100% ACN. Equilibrate Zip-tip 3 times with 10 µl of ddH_2O containing 0.1% FA.

6.3 Bind the peptides by aspirating and dispensing peptide solution; use up to 10 cycles.

6.4 Wash 6 times with 10 µl of ddH_2O containing 0.1% FA.

6.5 Elute peptides with 10 µl of 50% ACN/ 0.1% FA by aspirating and dispensing peptide solution; use up to 10 cycles. Repeat step to give a combined solution.

6.6 Dry combined solution using a Speed Vac.

6.7 Prepare sample for LC-MS/MS analysis: resolubilize the desalted peptide with ddH_2O containing 0.1% FA.

7. LC condition

Buffer A: ddH_2O/0.1% formic acid (FA)

Buffer B: 100% ACN/0.1% formic acid (ACN-acetonitrile)

Gradient:

Time (minutes)	% A	% B	Flow rate	Sample loading
0	95	5	300 nl/minute	10 µl (0.1% FA)
4.5	95	5		
31	65	35		
32	10	90		
52	10	90		
53	95	5		
70	95	5		

Analytical column: Acclaim PepMap C18, 75 µm I.D. x 25 cm nanoViper, 2 µm, 100 Å, Thermo Fisher Scientific

8. MS condition

Positive ion ESI mode

Gas 1: 15

Gas 2: 0

Curtain gas: 30

Ion Spray voltage was set at +2500 v

Interface heater temperature at 150℃

Column oven temp: 35 ℃

Declustering potential (DP): 80 V

IDA mode

TOF-MS scan range : 350 ~ 1250 m/z , acclimated for 0.25 seconds

MS/MS scan range : 65 ~ 1800 m/z , acclimated for 0.1 seconds

Collision energy (CE): rolling collision energy voltage

Charge: +2 ~ +4

Counts > 100

Top 20 parent ions will be selected following MS/MS

Database search program: Mascot

9. Ziptip cleanup

Buffer: 100% ACN / 50% ACN/0.1% formic acid / 0.1% formic acid

APPENDIX I

IN VITRO CULTURE

MS medium compositions (Murashige and Skoog, 1962)

Components	Quantity (mg L^{-1})
Macroelements	
Ammonium Nitrate (NH_4NO_3)	1,650.000
Potassium nitrate (KNO_3)	1,900.000
Calcium Chloride 2 hydrate ($CaCl_2.2H_2O$)	440.000
Magnesium sulfate 7 hydrate ($MgSO_4.7H_2O$)	370.000
Potassium Phosphate, Monobasic (KH_2PO_4)	170.000
Microelements	
Manganese Sulfate 4 hydrate ($MnSO_4.4H_2O$)	22.300
Zinc Sulfate 4 hydrate ($ZnSO_4.4H_2O$)	8.600
Boric Acid (H_3BO_3)	6.200
Potassium iodide (KI)	0.830
Sodium Molybdate (VI) dihydrate ($Na_2MoO_4.2H_2O$)	0.250
Cupric Sulfate 5 hydrate ($CuSO_4 \cdot 5H_2O$)	0.025
Cobalt Chloride 6 hydrate ($CoCl_2.6H_2O$)	0.025
Iron	
Na_2 EDTA (Na_2 $C_{10}H_{16}N_2O_8$)	37.250
Ferrous Sulfate 7 hydrate ($FeSO_4.7H_2O$)	27.850
Vitamin	
Glycine (NH_2CH_2COOH)	2.000
Thiamine - HCl ($C_{12}H_{17}ClN_4OS$. HCl)	0.100
Nicotinic acid ($C_6NH_5O_2$)	0.500
Pyridoxine - HCl ($C_8H_{11}NO_3$. HCl)	0.100
Myo-inositol	
Myo-inositol ($C_6H_{12}O_6$)	100.000
Sucrose	30,000.000

Adding 0.7% agar for a solid medium

Adjusting to pH 5.83

APPENDIX J

AMINO ACID ABBREVIATION

Full name	Abbreviation (3 letters)	Abbreviation (1 letter)
Alanine	Ala	A
Arginine	Arg	R
Asparagine	Asn	N
Aspartate	Asp	D
Cysteine	Cys	C
Glutamate	Glu	E
Glutamine	Gln	Q
Glycine	Gly	G
Histidine	His	H
Isoleucine	Ile	I
Leucine	Leu	L
Lysine	Lys	K
Methionine	Met	M
Phenylalanine	Phe	F
Proline	Pro	P
Serine	Ser	S
Threonine	Thr	T
Tryptophan	Trp	W
Tyrosine	Tyr	Y
Valine	Val	V

VITAE

Name Miss Nilubol Nuanjunkong

Student ID 5510230024

Educational Attainment

Degree	Name of Institution	Year of Graduation
Bachelor of Science (Biology) (First Class Honor)	Prince of Songkla University	2009
Master of Science (Botany)	Prince of Songkla University	2011

Scholarship Awards during Enrolment

- Science Achievement Scholarship of Thailand (SAST)
- Scholarship for Support Exchange Students and International Credit Transferred through ASEAN Community, Graduate School, Prince of Songkla University, Thailand

List of Publication and Proceedings

Nuanjunkong N., Tongurai, C. and Meesawat, U. Developmental evidence of male and female gametophytes of physic nut (*Jatropha curcas* L.): pollen capability and stigma receptivity. Walailak Journal of Science and Technology.

Nuanjunkong N., Tongurai, C., Tzen, J. T. C., Jiang, P. L. and Meesawat, U. Features of *Jatropha curcas* seed oil in relation to different pollination methods. Songklanakarin Journal of Science and Technology.